

ESTIMATION OF TANGENTIAL MOMENTUM ACCOMMODATION COEFFICIENT
USING MOLECULAR DYNAMICS SIMULATION

by

GEORGE WAYNE FINGER
B.S. University of Florida, 1975
M.S. University of Central Florida, 2002

A dissertation submitted in partial fulfillment of the requirements
for the degree of Doctor of Philosophy
in the Department of Mechanical, Materials and Aerospace Engineering
in the College of Engineering
at the University of Central Florida
Orlando, Florida

Fall Term
2005

Major Professor: Jayanta Kapat

© 2005 George Wayne Finger

ABSTRACT

The Tangential Momentum Accommodation Coefficient (TMAC) is used to improve the accuracy of fluid flow calculations in the slip flow regime. Under such conditions (indicated by Knudsen number greater than 0.001), the continuum assumption that a fluid velocity at a solid surface is equal to the surface velocity is inaccurate because relatively significant fluid “slip” occurs at the surface. Prior work has not led to a method to quickly estimate a value for TMAC - it is frequently assumed. In this work, Molecular Dynamics techniques are used to study the impacts of individual gas atoms upon solid surfaces to understand how approach velocity, crystal geometry and interatomic forces affect the scattering of the gas atoms, specifically from the perspective of tangential momentum. It is a logical step in the development of a comprehensive technique to estimate total coefficient values to be used by those investigating flows in micro- and nano-channels or on orbit spacecraft where slip flow occurs. TMAC can also help analysis in transitional or free molecular regimes of flow.

The gas – solid impacts were modeled using Lennard Jones potentials. Solid surfaces were modeled with approximately 3 atoms wide by 3 atoms deep by 40 or more atoms long. The crystal surface was modeled as a Face Centered Cubic (100). The gas was modeled as individual free gas atoms. Gas approach angles were varied from 10° to 70° from normal. Gas speed was either specified directly or by way of a ratio relationship with the Lennard-Jones energy potential (Energy Ratio). In order to adequately model the trajectories and maintain conservation of energy, very small time steps (on the order of 0.0005τ , where τ is the natural time unit) were

used. For each impact the initial and final tangential momenta were determined and after a series of many impacts, a value of TMAC was calculated for those conditions.

The modeling was validated with available experimental data for He gas atoms at 1770 m/s impacting Cu over angles ranging from 10° to 70° . The model agreed within 3% of the experimental values and correctly predicted that the coefficient changes with angle of approach.

Molecular Dynamics results estimate TMAC values from a high of 1.2 to a low of 0.25, generally estimating a higher coefficient at the smaller angles. TMAC values above 1.0 indicate backscattering, which has been experimentally observed in numerous instances. The ratio of final to initial momenta, when plotted for a given sequence of gas atoms spaced across a lattice cycle typically follows a discontinuous curve, with continuous portions indicating forward and back scattering and discontinuous portions indicating multiple bounces. Increasing the Energy Ratio above a value of 5 tends to decrease the coefficient at all angles. Adsorbed layers atop a surface influence the coefficient similar to their Energy Ratio. The results provide encouragement to develop the model further, so as to be able in the future to evaluate TMAC for gas flows with Maxwell temperature distributions involving numerous impact angles simultaneously.

ACKNOWLEDGMENTS

It is a pleasure to have this opportunity to thank my advisor for the past 5 years, Dr. Jay Kapat for his patient guidance, weekly advice, direction and constant support towards completing my coursework and this research work. I also acknowledge and offer thanks to my committee of Dr. R. Kumar, Dr. A. Bhattacharya, Dr. Q. Chen and Dr. D. Srivastava for their support and guidance.

I thank the UCF MMAE department staff (especially J. Clements) for their assistance and efficient support.

A special thanks goes to my employer, RS&H, Inc. who has provided a flexible work schedule and tuition reimbursement.

None of this would have been possible without the unconditional and constant support and encouragement of my wife Alice.

TABLE OF CONTENTS

LIST OF FIGURES	xii
LIST OF TABLES	xv
LIST OF ACRONYMS/ABBREVIATIONS	xvi
CHAPTER ONE: INTRODUCTION.....	1
Spacecraft.....	1
Micro-channels & Nano-channels	2
Micro-seals and Micro-gaps	4
Heat Transfer	5
Objective of this Work.....	5
CHAPTER TWO: BACKGROUND	7
Continuum Flow at a Surface	7
Slip Flow & Slip Coefficient	8
Mean Free Path	9
Knudsen Number	10
Maxwell’s Concepts for Interactions at the Gas / Surface Interface	11
Probabilistic Models of Gas / Surface Interactions.....	15
TMAC of Maxwell	15
TMAC Defined for this Work.....	15
Backscattering.....	17
Typical Values of TMAC	18

Scattering Kernels.....	18
Slip Coefficient from TMAC (f).....	19
Deterministic Models.....	20
Molecular Models.....	20
Lennard-Jones Potential.....	20
Tersoff – Brenner Potential.....	22
Surface Geometry Characteristics.....	22
Surface Material Characteristics.....	23
Velocity Distribution of Gas.....	25
Governing Equations.....	26
Newton’s Laws of Motion.....	26
Lennard-Jones Potential.....	27
Composite Lennard-Jones Coefficients.....	28
Conservation of Energy.....	28
CHAPTER THREE: LITERATURE REVIEW.....	29
Previous Experimental Works which provide TMAC Data.....	29
Experimental Work of Primary Interest - Seidl.....	29
Experimental Works of Secondary Interest.....	32
Saltsburg.....	33
Arkilic.....	33
Liu.....	34
Boring.....	34
Knetchtel.....	35

Thomas.....	35
Bentz and Gabis	37
Suetin	37
Porodnov.....	38
Lord.....	40
Maegley	42
Other	43
Previous Works which demonstrate need of a TMAC MD model.....	44
Logan	44
Bird	45
Previous Analyses Involving TMAC.....	46
Molecular Dynamics Simulations.....	46
Koplik, Banavar & Willemsen.....	47
Yang.....	48
Koplik	48
Cieplak	49
Tomassone	50
Vergeles	50
Oman.....	50
Knetchtel.....	51
Finger	52
Monte Carlo Simulations	52
Other Numerical Models.....	53

Analytical Models.....	54
CHAPTER FOUR: METHODOLOGY	56
Objective.....	56
Simplifying Assumptions and Their Justification	57
Assumption: A Single Gas Atom is Involved in each Gas-to-Solid Interaction.....	58
Assumption: Adiabatic Approximation is used	58
Assumption: Surface Relaxation and Rumpling of the Solid are Neglected	61
Quantitative Values Used	62
Lennard – Jones Coefficient Values	62
Cut Off Radius	62
Natural Time Unit and Time Step.....	65
Convergence of the Numerical Solution.....	66
Time Step Cut Off and Bounce Cut Off	67
Gas Starting Height and Mean Free Path.....	69
Limitations of the Model	70
Development of the MD Simulation Model	70
Technical Approach to MD Simulation Model	71
Main Issues in Computer Simulations	71
Select Software	72
Gather the Key Input Data	72
Setup Variables for MD Simulation	73
Calculate the initial conditions for the solid atoms.....	74
Run the MD Simulation for each gas atom.....	74

Analyze and Post Process the MD Model Data	75
Perform Energy Checks	75
Perform Momentum Analyses and Checks.....	75
Technical Approach to Design of the Experiments	77
General Topics in TMAC Experiment Design	77
Specific Experiments Planned	78
Baseline Validation with Data Methodology.....	79
Reasonableness Inspection of Typical Results Methodology.....	83
Energy Ratio Analysis Methodology.....	84
Adsorbed Layer Analysis Methodology	87
Atomic / Nano Scale Geometry Analysis Methodology.....	89
CHAPTER FIVE: FINDINGS.....	92
Baseline Validation Findings.....	92
Validation Experiment with Two Layers of Adsorbent.....	92
Validation Experiment with Three Layers of Adsorbent:.....	94
MD Model Validation Summary	96
Reasonableness Inspection of Typical MD Results.....	97
Gas atom position vs. time step	97
Gas atom velocity vs. time step	99
Gas atom acceleration vs. time step.....	101
Lennard Jones potential vs. time step	102
Number of solid atoms involved in the collision vs. time step.....	102
Total energy vs. time step.....	103

Kinetic Energy ratio (final/initial) vs. each gas atom	104
Tangential Momentum ratio (final/initial) vs. each gas atom.....	105
Normal Momentum Ratio (final/initial) vs. each gas atom	107
Summary – Reasonableness Check	107
Energy Ratio Analysis Findings	108
Adsorbed Layer Analysis Findings.....	116
Effect of Single and Multiple Adsorbed Layers with large ER difference.....	116
Effect of Single and Multiple Adsorbed Layers with small ER difference	120
Effect of Change of ER of Adsorbed Layer.....	120
Nano & Sub Nano Geometry Analysis Findings.....	122
Sub Nano Geometry Findings (Ratio of σ / Lattice Spacing)	122
Nano Geometry Findings – Single Atom Bumps Atop FCC 100 Crystal	124
Energy Ratio Surface Plot Analysis.....	128
CHAPTER SIX: CONCLUSION.....	131
Basic Conclusions about TMAC	131
Conclusions Based on Broad Parameters	132
Thoughts on MD Modeling of TMAC.....	132
APPENDIX: RECOMMENDATIONS FOR FOLLOW ON RESEARCH.....	134
LIST OF REFERENCES.....	141

LIST OF FIGURES

Figure 1 Specular Model.....	12
Figure 2 Molecule Striking Sphere.....	12
Figure 3 Diffuse Model.....	13
Figure 4 Intermediate Model.....	14
Figure 5 Plot of typical Lennard-Jones potential.....	21
Figure 6 Example Maxwell Speed Distribution (Halliday).....	26
Figure 7 Seidl Experiment Apparatus.....	30
Figure 8 Seidl Experimental TMAC Data 1.....	31
Figure 9 Seidl Experimental TMAC Data 2.....	32
Figure 10 Liu TMAC Data.....	34
Figure 11 Knechtel TMAC Argon ion on Aluminum.....	35
Figure 12 Maegley Data (figure 2 of reference).....	42
Figure 13 Maegley Data (figure 6 in reference).....	43
Figure 14 Effect of Cut Off Radius on TMAC Error.....	64
Figure 15 Effect of Cut Off Radius on Number of Solid Atoms Involved.....	64
Figure 16 Effect of Bounce Cut Off on Error.....	67
Figure 17 Effect of Terminated Gas Atoms on TMAC Error.....	68
Figure 18 Seidl Data.....	79
Figure 19 Atomic / Nano Scale Irregularities.....	91
Figure 20 Baseline Validation Data Summary – 2 Layer Model.....	93
Figure 21 Baseline Validation Data Summary – 2 Layer Model.....	95

Figure 22 Typical Gas Atom Path – Single “Bounce”; Negative Final Tangential Momentum ..	98
Figure 23 Typical Gas Atom Path – Single “Bounce”; Positive Final Tangential Momentum ...	98
Figure 24 Typical Gas Atom Paths – Multiple “Bounces”; Variable Result.....	99
Figure 25 Typical Gas Atom Velocity vs. Time Step.....	100
Figure 26 Typical Gas Atom Acceleration vs. Time Step	101
Figure 27 Typical Lennard Jones Potential vs. Time Step	102
Figure 28 Typical Number of Solid Atoms Involved in Collision vs. Time Step	103
Figure 29 Typical Total Energy vs. Time Step.....	104
Figure 30 Typical Kinetic Energy Ratio for Each Gas Atom.....	105
Figure 31 Typical Tangential Momentum Ratio Plot for Each Gas Atom.....	106
Figure 32 Typical Normal Momentum Ratio Plot for Each Gas Atom.....	107
Figure 33 Energy Ratio - Data Summary	108
Figure 34 Energy Ratio – Effect at Large Angles.....	109
Figure 35 Energy Ratio – Effect at Small Angles.....	109
Figure 36 Energy Ratio - Tangential Momentum Ratio - 4 Cases	111
Figure 37 Energy Ratio - Gas Atom 100 in 4 Cases.....	113
Figure 38 Energy Ratio - Gas Atom 200 in 4 Cases.....	114
Figure 39 Adsorbed Layers - Data Summary for Large ER Difference.....	116
Figure 40 Adsorbed Layers – Examples at 10 Degrees.....	118
Figure 41 Adsorbed Layers – Gas Atom Path Plots (10 sample atoms each)	119
Figure 42 Adsorbed Layers - Data Summary for Small ER Difference.....	120
Figure 43 Adsorbed Layers – ER 1 Layer	121
Figure 44 Adsorbed Layers – ER 2 Layers.....	121

Figure 45 Nano Geometry - Ratio of Sigma to Solid Lattice Spacing Concept.....	122
Figure 46 Nano Geometry – Ratio of Sigma to Solid Lattice Spacing Data	123
Figure 47 Nano Geometry – Ratio of Sigma to Solid Lattice Spacing, 10 & 70 Degrees	124
Figure 48 Nano Geometry – Surface “Bumps” Summary Data	125
Figure 49 Nano Geometry – Surface “Bumps”	126
Figure 50 Nano Geometry – Surface “Bumps” Reducing Backscattering	126
Figure 51 Nano Geometry - 1 /8: Most Gas Atoms miss "Bump" (10 sample atoms).....	127
Figure 52 Height Contour Plot of L-J Potential Corresponding to ER of 1 (Unit Cell).....	128
Figure 53 Height Contour Plot of L-J Potential Corresponding to ER of 1 (Larger Surface)....	129
Figure 54 Height High-Low-Average Corresponding to Various ER.....	130
Figure 55 Standard Deviation of Height Corresponding to Various ER	130

LIST OF TABLES

Table 1 Values of TMAC	18
Table 2 Arkilic	33
Table 3 Thomas.....	36
Table 4 Suetin	38
Table 5 Suetin	38
Table 6 Porodnov.....	39
Table 7 Porodnov.....	39
Table 8 Lord.....	40
Table 9 Lennard Jones Coefficients.....	62
Table 10 Typical MD Simulation Convergence.....	66
Table 11 Seidl Experimental Error	80
Table 12 Baseline Data MD Experimental Conditions.....	81
Table 13 Energy Ratio MD Experimental Conditions.....	85
Table 14 Adsorbed Layer MD Experimental Conditions.....	87
Table 15 Nanoscale Geometry MD Experimental Conditions	89
Table 16 Comparison MD Model Results (2 Layers) to Seidl Data.....	93
Table 17 Comparison MD Model Results (3 Layers) to Seidl Data.....	95

LIST OF ACRONYMS/ABBREVIATIONS

<u>ACRONYM</u>	<u>Definition of Acronym</u>
DSMC	Direct Simulation Monte Carlo
ER	Energy Ratio
$f(r_{ij})$	Lennard Jones Force
J	Joules
Kn	Knudsen Number
MD	Molecular Dynamics
MEMS	Micro Electro Mechanical Systems
NEMS	Nano Electro Mechanical Systems
NMAC	Normal Momentum Accommodation Coefficient
R_c	Cut Off Radius
s	Seconds
TMAC	Tangential Momentum Accommodation Coefficient
$u(r_{ij})$	Lennard Jones Potential
U	Gas Velocity
δ	Boundary Layer Thickness
ε	Lennard Jones Coefficient – Characteristic Energy
λ	Mean Free Path
η	Viscosity
σ	Lennard Jones Coefficient – Characteristic Distance
v	Mean Particle Speed

τ	Natural Time Unit
τ_{wall}	Shear Stress at Wall
Θ_d	Debye Temperature
ξ	Slip Coefficient / Slip Length

CHAPTER ONE: INTRODUCTION

In most applications, a continuous environment is sufficient to describe the flow phenomena.

The sample sizes are large enough and the materials dense enough such that individual molecular actions are not significant. We use terms like density, temperature and pressure to describe the collective behavior of countless gas atoms or molecules acting as a continuum.

However, situations exist where this is an inappropriate model. Some real applications result in situations where the gas is so dilute or the sample size so small that few atoms are involved. Non continuum models are required to describe the behavior of these system. Primary examples of “slip flow” occur in outer space (where the gas is very dilute) and in micro or nano channels (where the sample size is very small).

The impact of rarefied gas atoms upon solid surfaces plays an important role in the performance of many systems. The impacts typically result in incomplete tangential momentum transfer. That is, some of the forward (tangential) momentum is transferred between the gas and the solid. If the system is conveying the gas, this contributes to the friction loss of the gas, reducing its flow. If the system is moving through the stationary gas it results in drag force which slows the system.

Spacecraft

Satellites on orbit move through a rarefied gas environment. The impact of these gas atoms on surfaces of the spacecraft moving through them results in a drag force upon the spacecraft [1] .

For spacecraft in a geosynchronous orbit (at approximately 22,000 miles) this drag force requires the use of station keeping propellant to maintain the exact orbital placement slot assigned and to which the earth station antennae are pointed. This satellite effectively loses functionality soon after its propellant is depleted.

For spacecraft in low earth orbit such drag leads to a loss of altitude, orbital decay and eventual atmospheric reentry. For example, depending on orbital orientation, the Space Shuttle orbiter at an orbital altitude of 220 kilometers degrades between 1 and 5 kilometers in altitude per day because of drag [2]. For smaller satellites, on the order of 1 m in size, in orbits as low as 150 km the Knudsen number can still be between 30 and 40, indicating a highly rarefied environment [3].

Therefore a method to better understand the tangential momentum transfer will lead to improved understanding of the drag forces and thruster jet impingement [4] and more appropriate propellant allocations for optimum life. Additionally, a method to understand and predict tangential momentum transfer can result in improved surfaces design which could lower drag overall, and result in less station keeping propellant being required or longer life of the spacecraft or more reliable reentry into other planets [5] [6] .

Micro-channels & Nano-channels

Micro-channels and Nano-channels are used in many micro-electromechanical systems (MEMS) and nano-electromechanical systems (NEMS). These channels convey gasses for chemical

analysis, actuation and basic gas delivery. Micro channels are also being investigated for heat transfer [7], [8]. The channels are frequently on the order of 1 micrometer in width [9] with depths as small as 500 nanometers [10]. In these small channels, the surface to volume ratio may be a million times the typical value experienced at macro scale, leading to significant effects from these surface interactions [11]. At this small sample size the gas is not in a continuous flow regime [12].

As the gas moves through the micro- or nano-channel, its flow rate is affected by the tangential momentum transfer among the gas and the channel wall. Friction loss results. The flow rate is affected [13]. This change in flow rate can affect the accuracy of the MEMS chemical analysis being performed, the speed of the analysis, the amount of gas delivered and other factors. It can result in a greater pressure differential to perform the required flow task.

Therefore a method to better understand the tangential momentum will lead to improved understanding of the friction forces, more appropriate friction estimates and better designs of such MEMS and NEMS. This should lead to improved accuracy of the devices manufactured. Additionally, a method to understand and predict tangential momentum can result in improved surfaces design which could lower friction overall, and result in less differential pressure being required which may be the enabling technology for new applications.

Micro-seals and Micro-gaps

Development of MEMS or NEMS rotating machinery (turbines, Wankel rotary engines, Wankel rotary compressors) results in a difficulty in sealing the tips of the rotating components against the stationary surface [14, 15]. Other small rotating machinery (such as computer disc drives) maintains small gaps [16]. For example, Winchester type hard disk drives have a read/write head which floats 50 nanometers above the surface of the spinning platter [17]. At this small sample size the gas is not in a continuous flow regime. MEMS accelerometers using gas film damping are operating in the non continuum range [18] .

As the gas moves through the tip clearance zones, its flow rate is affected by the tangential momentum transfer among the gas and both the stationary outer wall and the rotating tip. Friction loss results. This reduces power output of the engine or increases power consumption of the compressor. Additionally, some of the intervening gas travels through the clearance opening and degrades performance of the device.

Therefore a method to better understand the tangential momentum will lead to improved understanding of these friction forces, more appropriate friction estimates and better designs of such devices. This should lead to overall better performance in both the power and throughput areas.

Heat Transfer

In many of the cases described above, complementary issues exist in the area of heat transfer. Applications include miniaturized heat exchangers to cool integrated circuits, micro reactors [19], micro turbines and engines. Just as friction and drag are related to tangential momentum transfer, heat transfer is frequently related to normal momentum transfer. Therefore improving the understanding of tangential momentum transfer is hoped to shed some additional light on its perpendicular complement, normal momentum transfer [20] [21].

Objective of this Work

The objective of this work is to perform a numerical simulation of non continuum gas atoms impacting a solid surface while monitoring their tangential momentum before, during and after the impact so that the simulation may be used as a tool to better understand and design the above type systems.

An established indicator of tangential momentum transfer is the TMAC – Tangential Momentum Accommodation Coefficient. Much of the past work has either assumed a value for the TMAC or analyzed experimental data to develop statistical value for the TMAC for a given set of conditions. This work will develop a deterministic model for a given set of conditions which can be used to estimate the TMAC and provide greater insight into the various factors affecting its value.

This work develops a simple free molecular regime deterministic simulation model which can be used to estimate the TMAC of rare gas to solid surface interactions, for a given set of conditions. The model was validated with data from prior experimental work. The model was revised and expanded, as required, based on the validation data. Using the validated model, simulations were conducted to draw conclusions about the various physical characteristics which may affect TMAC values for a specific application.

CHAPTER TWO: BACKGROUND

Continuum Flow at a Surface

Under continuum conditions the tangential velocity of a fluid at the surface (relative to the surface's velocity) is reduced to zero and the forces exerted on fluid moving past a solid (or a solid body moving through a fluid) are determined by characteristics of the flow field.

For a continuum, this results in a boundary condition of zero velocity at the wall surface – the so named “no slip condition”.

$$U(\text{at } y = 0) = 0 \quad (\text{The gas velocity at the surface is zero})$$

This zero surface velocity in combination with the fluid viscosity results in significant drag. Barwinkel [22] notes that frictional force amounts to about 80% of total drag for normal airplanes. This force is calculated by integrating the shear stress over the entire airplane's exterior surface. The shear stress at the surface is calculated from the velocity gradient at the surface:

$$\tau_{\text{wall}} := \eta \frac{d}{dy} u \quad \text{at } y=0$$

Where u is the moving gas velocity, y is the distance normal from the surface, τ_{wall} is the shear stress at the wall and η is viscosity.

Slip Flow & Slip Coefficient

Under certain rarefied gas conditions a slipping action does take place at the wall surface. This results in a situation where the relative gas velocity at the wall is a non zero amount. This non zero amount is the amount of “slip” present at the surface. The effect exists in both laminar and turbulent flows [23] .

It is common to quantify the amount of slip as an imaginary distance. This method linearly extrapolates U until it reaches a zero velocity at an imaginary depth within the surface. This depth (ξ) is a virtual distance and commonly called the “Slip Coefficient”. As ξ approaches zero, the slip effect becomes smaller.

The ratio of ξ to the boundary layer thickness (δ) is an indicator of the significance of the slip flow. If the slip coefficient is more than 1% of the boundary layer thickness, it is generally considered too large to neglect.

$$\frac{\xi}{\delta} > 0.01$$

This then becomes a indicator to the “Slip Flow” regime.

Mean Free Path

As gas molecules move about they are subject to collisions with other gas molecules. Between collisions they move with constant speed along a straight line. The average distance between successive collisions is termed the "Mean Free Path." The Mean Free Path is obviously affected by the number density of the gas (number of molecules per unit volume) and the size of the molecules themselves.

In the derivation of the Mean Free Path formula, one envisions the path created by a molecule traveling at velocity v during a time period Δt . The Mean Free Path is then the length of the path traveled divided by the number of other gas molecules present in the volume traveled (which would result in collisions):

$$\lambda := \frac{v \cdot \Delta t}{\pi \cdot \sigma^2 \cdot v_{\text{rel}} \cdot \Delta t \cdot \left(\frac{N}{V}\right)}$$

Where v is the mean speed of the molecule relative to space and v_{rel} is the mean speed of the molecule relative to the other molecules (which are moving). When taking into account the actual speed distribution of the molecules, v_{rel} equals $2^{1/2} v$ [24].

The Mean Free Path (λ) is then given by:

$$\lambda := \frac{1}{2^{0.5} \cdot \pi \cdot \sigma^2 \cdot n}$$

Where σ is the effective diameter of the molecule and n is the number density (N/V).

For air at standard conditions, the molecular Mean Free Path is approximately 50 -70 nanometers [25] . For spaceflight at an altitude of 120 kilometers, the Mean Free Path is approximately 1 meter. [16]

Another boundary to the Slip Flow regime is reached as the mean free path of the atoms (λ) approaches the boundary layer thickness. As this ratio becomes significant, interactions at the surface begin to lose their continuum characteristics. This becomes an indicator of the “Slip Flow” regime.

$$\frac{\lambda}{\delta} < 0.1$$

Knudsen Number

The Knudsen Number (Kn) represents the dimensionless ratio of the Mean Free Path to a characteristic length.

$$Kn := \frac{\lambda}{L}$$

The Knudsen Number is an indicator of the type of flow regime and a guide to determine the best ways of modeling the flow [26].

Continuum Regime: If the $Kn < 0.01$, it indicates Continuum Flow. The Navier-Stokes equations are valid for modeling the behavior. Most of the studies over the years have been in this regime.

Slip Flow Regime: If $0.01 < Kn < 0.1$, it indicates Slip Flow. The Navier-Stokes equations must be adjusted for modeling the behavior by using a slip boundary condition at the wall.

Transition Regime: If $0.1 < Kn < 3$, it indicates Transition Flow. The Navier-Stokes equations do not provide a good model, even if adjusted with slip boundary conditions. Good analysis techniques for this regime are difficult to determine. Much of the information in this regime is empirical.

Free Molecular Regime: If $3 < Kn$, it indicates Free Molecular Flow. Within this regime intermolecular gas collisions are assumed to be negligible. Typically fewer particles are involved, making probabilistic (and even deterministic) Molecular Dynamics calculations practical.

Maxwell's Concepts for Interactions at the Gas / Surface Interface

Concepts for the interaction of gas molecules impacting a solid surface include the following by Maxwell.

Maxwell [27] suggests consideration of a perfectly elastic smooth fixed surface which reflects at the angle of incidence (Specular Model). The gas can therefore only exert a normal force on this surface. Because of the perfect reflection of this gas molecules, no tangential force is exerted. This type of surface is commonly referred to as “Specular”. Such an ideal model is not particularly useful because gasses regularly exert tangential force against real surfaces.

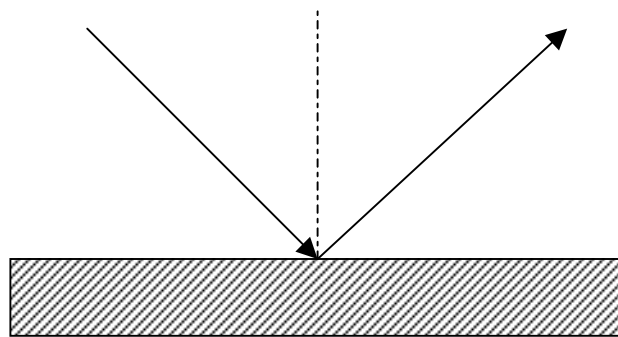


Figure 1 Specular Model

Maxwell next suggests consideration of a molecule striking a single fixed elastic sphere with a given velocity vector, but unknown position. Its final velocity could therefore be in any direction with equal probability.

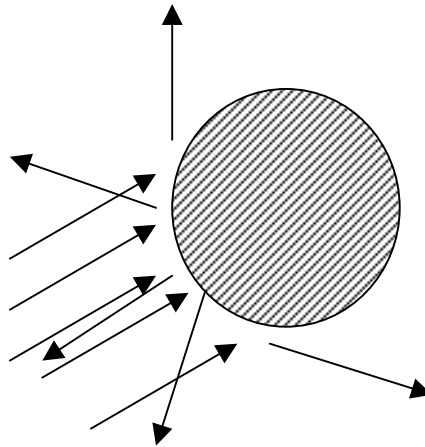


Figure 2 Molecule Striking Sphere

Maxwell then suggests consideration of a stratum of such fixed elastic spheres, placed so far apart from one another that any one sphere is not significantly shielded by any other sphere from the impact of molecules. The stratum is assumed to be deep enough that no molecule can pass through it without striking at least one sphere. Behind this stratum is a perfectly elastic smooth surface. Then every molecule of gas moving towards the surface must strike one or more spheres and all directions of its velocity become equally probable. The velocity is, of course, away from the surface. However any particular magnitude and direction would be similar to a gas at rest with respect to the surface. Maxwell suggests that those molecules leaving the stratum have the temperature of the solid and a density such that the number of molecules per unit time from the gas striking the stratum (“absorbed” gas) is equal to that leaving the surface (“evaporated” gas). This type of surface is commonly referred to as “Diffuse”.

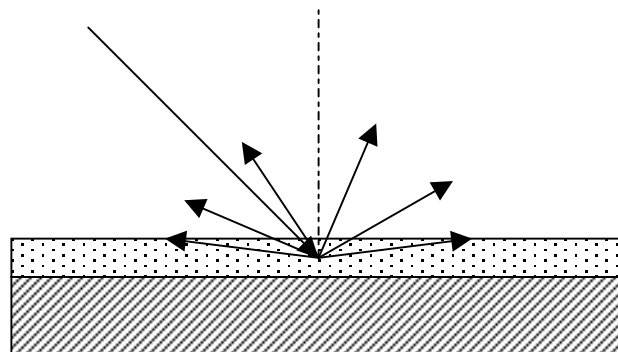


Figure 3 Diffuse Model

Maxwell next suggests consideration of a collection of spheres so close together that they partially shield each other from impacts. If the point on each sphere furthest from the solid is called the “pole”, then there will obviously be more strikes near the pole than near the “equator” of a sphere. For gas molecules traveling normal to the solid, all of its rebounding velocity directions are equally probable. However, the greater the tangential velocity of the gas molecule, the greater the likelihood that it will strike a sphere near a pole; therefore, the greater the probability that it will retain all or part of its tangential velocity. This type of surface is intermediate between the two ideal models previously described above, with molecules traveling normal to the surface more likely to be being diffused and molecules traveling tangential to the surface more likely to be reflected.

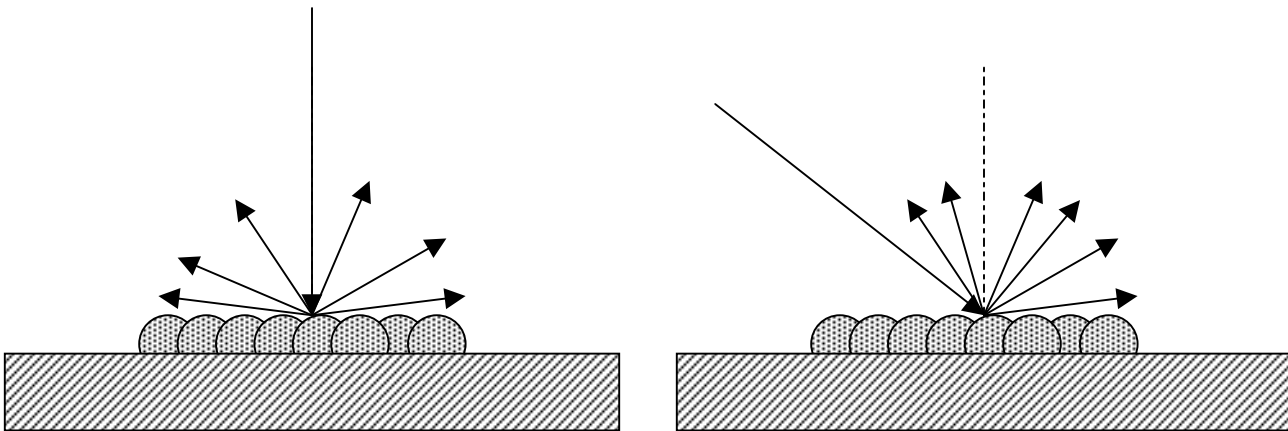


Figure 4 Intermediate Model

Maxwell also suggests a surface with a great number of “asperities” (asper ~ rough), but declines to analyze the case because of the difficulty.

Probabilistic Models of Gas / Surface Interactions

TMAC of Maxwell

Maxwell [27] suggests a coefficient “f” which represents the portion of incident molecules absorbed into the surface and “evaporated” with velocities corresponding to those of the still gas at the temperature of the solid. Then the remaining portion of incident molecules (1 – f) is perfectly reflected by the surface.

TMAC Defined for this Work

Barwinkel [22] states that Accommodation Coefficients (AC) are introduced to describe specific interactions involving flux of a physical quantity (momentum) incident and reflected from a wall. For the Tangential Momentum Accommodation Coefficient (AC), ϕ is the flux, i is the quantity of flux incident on the wall, r indicates the flux perfectly reflected from the wall and eq indicates the flux carried by a Maxwellian distribution coming from the wall at its temperature.

$$AC := \frac{\phi_i - \phi_r}{\phi_i - \phi_{eq}}$$

Arkilic [28] defines a TMAC as the “average stream wise (or tangential) momentum exchange between impinging gas molecules and the solid surface.” Their coefficient σ is:

$$\sigma := \frac{u_r - u_i}{U_w - u_i}$$

Where, u is the flux, i indicates the average stream wise velocity of the molecules incident on the wall, r indicates the average stream wise velocity of the molecules perfectly reflected from the wall and w indicates the average stream wise velocity of the wall.

For a perfectly diffuse surface, Maxwell's "f", Barwinkel's "AC" and Arkilic's " σ " all yield an accommodation coefficient of 1. For a perfectly specular surface, they all yield a value of zero.

They all being similar and describing the same situation, this paper will utilize the following definition, to describe the TMAC in the context of an MD analysis:

$$\text{TMAC} := \frac{\sum_N m \cdot V_i - \sum_N m \cdot V_f}{\sum_N m \cdot V_i}$$

Where N is the total number of gas atoms in the sample, m is the mass of a gas atom, V is the tangential velocity of the gas atom, i is the initial value and f is the final value.

The TMAC is used to directly calculate the amount of velocity slip occurring at the wall using the following relationship [29] :

$$u_{\text{gas}} - u_{\text{wall}} := \left[\frac{2 - \text{TMAC}}{\text{TMAC}} \cdot \lambda \cdot \left(\frac{\delta u}{\delta y} \right)_w \right] + \left[\frac{3}{4} \cdot \frac{\mu}{\rho \cdot T_{\text{gas}}} \cdot \left(\frac{\delta \Gamma}{\delta x} \right)_w \right]$$

The difference between the velocity of the gas at the wall (u_{gas}) and the velocity of the wall itself (u_{wall}) is a function of the TMAC, mean free path (λ), the strain rate at the wall $[(\delta u/\delta y)_w]$, fluid

density (ρ), fluid viscosity (μ), temperature of the gas adjacent to the wall (T_{gas}) and temperature change rate at the wall $[(\delta T/\delta x)_w]$. Note for a gas and wall with no heat flux (energy transfer) at the wall, the equation simplifies to an adiabatic condition which Maxwell suggested [27] :

$$u_{\text{gas}} - u_{\text{wall}} := \left[\frac{2 - \text{TMAC}}{\text{TMAC}} \cdot \lambda \cdot \left(\frac{\delta u}{\delta y} \right)_w \right]$$

Backscattering

Based on the above discussion, one would normally expect the TMAC to fall within the range of 0 to 1. However, there are some experiments which have resulted in a reflection scheme which reversed the flow so that tangential momentum was reversed to a small amount. This is termed “backscattering.” Berman [30] suggests using a backscattering value of about 6% to improve agreement with experimental data taken when the surfaces involved are not highly polished. Several others [31] [32] [33] [34] [35] also developed experimental data which supported the concept of Backscattering.

The consequence of this is that the TMAC, as defined above can conceivably have values greater than 1.

Typical Values of TMAC

Typical values for TMAC are shown in Table 1:

Table 1 Values of TMAC

TMAC Values			
Experimenter	Largest TMAC Measured	Smallest TMAC Measured	Reference
Bentz	1.11	0.83	[36]
Knetchtel	0.95	0.45	[37]
Lord	0.95	0.35	[38]
Porodnov	1.059	0.803	[39]
Seidl	1.20	0.20	[33]
Thomas	1.075	0.824	[34]
Liu and several others	Approximately 1.0		[40]

As shown by the range of data in the table, TMAC values have been measured from a high of about 1.2 to a low of about 0.2. These extremes are not typical. A majority of the experimental measurements are in the 1.06 to 0.85 range.

Scattering Kernels

Scattering Kernels are probability based models. Per Dadzie, the kernel represents “the density of probability that a molecule impinging a wall at any point of the wall with velocity V' is reflected at the same point with a velocity V'' ” [41]. Kernels have been suggested since Maxwell. The CLL model by Cercignani-Lampis [42] uses three separate accommodation coefficients (one normal, one tangential and one energy). A model by Dadzie uses three separate accommodation coefficients (one normal and two tangential) to describe surfaces with anisotropic character.

Scattering Kernels turn impinging molecules into reflected ones on a probability density basis. These Kernels use the tangential, normal (and other) accommodation coefficients as weighting factors in their modeling process. Therefore, better understanding of these accommodation coefficients can result in improved weighing factors to improve these kernels.

Slip Coefficient from TMAC (f)

The Slip Coefficient may be calculated from “f”. For no inequalities in temperature, a coefficient G is developed (Helmholtz and Piotrowski), as a function of the coefficient “f” and of the mean free path of a molecule, λ . According to Maxwell:

$$G = \frac{2}{3} \left(\frac{2}{f} - 1 \right) \lambda$$

“If, therefore, the gas a finite distance from the surface is moving parallel to the surface, the gas in contact with the surface will be sliding over it with the finite velocity “v”, and the motion of the gas will be very nearly the same as if the stratum of depth “G” had been removed from the solid and filled with the gas, there being now no slipping between the new surface of the solid and the gas in contact with it.”

The coefficient “G” is referred to as the Gleitungs-coefficient, or coefficient of slipping (ξ).

Deterministic Models

Molecular Models

Molecular Models seek to duplicate the forces between real molecules which are strongly repulsive at short distances and weakly attractive at larger distances. Some types of “Hard Sphere” and “Soft Sphere” models only include the repulsive force, neglecting the attractive force. The “Square Well” model includes a uniform attractive component to one of the repulsive models. The better molecular models combine more general attractive and repulsive potentials. [43] [44] [45] .

Lennard-Jones Potential

The best known of the attractive and repulsive potential models is the Lennard-Jones potential, which adds an inverse power law attractive component to an inverse power law model [43].

The repulsive portion of the potential represents the resistance to compression among atoms, so it repels at close range. The attractive portion of the potential represents the attractive van der Waals interactions which bind atoms together in liquid and solid states. This results in the Lennard-Jones Potential whose equation is given below. [46]

For two atoms (i and j) with location vectors of r_i and r_j the potential energy is given by:

$$u(r_{ij}) = \begin{cases} 4\epsilon \left[\left(\frac{\sigma}{r_{ij}} \right)^{12} - \left(\frac{\sigma}{r_{ij}} \right)^6 \right] & r_{ij} < r_c \\ 0 & r_{ij} \geq r_c \end{cases}$$

Where r_{ij} represents the absolute value of the difference between the location vectors.

The strength of the energy potential is represented by ϵ . A characteristic distance is represented by σ . Generally there is a “cut off radius” (r_c) beyond which the potential is taken to be zero. The cut off radius is typically 2.5σ to 5.0σ [47]. The potential is summed over all the involved molecular pairs. Techniques exist to adjust this calculation to abate the error caused by imposing a cut off radius

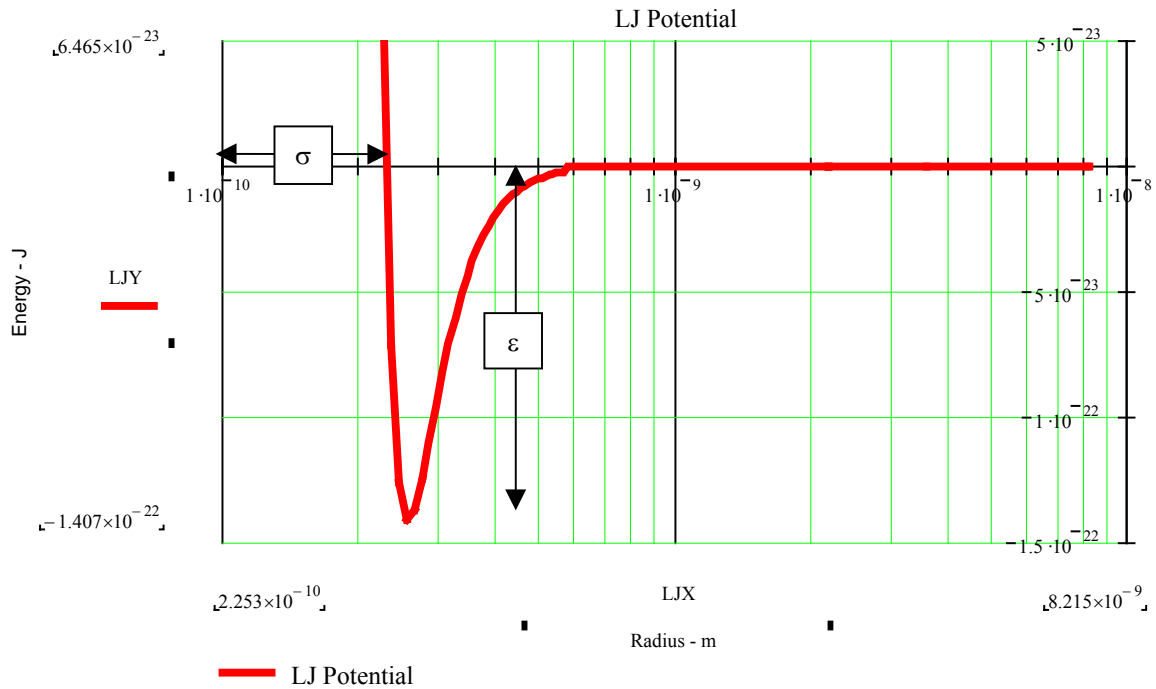


Figure 5 Plot of typical Lennard-Jones potential

The force associated with this potential is given by the gradient of the potential:

$$\mathbf{f} = -\nabla u(r)$$

Which yields:

$$\mathbf{f}_{ij} = \left(\frac{48\epsilon}{\sigma^2}\right) \left[\left(\frac{\sigma}{r_{ij}}\right)^{14} - \frac{1}{2} \left(\frac{\sigma}{r_{ij}}\right)^8 \right] \mathbf{r}_{ij}$$

Tersoff – Brenner Potential

The Tersoff – Brenner potential represents another attraction – repulsion model which is applicable to solids held in a lattice structure, such as body centered cubic or face centered cubic .[47] This potential would become involved if it were necessary to allow movement of the solid atoms in the model.

Surface Geometry Characteristics

The physical surface of the solid is of particular interest. The surface may be described a variety of ways, each of which will affect the outcome of the analysis. The following terms are defined for the purposes of this work:

Physically Irregular (macro scale): A surface may have machining grooves, grinding marks or other surface irregularities that exist on a scale of 100 micrometers or more.

Physically Irregular (micro scale): A surface may have polishing grooves or other surface irregularities that exist on a scale of 1 to 100 micrometers.

Physically Irregular (nano scale): A surface may have polishing grooves or other surface irregularities that exist on a scale of 100 to less than 1000 nanometers

Atomically Smooth: A surface may be prepared such that it represents a crystal plane cut, however with irregularities of + or – one atom.

Ideal Crystal Plane: A surface may be described as a perfect crystal plane.

Ideally Smooth Plane: A surface may be described as an ideally smooth perfect plane.

Surface Material Characteristics

Surfaces may or may not actually present the base material atoms as the material for impact.

Contaminated Surfaces : Contaminants may be present within the base material and present at the surface. Contaminants or Oxide Layers may have formed at the surface.

Electrolytically Polished Surfaces: Surfaces which have been electrolytically treated to remove material from the high points by the passage of an electric current to produce a smoother surface.

Adsorbed Layer Surfaces: Adsorption is the process by which molecules adhere to the surface of a solid. The term Physical Adsorption describes molecules held to the surface of the adsorbent by van der Waals forces [48]. It has been suggested that some materials assume a specific orientation upon adsorption [49] . In the case of noble gas atoms adsorbed onto metals, physical adsorption is the main form of interaction, and can result in spacing of the adsorbed atoms at distances other than the simple “sum of radii” spacing which might be expected [50] .

Ideally Clean Surfaces: If one assumes the surface is free of all contaminated and adsorbed atoms, the surface may be considered Ideally Clean. (However, even an ideally clean surface could have the impinging gas atoms or contaminant atoms adsorbed onto its surface and quickly become an Adsorbed Layer Surface.)

Velocity Distribution of Gas

Even when a volume of gas is at an equilibrium temperature, not all gas atoms have the same speed. Maxwell first solved the question of distribution of speed of a large number of atoms (or molecules) in a gas, yielding the following equations:

$$N(v) = 4\pi N(m/2\pi kT)^{3/2} v^2 e^{-mv^2/2kT}.$$

$$N = \int_0^{\infty} N(v) dv.$$

Here $N(v) dv$ is the number of molecules in the gas sample having speeds between v and $v+dv$.

Other factors are: k (Boltzmann's constant); T (absolute temperature) and m (mass of a molecule). N is the total number of molecules in the sample [24].

The result is not a symmetrical distribution about the mean. This is because there is a lower boundary to speed (zero), but no upper boundary. An example distribution of speeds for oxygen molecules is shown below.

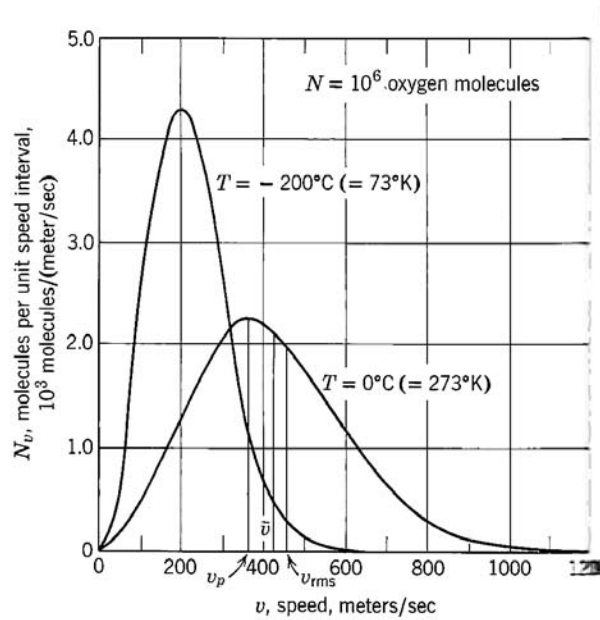


Figure 6 Example Maxwell Speed Distribution (Halliday)

Governing Equations

Newton's Laws of Motion

The primary equations which govern this work are Newton's first two laws of motion.

Newton's First Law states, "Every body persists in a state of rest or uniform motion in a straight line unless it is compelled to change that state by forces impressed upon it" [24]. This is the situation for the candidate gas molecule when it is outside the cut off radius of all other atoms.

Newton's Second Law states that the vector sum of all forces acting on a body are equal to the change in momentum (mass times velocity) with time. Since the mass of the atom is taken to be constant, this reduces to:

$$\sum_n \mathbf{F} := m \mathbf{a}$$

This is the situation for the candidate gas molecule which is within the cut off radius and is exposed to the sum of all the Lennard-Jones pair forces.

Lennard-Jones Potential

The previously stated Lennard-Jones energy potential equation and force equation are applied to determine the forces and energy.

$$u(r_{ij}) = \begin{cases} 4\epsilon \left[\left(\frac{\sigma}{r_{ij}} \right)^{12} - \left(\frac{\sigma}{r_{ij}} \right)^6 \right] & r_{ij} < r_c \\ 0 & r_{ij} \geq r_c \end{cases}$$

$$\mathbf{f}_{ij} = \left(\frac{48\epsilon}{\sigma^2} \right) \left[\left(\frac{\sigma}{r_{ij}} \right)^{14} - \frac{1}{2} \left(\frac{\sigma}{r_{ij}} \right)^8 \right] \mathbf{r}_{ij}$$

Composite Lennard-Jones Coefficients

For unlike molecules, the Lennard-Jones coefficients are determined as arithmetic and geometric means as follows [51]:

$$\sigma_{ij} = \frac{\sigma_i + \sigma_j}{2}$$
$$\varepsilon_{ij} = (\varepsilon_i \varepsilon_j)^{1/2}$$

Conservation of Energy

For conservation of energy, a molecule's energy is equal to the sum of its kinetic energy and its potential energy among all involved pairs.

$$E_i := \left[\frac{1}{2} \cdot m_i \cdot (V_i)^2 \right] + \sum_{(j \neq i)} \phi(r_{i,j})$$

CHAPTER THREE: LITERATURE REVIEW

Previous Experimental Works which provide TMAC Data

Experimental Work of Primary Interest - Seidl

A work of primary interest to the proposed work was performed by Seidl [33]. An electronic microbalance was used to measure the TMAC from a uniform molecular beam under a range of angles of approach. The fluxes of the tangential momenta of incident and scattered molecules were determined by measuring the force exerted from the molecular beam onto the plane specimen by means of a beam microbalance. In order to separate the normal and tangential forces, for each angle of incidence θ two measurements were carried out with different angles φ between molecular beam and beam of microbalance.

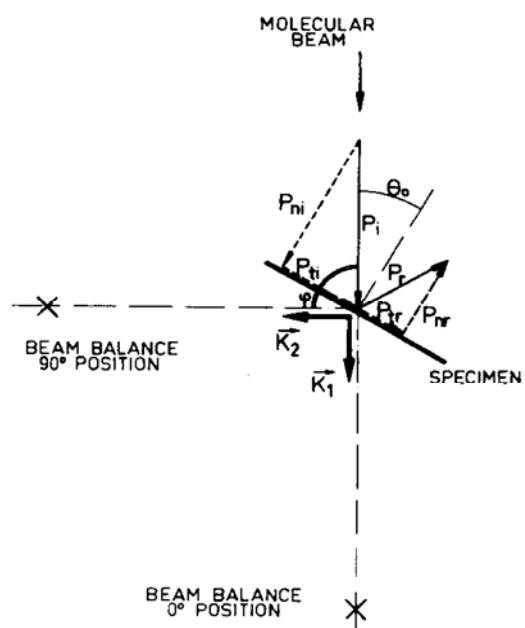


Figure 7 Seidl Experiment Apparatus

Much work was done with understanding the surface characteristics of the solid material, and altering the surface through various cleaning methods. The resulting data lends itself to this

work's plans to model this behavior in such a manner as to be able to estimate the TMAC for certain materials and conditions.

Pertinent data from Seidl are shown below:

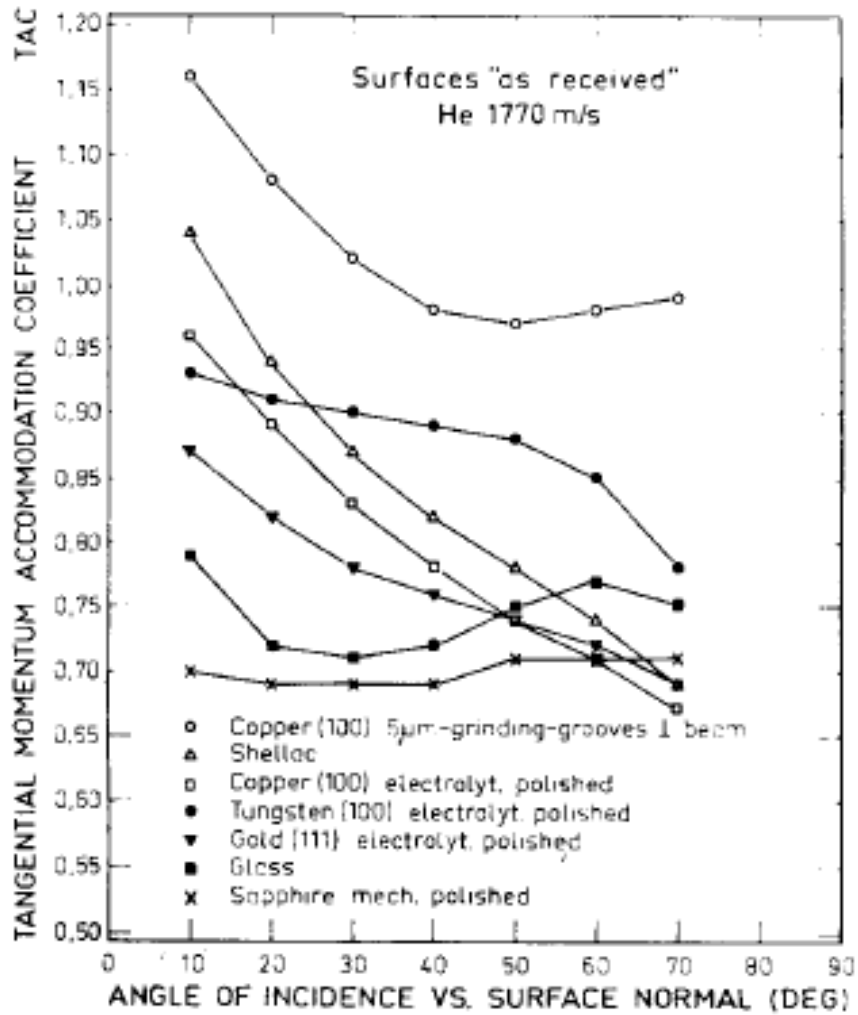
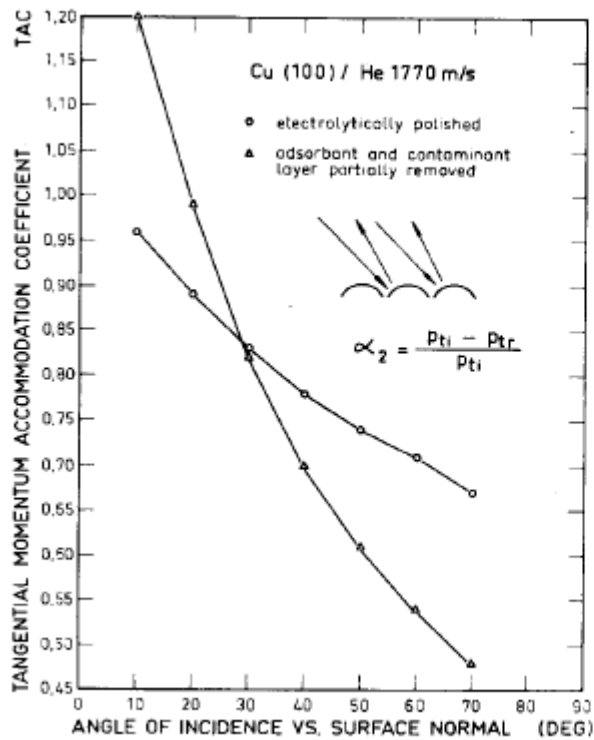


Figure 8 Seidl Experimental TMAC Data 1



Effect of surface cleaning on an atomically rough surface

Figure 9 Seidl Experimental TMAC Data 2

Based on the experimental methodology used and the data presented, it is planned to use certain data available from this paper as a validating method for the resulting model. Specifically the data given on Helium gas as it impacts upon Copper surfaces is of interest.

Experimental Works of Secondary Interest

In general, these works provide experimental data involving Helium gas, which provides background data for the proposed work.

Saltsburg

Saltsburg [52] also investigated molecular beam impacts upon surfaces. Their work included He impacts upon Ag surfaces at a variety of angles. The data was not presented in a way which allows ready evaluation of the TMAC. It does provide supplemental information and provides interesting insight into the effects of impacts upon surfaces which are at a different temperature than the gas.

Arkilic

Arkilic [9] performed an experiment which flowed Helium through a micro channel with the following characteristics:

Table 2 Arkilic

Parameter	Nominal Value(μm)	Variation(μm)
length (L)	7500	± 10
width (w)	52.25	± 0.25
height (H)	1.33	± 0.01
surface roughness	$\leq 0.65 \times 10^{-3}$	NA

The results of the experiment indicated a TMAC value of 1.

Liu

Liu et al [40] performed experiments to investigate satellite drag coefficients of He at 7,000 m/s impacting a cleaned aluminum (6051-T6) surface at varying angles of incidence. They determined that the TMAC was approximately 1 for all investigated angles.

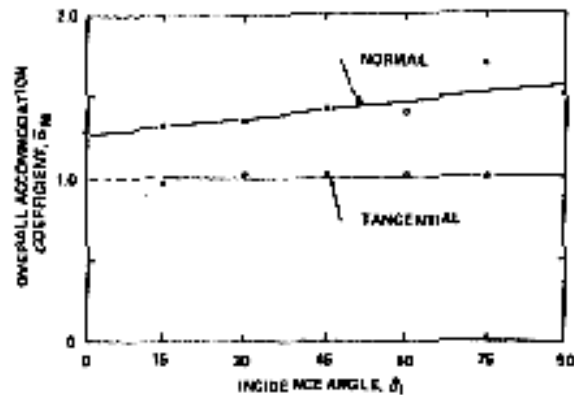


Fig. 6 Overall normal and tangential momentum accommodation coefficient as a function of incidence angle for cleaned 6051-T6 aluminum surface.

Figure 10 Liu TMAC Data

Boring

Boring et al performed experiments measuring at satellite orbital speeds (7 to 37 km/s) investigating momentum transfer. Surface conditions were not rigidly controlled. No TMAC data was presented [53].

Knetchtel

Knetchtel et al measured lift and drag forces on aluminum and gold surfaces inclined to a stream of argon ions. The TMAC was determined for a limited number of angles. The gas velocities used were all above 8000 m/s. (13eV for Argon is approximately 7800 m/s.) Shown in the figure below are plots of Argon ions impacting an aluminum surface. [37]

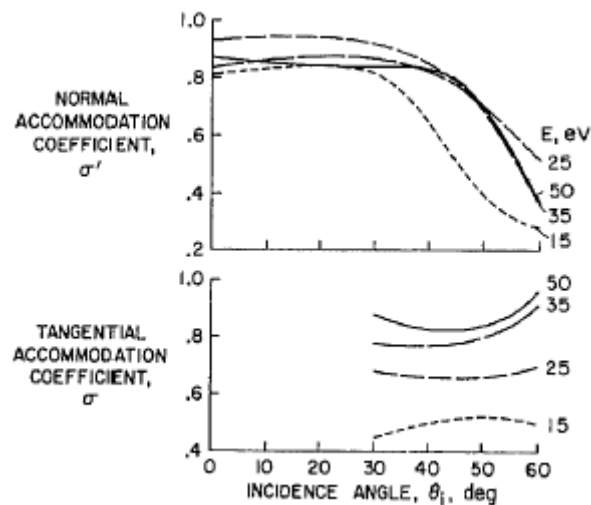


Figure 11 Knechtel TMAC Argon ion on Aluminum

Thomas

Thomas and Lord [34] experimentally determined Tangential Momentum (and Thermal) Accommodation Coefficients for polished and roughened steel balls. The ball was magnetically levitated in a rarefied gas and spun. The deceleration of the spin was observed and measured.

Therefore, instead of the gas flowing over the surface, the surface of the ball was moving with respect to the gas. The value of their TMAC was defined as the ratio of the observed angular deceleration to the calculated theoretical deceleration assuming all the molecules striking the surface are reemitted with the tangential velocity pertaining to the latitude on the sphere at which they impinge.

Table 3 Thomas

Steel Ball Dia	Surface Roughness	Gas	TMAC	Conditions
0.25 inches	0.1 μ rms	He	0.824	25 ° C, High Vacuum, (Kn approx = 1 to 5*)
0.25 inches	0.1 μ rms	Ne	0.918	25 ° C, High Vacuum, (Kn approx. = 1 to 5*)
0.25 inches	0.1 μ rms	Ar	0.931	25 ° C, High Vacuum, (Kn approx. = 1 to 5*)
0.25 inches	0.1 μ rms	Xe	0.943	25 ° C, High Vacuum, (Kn approx. = 1 to 5*)
0.25 inches	“roughened”	He	1.040	25 ° C, High Vacuum, (Kn approx. = 1 to 5*)
0.25 inches	“roughened”	Ne	1.035	25 ° C, High Vacuum, (Kn approx. = 1 to 5*)
0.25 inches	“roughened”	Ar	1.049	25 ° C, High Vacuum, (Kn approx. = 1 to 5*)
0.25 inches	“roughened”	Xe	1.075	25 ° C, High Vacuum, (Kn approx. = 1 to 5*)
				* Inferred from Thermal experiment data

In addition to the data, there are two additional topics of note in this work:

- The roughened steel balls displayed a TMAC greater than 1. Thomas investigated and concluded that the TMAC for these balls was indeed greater than 1 because of the extensive roughness.
- Both the polished and roughened steel balls were heated until oxidized and “blued”. This created a roughened oxidized surface on the previously polished and roughened balls. After “bluing”, the TMAC of the polished balls increased significantly (amount not stated). However, the roughened ball’s TMAC did not change significantly. This indicates that surface oxidation effects are significant in the context of highly polished surfaces, but are insignificant with respect to very rough surfaces.

Bentz and Gabis

Gabis et al used a spinning rotor gauge to measure TMAC of various gasses including Helium (approx 0.9) [54] .

Bentz et al [36] used a spinning rotor gauge to measure TMAC for N₂ (ranging from 0.83 to 0.89) and CH₄ (ranging from 0.98 to 1.11).

Suetin

Suetin [55] performed experiments in capillaries and observed that the TMAC is not only a function of Knudsen number. It is also a function of the gas type and surface type. They experimented with two packets of glass capillaries with molten walls. The length to diameter

ratio was 600. The deviation of radii among the capillaries was less than 2%. They used the experimental data to estimate the tangential momentum accommodation at the walls.

For free molecular flow, they obtained the following:

Table 4 Suetin

Suetin Results for Free Molecular Flow:	TMAC
Helium	0.935
Neon	0.929
Argon	0.975

For slip flow, they obtained the following:

Table 5 Suetin

Suetin Results for Viscous Slip Flow:	TMAC
Helium	0.895
Neon	0.865
Argon	0.919

Porodnov

Porodnov, Suetin, Borisov and Akinshin [39] conducted experiments on viscous slip flow and free molecular flow through slits and capillaries. They observed that channel flow conductivity

essentially depended on the channel surface roughness and on the kind of gas involved. Their data was analyzed for the case of flow through slits to yield the following:

Table 6 Porodnov

Gas	Flow Regime	Slit Material	Roughness Height (um)	Temperature K	TMAC
He	Free Molecular	Glass	1 - 5	293	0.961
He	Free Molecular	Glass	0.05	293	0.870
He	Free Molecular	Glass w/ oil film	--	293	0.857
He	Free Molecular	Flouro Plastic	1 - 5	293	1.059
Ne	Free Molecular	Glass	1 - 5	293	0.957
Ne	Free Molecular	Glass	0.05	293	0.847
Ne	Free Molecular	Glass w/ oil film	--	293	0.838
Ne	Free Molecular	Flouro Plastic	1 - 5	293	0.803
Ar	Free Molecular	Glass	1 - 5	293	0.934
Ar	Free Molecular	Glass	0.05	293	0.880
Ar	Free Molecular	Glass w/ oil film	--	293	0.926
Ar	Free Molecular	Flouro Plastic	1 - 5	293	0.919
Kr	Free Molecular	Glass	1 - 5	293	0.922
Kr	Free Molecular	Glass	0.05	293	0.904
Xe	Free Molecular	Glass	1 - 5	293	0.926
Xe	Free Molecular	Glass	0.05	293	0.908
H ₂	Free Molecular	Glass	1 - 5	293	0.969
H ₂	Free Molecular	Glass	0.05	293	0.911
H ₂	Free Molecular	Flouro Plastic	1 - 5	293	0.880
D	Free Molecular	Glass	1 - 5	293	0.949
D	Free Molecular	Glass	0.05	293	0.897
D	Free Molecular	Glass w/ oil film	--	293	0.844
D	Free Molecular	Flouro Plastic	1 - 5	293	0.911
CO ₂	Free Molecular	Glass	0.05	293	0.961

They present the following data for the viscous slip flow regime in capillaries:

Table 7 Porodnov

Gas	Flow Regime	Capillary Packet Material	Roughness Height (um)	Temperature K	TMAC
He	Viscous Slip	Glass	“molten walls”	293	0.895
He	Free Molecular	Glass	“molten walls”	293	0.935
Ne	Viscous Slip	Glass	“molten walls”	293	0.865
Ne	Free Molecular	Glass	“molten walls”	293	0.929
Ar	Viscous Slip	Glass	“molten walls”	293	0.927
Ar	Free Molecular	Glass	“molten walls”	293	0.975

Kr	Viscous Slip	Glass	“molten walls”	293	0.995
Xe	Viscous Slip	Glass	“molten walls”	293	1.010
H ₂	Viscous Slip	Glass	“molten walls”	293	0.957
D	Viscous Slip	Glass	“molten walls”	293	0.934
N ₂	Viscous Slip	Glass	“molten walls”	293	0.925
CO ₂	Viscous Slip	Glass	“molten walls”	293	0.993
He	Free Molecular	Glass	“molten walls”	293	0.870

Gas	Flow Regime	Capillary Sieve Material	Roughness Height (um)	Temperature K	TMAC
He	Free Molecular	Glass	“molten walls”	293	0.944
Ne	Free Molecular	Glass	“molten walls”	293	0.934
Ar	Free Molecular	Glass	“molten walls”	293	0.982
Kr	Free Molecular	Glass	“molten walls”	293	0.991
Xe	Free Molecular	Glass	“molten walls”	293	1.000
H ₂	Free Molecular	Glass	“molten walls”	293	0.976
D	Free Molecular	Glass	“molten walls”	293	0.969
N ₂	Free Molecular	Glass	“molten walls”	293	0.977
CH ₄	Free Molecular	Glass	“molten walls”	293	0.992
CO ₂	Free Molecular	Glass	“molten walls”	293	0.998

Lord

Lord [38] conducted experiments of TMAC on polycrystalline metal surfaces. What is interesting about these experiments is the methodology was used to prevent contamination from developing on the surfaces tested. Chemical getters (mischmetal or barium) were used to reduce the level of background contamination. Surfaces were cleaned using RF induction heating to heat just below the melting point of the material. The result was much different experimental values of the TMAC for cleaned vs. contaminated surfaces:

Table 8 Lord

Gas	Flow Regime	Material	Roughness Height (um)	Pressure	TMAC
He	Free Molecular	Mo metal foil, 25 um thick	Baked but unclean polycrystalline	A few milli torr	About 0.9
He	Free Molecular	Mo metal foil, 25 um thick	Cleaned polycrystalline	A few milli torr	0.20
Ne	Extrapolated to Free Molecular	Mo metal foil, 25 um thick	Cleaned polycrystalline	A few milli torr	0.31

A	Extrapolated to Free Molecular	Mo metal foil, 25 um thick	Cleaned polycrystalline	A few milli torr	0.67
Kr	Extrapolated to Free Molecular	Mo metal foil, 25 um thick	Cleaned polycrystalline	A few milli torr	0.85
Xe	Extrapolated to Free Molecular	Mo metal foil, 25 um thick	Cleaned polycrystalline	A few milli torr	0.95
He	Free Molecular	W metal foil, 25 um thick	Baked but unclean polycrystalline	A few milli torr	About 0.9
He	Free Molecular	W metal foil, 25 um thick	Cleaned polycrystalline	A few milli torr	0.35
He	Free Molecular	Ta metal foil, 25 um thick	Baked but unclean polycrystalline	A few milli torr	About 0.9
He	Free Molecular	Ta metal foil, 25 um thick	Cleaned polycrystalline	A few milli torr	0.46
Ne	Extrapolated to Free Molecular	Ta metal foil, 25 um thick	Cleaned polycrystalline	A few milli torr	0.59
A	Extrapolated to Free Molecular	Ta metal foil, 25 um thick	Cleaned polycrystalline	A few milli torr	0.78
Kr	Extrapolated to Free Molecular	Ta metal foil, 25 um thick	Cleaned polycrystalline	A few milli torr	0.85
He	Free Molecular	Pt metal foil, 25 um thick	Baked but unclean polycrystalline	A few milli torr	About 0.9
He	Free Molecular	Pt metal foil, 25 um thick	Cleaned polycrystalline	A few milli torr	0.35
He	Free Molecular	Ti metal foil, 25 um thick	Baked but unclean polycrystalline	A few milli torr	About 0.9
He	Free Molecular	Ti metal foil, 25 um thick	Cleaned polycrystalline	A few milli torr	0.38

Of interest was the observation that the TMAC generally increased with an increase in molecular weight of the gas. However, no correlation was made with any property of the surface material.

Maegley

Maegley [32] investigated flow through annuli over a range of Knudsen numbers from about 0.01 to 450. The experimental data was compared to theoretical flows based on a perfectly diffuse scattering of molecules at the surface. They developed a term “W” (reduced flow), defined as a dimensionless quantity – the ratio of the flow through the system to the free molecule flow through an orifice having the same cross sectional area and pressure drop. Then they developed the term “ $W/W_{o,d}$ ” (transport ratio) where $W_{o,d}$ is the theoretical free molecular transmission determined by diffuse scattering at the annulus walls.

Two of the key data graphs from the paper are shown below:

“Maegley Figure 2” shows how the transport ratio varies along the range of Knudsen numbers, and is different for He than for Ar.

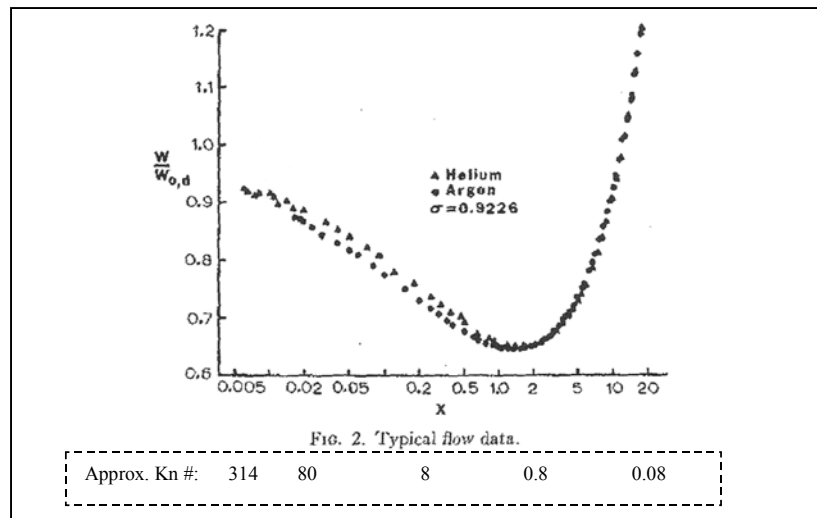


Figure 12 Maegley Data (figure 2 of reference)

“Maegley Figure 6” shows how the “reduced flow” term can be estimated more accurately if instead of pure diffuse reflection, diffuse plus a 6% backscattering term is included.

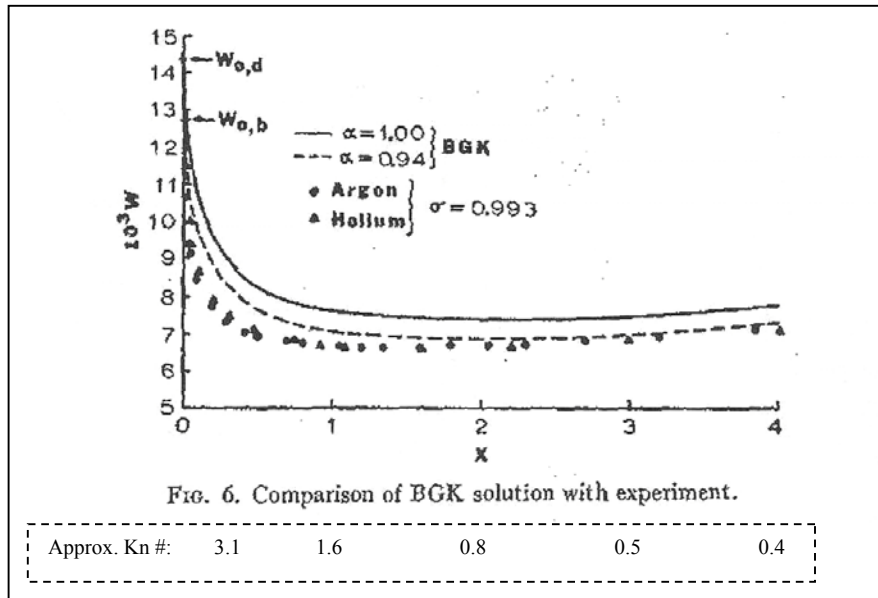


Figure 13 Maegley Data (figure 6 in reference)

They conclude that transmission probability is not independent of the gas type involved and that backscattering occurs because of the surface roughness effects of typical surfaces.

Other

Other experimental work has determined the TMAC of He in the range of 0.93 [56]; in the range of 1.0 [20] and (as a function of oxygen surface contamination) 0.71 to 0.96 [57].

Cooper et al investigated gas transport through carbon nanotubes and determined a TMAC value of 0.52 +/- 0.1 for argon, nitrogen and oxygen [58].

Jang et al investigated TMAC in glass and silicon microchannels cut by Deep Reactive ion Etching. The TMAC was found to be 0.204 for air flowing at atmospheric conditions [59].

Other work has been performed to experimentally determine NMAC as it relates to surface preparation and angle of incidence [60].

Previous Works which demonstrate need of a TMAC MD model

Logan

Logan [61] developed a classical model for the scattering of gas atoms from a solid surface.

Their initial classical model assumed that:

- The scattering pattern is 2-D, “in plane”.
- Both the gas and surface atoms are rigid elastic particles, with impulsive potential.
- Collisions with the surface do not change the tangential momentum component (smooth surface).
- Surface atoms are independent particles.
- Velocity distribution of the surface atoms is Maxwellian.

Since the Tangential component was assumed to be unchanged, the initial work was of most interest in analyzing the normal velocity components.

Subsequently, they introduced a surface roughness into the classical model with the following changes in assumptions:

- The scattering pattern was allowed to be 3-D to include “out of plane” scattering.
- The surface was not perfectly smooth.

Their results concluded that the principal parameters of the scattering distribution were:

- the incident angle, measured from the surface normal,
- the mass ratio of the gas atom to the surface atom
- the ratio of the mass of the surface atom multiplied by the temperature of the surface to the mass of the gas atom multiplied by the temperature of the gas.

For a fixed approach angle of 45 degrees, it was noted that in plane scattering increased with increasing asymmetrically with roughness. It is also noted that out of plane scattering increased symmetrically with increasing roughness. It was suggested that measurement of out of plane scattering could be useful as a way of measuring surface roughness.

No formal analysis of TMAC was performed.

Bird

G. A. Bird wrote, “Any physical model for the interaction of a molecule with a surface would have to be far more complex than the models that have been presented for intermolecular collisions in the gas phase. This applies even to the ideal case of a microscopically flat surface

with no adsorbed gas layer. There is no model of gas surface interactions that is adequate for quantitative studies over a wide range of parameters for all combinations of gases and surfaces, and it is unlikely that one will be forthcoming. If sufficient experimental data were to become available for a particular application, it could be used to determine the adjustable parameters of an empirical model that satisfies the physical constraints. In the absence of such a model, non-diffuse reflection has most frequently been represented by assuming some fraction ϵ of the molecules are reflected specularly, while the remainder are reflected diffusely. However, this model cannot reproduce the molecular beam data that has been obtained for the particular cases and there is no justification for the implicit assumption that the result should lie between the limits set by the completely diffuse and completely specular reflection. There is, therefore a need for a more general empirical model” [43]

Previous Analyses Involving TMAC

Molecular Dynamics Simulations

Molecular Dynamics (MD) simulations are a method to model micro systems on a molecular scale. Such micro-systems may have a large number of molecules, each with their initial conditions and do not lend themselves to an analytical solution. MD applies Newton’s laws with computer based integration methods, using finite difference equations to numerically solve such systems. Its primary applications involve systems where relativistic effects are not observed and

quantum effects can be incorporated as corrections. [The emerging field of computational nanotechnology is addressing these quantum effects [62].]

MD has proven itself over many decades of use, and continues to grow in use as computer capabilities and economies improve [63] .

MD simulations to date have frequently treated gas to surface impacts in an average sense and as a statistical notion [46]. Other MD simulations have investigated slip length using an assumed TMAC value of 1 [64].

Koplik, Banavar & Willemsen

Koplik, Banavar and Willemsen [65] used Molecular Dynamics to model Pouseuille Flow and Moving Contact Lines. A Lennard-Jones potential was used along with a cut off radius of 2.5σ . The wall molecules were modeled as two layers of very heavy molecules arranged in an FCC lattice. The wall molecule's mass was set to be 10^{10} the mass of the gas atom, thereby providing a means to conserve energy at impacts and also to hold the structure together for the duration of the simulation. The results were in accordance with bulk continuum flow, and gave the authors the confidence to continue exploring fluid flows with MD simulations.

(Although the next 5 papers are titled only by the name of the first author, it is worth noting that Banavar served as co-author on them all and Koplik was a frequent co-author.)

Yang

Yang et al [66] used Molecular Dynamics to model a drop of liquid spreading across a surface. This simulation resulted in wetting occurring in distinct layers. The layers were terraced and ordered, but not solid. Some of the vapor condensed on the solid surface before the drop spread and was rather “static.”

Koplik

Koplik et al [67] used Molecular Dynamics to model a liquid mixture with a “No Slip” condition at the wall. For the liquid conditions evaluated, no slip was confirmed for both liquid species present. The actual zero velocity was reached at a nominal wall position, which was described as within one or two atomic distances from the wall.

Koplik et al [68] also used Molecular Dynamics to model fluid wall interactions. The discussion recognizes that assuming perfectly specular or perfectly diffuse (or “thermal”) walls essentially assumes the answer. They discuss modeling of molecular walls four ways: (i) Fixed solid molecules located at the lattice sites, (ii) Replacing the discrete molecule centers of each solid plane by a continuous distribution of molecules with a uniform planar density, (iii) Replacing the continuously distributed wall with a Boltzman weighted wall, whose potential is proportional to the probability that a molecule is at a distance z from the surface and (iv) Where the wall potential is assumed to be infinite when a liquid molecule strays into the wall and zero otherwise. Their Molecular Dynamics wall were modeled essentially as (i) above (static / immovable, with molecules located at the lattice sites) because the mass of their solid molecule

was set to be 10^{10} time the mass of the liquid molecule. One of their findings was the formation of layered fluid molecules, at rest, adjacent to the walls – essentially a “no slip” condition at the boundary.

Cieplak

Cieplak et al [69] suggest an atomistic model of the fluid and the walls is useful for analyzing the boundary conditions at the surface. They found specular collisions and thermal (diffuse) collisions with the walls, determined primarily by the attractive component of the interactions. They focussed on purely repulsive walls by using a modified Lennard-Jones potential which allows adjustment to specify the attractive and repulsive nature of the walls. For the repulsive wall case an exclusion zone existed near the wall one or two atomic layers thick. The analysis included a collision kernel which predicts short collision residence times for specular collisions and long collision residence times for thermal (diffuse) collisions.

Cieplak et al [70] investigated boundary conditions at the fluid-solid surface. They found that slip increased with weakening wall-fluid attraction. Their MD analysis used two parallel walls and a modified Lennard-Jones potential which allows adjustment to specify the attractive and repulsive nature of the walls. The adjustment to create attractive and repulsive walls was an effort to model purely thermal (diffuse) and purely specular walls. For the attractive wall, fluid density at the wall surface established one layer of molecules in thickness, independent of density. A second layer also forms, although its was affected by fluid density.

Tomassone

Tomassone et al [71] used MD to evaluate the phase behavior of surfactants adsorbed on an interface for both soluble and insoluble situations. Their initial conclusion was that adjustment of the Lennard-Jones attraction -repulsion potential allows smooth and systematic modeling of the system properties.

Vergeles

Vergeles et al [72] used MD to study the motion of a sphere as it moved through a fluid and approached a wall. They used a Lennard Jones potential model and found that fluid molecules form well pronounced layers around diffusing particles that are quite stable.

Oman

Oman et al developed a numerical model of gas – surface interactions, calculating classical trajectories of gas molecules impacting crystal surfaces represented by point centers using a Lennard Jones potential model. The model assumed a single solid atom dominated the collision. It used a one atom repulsive potential and a composite potential from the field of atoms as the attractive potential. The effort modeled accommodation coefficients for energy, tangential momentum and normal momentum. Solid atoms were allowed to move to model the energy transfer. Computational limitations at that time also limited the number of gas and solid atoms involved so other simplifying techniques were incorporated. The model demonstrated that such

an MD model of gas – solid collisions can yield insight into the collision, that a number of collisions must be evaluated and averaged over a lattice spacing and the importance of the top surface layer of solid atoms in the interaction [73] .

The model was used for analysis of both energy and momentum accommodation study. Multiple gas atoms were averaged to determine the accommodation coefficients. No TMAC as a function of angle of impact was reported. However, TMAC values were shown to vary with azimuth angle for a type 100 crystal, with generally the closer packed planes having lower accommodation coefficient values. They suggest that the properties of an adsorbed layer play a dominating role momentum accommodation, with even one layer of adsorbent dominating. A phenomenological model was developed which assumes that if a gas atom experiences a second collision, it is fully accommodated [74] .

Knetchtel

Knetchtel et al developed a simplified model, approximating the surface with hard spheres and a one dimensional attractive field over the surface to represent the attraction of all surface atoms. A number of atoms were directed at the surface all at a fixed angle of incidence and the average momentum accommodation calculated.. Results were compared to experimental data of N_2^+ ions on aluminum. In general, the magnitudes of the data did not reliably compare well with the model. For some data sets the general trend for the data was in agreement. Agreement was generally better for NMAC than for TMAC [75] . They suggest that modeling of TMAC requires a three dimensional model

Finger

Finger et al developed the work described in this Dissertation, which was accepted for presentation at the 44th AIAA Aerospace Sciences Meeting [76] .

Monte Carlo Simulations

A method known as Direct Simulation Monte Carlo (DSMC) provides a particle based, numerical technique for solving the Boltzman Equation. Over the past 20 years, it has shown to have good applicability in the non-continuum regimes and can be much faster than the Molecular Dynamics method.

Collisions among gas particles are determined based on being located within the same evaluation cell. At each time step, particles within an evaluation cell are randomly selected for a collision. DSMC uses scattering rates and post collision velocity distributions to simulate the collision results. For gas to wall surface interactions, the TMAC is used within a probability algorithm (“scattering kernel”) to determine the outcome of the collision. A single gas particle is used as a representative for many others, reducing the sample size involved in the calculation [16]. DSMC simulations of such flows frequently assume a TMAC value of 1 in the absence of other data [77], [78], [79]. Other DMAC simulations use multiple analyses at multiple specified TMAC values, such as 0.5, 0.8 and 1.0 [80] . Similar DSMC modeling has been performed for gases impacting solid particles in a rarefied flows, such as solid rocket motor exhaust. Model assumptions effectively establish surrogate TMAC [81] [82] .

Other Numerical Models

Other numerical models have been developed.

Beskok has developed simulation models of heat and momentum transfer using a “spectral element technique.” These models have assumed a TMAC value of 1 for the calculations, although they acknowledge that other values may be more appropriate [83] [17].

Tang et al performed a study of gas flows in MEMS using the Lattice Boltzmann method. This model used an assumed “reflection coefficient” of 0.7 to take into account the differences between specular and “bounce back” wall surfaces [84] .

Jie et al performed Navier-Stokes simulations of gas flow in microdevices. These simulations assumed a TMAC of 0.8 for the calculations, acknowledging TMAC values are typically in the 0.2 to 0.8 range [85] .

Raju et al performed a numerical study of flow in a microchannel. Their study assumed a TMAC of 0.0 for an entrance length and a TMAC of 1.0 for the rest of the domain [86] .

Analytical Models

Logan [61] proposed and later updated a closed form analytical model for the scattering of gas atoms from a solid surface. Their initial model assumed that the surface was perfectly smooth and that collisions did not change the tangential component of the gas atom. A stationary potential well was used for the attractive solid potential. A later model included provisions for surface irregularities, which did provide for tangential component change. Their models did not take into account the possibility that more than one surface atom is included in the collision and did not include provisions for the gas atom to have multiple collisions with the solid. The results of their analytical model were not presented in terms of TMAC.

Ebert [87] performed an analytical evaluation of Slip Flow in ducts, using assumed values of 0.9 to 1.0 for the TMAC.

Morini [88] performed an analytical analysis of Slip Flow in micro tubes. Their analysis included a factor for TMAC and advised it was usually taken as 1.

Shapiro [89] Performed an analytical analysis of rarefied gas flow in channels, using a TMAC of approximately 1.

Barber et al [90] performed an analytical solution of flow past a sphere taking into account slip flow and the TMAC. However, the TMAC was assumed to be a value of 1.

Martin et al performed analysis of a Blasius boundary layer, using a technique which combined TMAC with other factors to define a non dimensional parameter. Results were in terms of this parameter and therefore do not directly yield TMAC values [91] .

Goodman developed a three dimensional hard sphere model of the interaction of monatomic gasses with surfaces which indicated some variation of TMAC with angle of impact [92] .

Jackson also developed a hard sphere model involving an ideal crystal surface with solid atoms at rest. Analyses were performed at varying angles and Energy Ratios, which indicated variable TMAC with both angle and ER [93] .

Epstein performed an analysis of an accommodation coefficient, concluding that the accommodation coefficient was substantially influenced by particle velocity [94] .

CHAPTER FOUR: METHODOLOGY

Objective

It has been clearly shown in the previous sections that the Tangential Momentum Accommodation Coefficient (TMAC) is used in many important analyses to predict and analyze flow of gases in the slip flow regime.

It is also evident from the previous work that today TMAC values are regularly assumed or approximated because no methodology exists to estimate or predict TMAC based on the mechanisms involved in the momentum transfer among rare gas and solid surface interactions.

Many experiments are performed to quantify the TMAC values because no methodology exists to predict a TMAC for a given set of conditions. Widely varying TMAC values are given sometimes without the complementary understanding of why they vary.

It is therefore concluded, based on the work previously done that a molecular dynamics simulation tool, which seeks to model the rare gas to solid surface interaction could be used to estimate the appropriate TMAC values to be used in predictive calculations for such applications in spaceflight, micro channels and assist in understanding the mechanisms for heat transfer.

The proposed work for this research was to:

“Develop a simple free molecular regime deterministic simulation model which can be used to estimate the TMAC of rare gas (He) to solid surface interactions, for a given set of conditions. (It is specified for this initial work that no heat (energy) transfer takes place across the boundary or, in other words, an adiabatic approximation is used. Such an approximation has been used in the past for lattice – electron interaction [95] .) Validate the model with data from prior experimental work. Revise and expand the model, as required, based on this and other validation data. Using the validated model, conduct simulations to draw conclusions about the various physical characteristics which may affect TMAC values for a specific application.”

Simplifying Assumptions and Their Justification

Simplifying assumptions for this model include:

A single gas atom is involved in each gas-to-solid interaction: The gas is specified to be sufficiently rare that during the gas to solid interaction, no other gas molecules influence the interaction.

Adiabatic Approximation is used: No energy transfer take place across the boundary. Internal vibrations of the solid are neglected. The gas and solid are specified to be at the same temperature. Solid atoms are assumed to be fixed in place.

Surface relaxation of the solid is neglected: It is assumed that the effects of relaxation of the metal crystal surface are small enough to be neglected.

Assumption: A Single Gas Atom is Involved in each Gas-to-Solid Interaction

The model begins and ends the gas atom on the order of 0.1λ (one tenth of a mean free path) from the surface of the solid. Therefore, the gas is sufficiently rare that during the entire gas to solid interaction that no other gas molecules are likely to influence the interaction.

Assumption: Adiabatic Approximation is used

It is specified for this initial work that no heat (energy) transfer takes place across the boundary or, in other words, an adiabatic approximation is used. Such an approximation has been used in the past for lattice – electron interaction [95] .

MD fluid –solid simulations by Banavar et al [68] [72] neglected solid atom motion (including vibrations) by setting the mass of the solid atoms as 10^{10} times the mass of the gas atoms. In this way the solid atoms were effectively fixed in space for the short time period of their MD simulations.

The following discussions explore why continued use of fixed solid atoms is also applicable for this particular MD simulation.

Justification Technique Based Debye Frequency:

In the development of the understanding of Heat Capacity of solids, Dulong & Petit first suggested that Heat Capacity of a monatomic crystal was a function of Boltzmann's constant and independent of temperature. However, the Dulong & Petit model breaks down at lower

temperatures. Einstein introduced the concept of quantization of energy levels for the atoms in a solid, where the energy level was a function of Planck's constant, the frequency of vibration and the energy state. At low temperatures this model has the effect to reduce the Heat Capacity more in agreement with the experimental data. However it over corrects and predicts an early decline in Heat Capacity. Debye suggested that the vibrations have a specific number of mode shapes and characteristic frequencies, superimposed on each other. There is a cut off frequency (ν) which is expressed in terms of a "Debye Temperature" (Θ_d), such that energy of the maximum frequency of the modes is related to that temperature. [96] [97] This is expressed as:

$$\nu := \frac{\Theta_d \cdot k_b}{h}$$

Where h is Planck's constant and k_b is Boltzmann's constant.

Typical Debye Temperatures for different crystal structures are:

Copper	$\Theta_d = 339 \text{ K}$ [98]
Aluminum	$\Theta_d = 418 \text{ K}$ [98]
Carbon (Diamond)	$\Theta_d = 3000 \text{ K}$ [96]

This yields Debye cut off frequencies (and periods of vibration) for these same materials of:

Copper	$\nu = 7 \times 10^{12} \text{ Hz}$	Period = $1.4 \times 10^{-13} \text{ s}$
Aluminum	$\nu = 9 \times 10^{12} \text{ Hz}$	Period = $1.1 \times 10^{-13} \text{ s}$
Carbon (Diamond)	$\nu = 6 \times 10^{13} \text{ Hz}$	Period = $1.6 \times 10^{-14} \text{ s}$

Therefore, the periods of vibration of the solid atoms in crystal lattices are on the order of 10^{-13} s to 10^{-14} s. If the period during which a collision takes place is less than or equal to this vibration period, it is possible that the gas atom could be significantly affected by the motion of the solid

atom. However, if the collision period is many times this solid vibration period, then it is expected that the solid atom completes many cycles during the collisions and its effects are averaged out.

For the analyses performed in this investigation, we consider the period of collision to be the time the gas atom is within the cut off radius. Typical time steps for the MD analyses performed are on the order of 10^{-15} s, with collisions periods usually involving more than 1000 time steps. This leads to a typical period of collision on the order of 10^{-12} s, which is one or two orders of magnitude greater than the vibration period of the solid atoms. Therefore, the solid vibrations would be expected to result in no more than a first order error and may be neglected for this analysis.

Justification Technique Based on Other Lattice Vibration Frequencies:

Other vibration spectra of many materials have been analyzed and the frequencies reported. These include “Acoustic Modes” in the general group velocity of sound and “Optical Modes” with frequencies in the infrared and can be excited by light. Reports of these frequencies [99] and their corresponding periods are shown below:

Carbon (Transverse Acoustical)	$\nu = 2.4 \times 10^{13}$ Hz	Period = 4.1×10^{-14} s
Carbon (Transverse Optical)	$\nu = 3.9 \times 10^{13}$ Hz	Period = 2.5×10^{-14} s
Silicon (Transverse Acoustical)	$\nu = 4.4 \times 10^{12}$ Hz	Period = 2.3×10^{-13} s
Silicon (Transverse Optical)	$\nu = 1.6 \times 10^{13}$ Hz	Period = 6.3×10^{-14} s

Note that these frequencies are of the same order of magnitude as the Debye Frequencies and therefore lead to the same conclusion that the solid vibrations may be neglected for this analysis.

Supplemental Discussion Based on Number of Solid Atoms:

Another related analysis examines the number of solid atoms involved in a typical collision. As the gas atom approaches the solid, the number of solid atoms within the cut off radius increases to a large number. At the time of closest approach, typically 30 or 40 solid atoms contribute forces which when summed together affect the gas atom. It would be required for all or most of these solid atoms to vibrate “in phase” to provide a large effect on the gas atom. Therefore, if they each move independently, it is unlikely that they would be "in phase" and would not present a significant effect. However, the solid atoms are in a 3 dimensional array with multiple mode shapes. In fact, large regions of the lattice can move together coherently, especially at lower frequencies. [98] Therefore it is possible that all moving together coherently could have some first order effect, but this was not further considered further, based on the period of vibration discussion given above.

Assumption: Surface Relaxation and Rumpling of the Solid are Neglected

At a horizontal surface of metal crystals, the vertical atomic spacing slightly changes. “Surface Relaxation” is defined as the difference of the average vertical distance of one layer of atoms to the adjacent layer, expressed as a percent. For a Cu (100) surface, the experimental values for relaxation are about –1% to –2%, indicating a slight shrinkage of the vertical crystal spacing [100] [101] .

Similarly, for contaminant imbedded in that surface, there exists a difference between the mean vertical position of the metal atoms and that of the contaminant atom (“rumpling”). Data for an Oxygen atom in a Mg (100) crystal indicate a Rumpling of +0.6% to +1.1%, indicating slight expansion of the vertical spacing [102] .

Since these percentages are small and to a certain extent self canceling, they are not considered further for this work.

Quantitative Values Used

Lennard – Jones Coefficient Values

The following Lennard – Jones coefficient values were used [103] [104]. The Lennard – Jones energy value (ϵ) is given in various forms, but converted to Joules (J) for this work:

Table 9 Lennard Jones Coefficients

Atom	σ	ϵ (as used)	ϵ (as given)	Data Source
Carbon	3.35×10^{-10} m	7.2×10^{-22} J	51.2 K (ϵ/k_B)	Tildesley & Madden 1981
Copper	2.3×10^{-10} m	9.3×10^{-20} J	3.5 eV ($e_b: \epsilon*6$)	Hess and Kroger, 2002
Hydrogen	2.81×10^{-10} m	1.2×10^{-22} J	8.6 K (ϵ/k_B)	Murad and Gubbins 1978
Helium	2.28×10^{-10} m	1.4×10^{-22} J	10.2 K (ϵ/k_B)	Maitland et al 1981
Oxygen	2.95×10^{-10} m	8.6×10^{-22} J	61.6 K (ϵ/k_B)	English and Venables 1974

Cut Off Radius

The “Cut off Radius” (R_c) is the nondimensionalized distance beyond which Lennard – Jones potentials and forces are neglected. In MD texts, it is recommended to set $R_c = 2.5$, where the

interaction energy is 0.016 of the well depth [46] . In MD simulations by Banavar and others involving fluid and solid interactions an $R_c = 2.5$ is also commonly used [68, 71].

For many MD simulations we are dealing with gas atoms spread out over a large volume. Few atoms are typically involved close to the cut off radius at any given time step. Neglecting the occasional atom at a distance has a small effect. However in simulations involving an interaction with a solid, there are numerous time steps in succession with many solid atoms lying just outside of this arbitrary cut off radius. Their cumulative effect on the dynamics of the gas atom may be significant. For this work, we are interested in these interactions at the solid surface, which may have dense solid atoms and additional layers of contaminants. Therefore the cumulative effect of this error could be significant.

In order to assess the effect of varying the Cut Off radius, a series of simulations was run with a solid 5 atomic layers deep by 3 atomic layers wide. The TMAC was evaluated at a fixed angle of approach for R_c varying from 1.5 to 4.5. Error was evaluated for each of the runs in comparison to the value determined with the R_c of 4.5 The results are shown below:

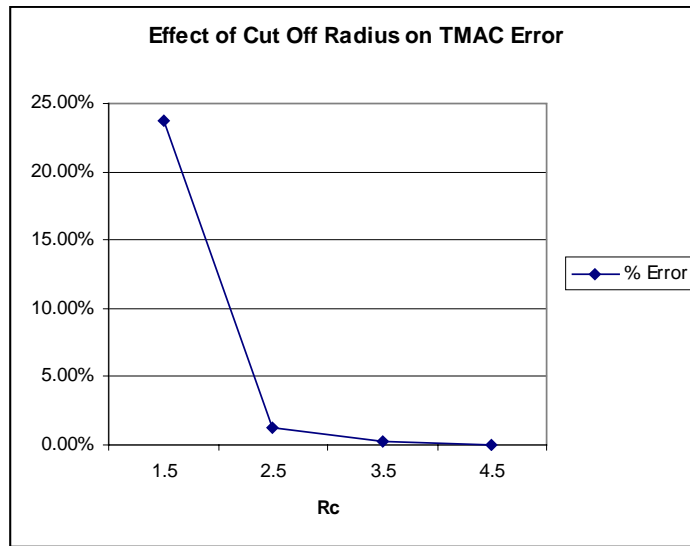


Figure 14 Effect of Cut Off Radius on TMAC Error

In order to make a judgement about what to select as a practical Rc, the number of solid atoms involved in each interaction was evaluated as a function of Rc, as shown below:

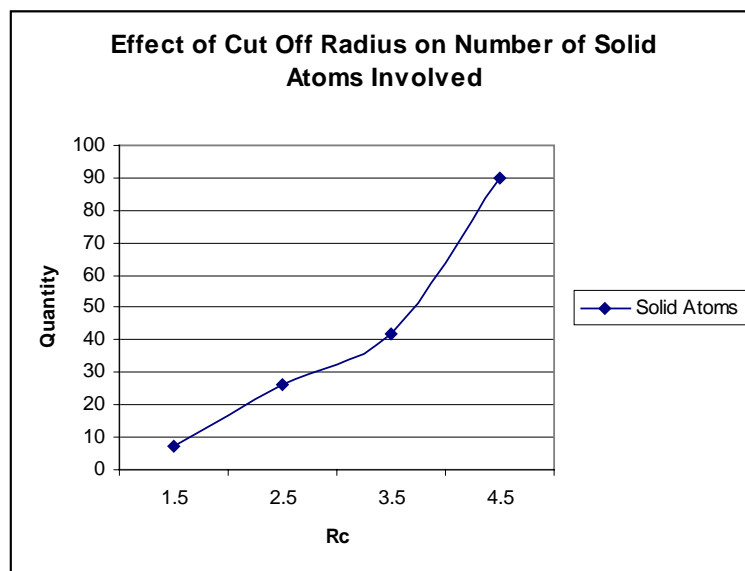


Figure 15 Effect of Cut Off Radius on Number of Solid Atoms Involved

Each increase in the number of solid atoms increases the accuracy, but also adds to the calculation time for the simulation.

Therefore, as a practical matter the cut off radius for this analysis was set to $R_c=3.5$, accepting an error of less than 1%.

Natural Time Unit and Time Step

The “Natural Time Unit” of this simulation is:

$$\tau := \left(\frac{m \cdot \sigma^2}{\varepsilon} \right)^{\frac{1}{2}}$$

Where τ is the Natural Time Unit, σ is the Lennard – Jones gas length, m is the mass of the gas atom and ε is the composite Lennard – Jones energy of the interaction. The Natural Time Unit for the Helium – Copper interaction is 1.3×10^{-12} seconds. Surface contaminants would change it slightly.

The Time Step used in the MD simulation is a fraction of the Natural Time Unit of the interaction. In MD texts, it is considered over the range of 0.001τ to 0.005τ [46]. In MD simulations by Banavar and others a time step of 0.005τ is also commonly used [68, 71].

For this simulation a Time Step of 0.0005τ was typically used to minimize error of the integration method incorporated into the simulation.

Convergence of the Numerical Solution

For each of the 500 gas molecules impacting the solid in a simulation run, the initial and final kinetic energy was compared and verified to be conserved. A typical conservation of energy plot is shown in Fig 29. As shown in the plot, the simulation conserves energy for each of the gas molecules to 3rd order or greater accuracy, even after thousands of time steps.

Convergence of the TMAC estimate and Conservation of Energy was tested as a function of Time Step. The simulation quickly converges for appropriate Time Steps, as shown in Table 10.

Table 10 Typical MD Simulation Convergence

Typical MD Simulation Convergence		
Time Step	%Variation from Base TMAC Estimate (Error)	Conservation of Energy, worst gas atom
0.10 τ	Does not Converge	-
0.05 τ	0.3714	10%
0.025 τ	0.0103	92%
0.010 τ	0.0005	99.8%
0.001 τ	0.0000	99.996%
0.0001 τ	0.0000	99.99985%
0.00001 τ	Base TMAC Value	99.99999%

Based on this analysis, the typical Time Step used was 0.0005 τ . This value is well within the convergence range and typically introduces error of less than 3rd order.

Time Step Cut Off and Bounce Cut Off

Occasionally a gas atom will undertake a long series of collisions with the solid. Rather than calculate through 20 or more collisions, it is terminated after certain number of collisions (or a certain number of Time Steps). The future path of the gas molecule is assumed to be completely randomized. The MD calculation is terminated for that atom and the gas atom is assigned the average Tangential velocity of a random atom leaving the surface (zero) and a normal velocity equal to that required to maintain conservation of Kinetic Energy.

In order to understand the effect of this process better, a sample set of MD simulations were run under conditions which did result in a large number of multiple collisions, so that this 1% limit was greatly exceeded. A series of 500 gas atoms were impacted upon a solid surface at a fixed angle of approach. The Bounce and Time Step limits were changed over the multiple runs in order to evaluate the effect, which is shown below:

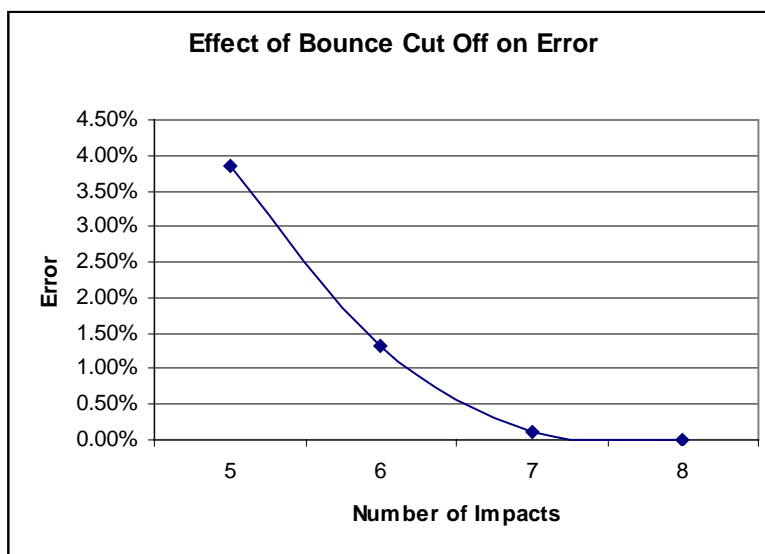


Figure 16 Effect of Bounce Cut Off on Error

It is interesting to note that even after 5 or 6 successive impacts, some effect on tangential momentum remains, and arbitrarily termination of the tangential momentum can introduce significant error.

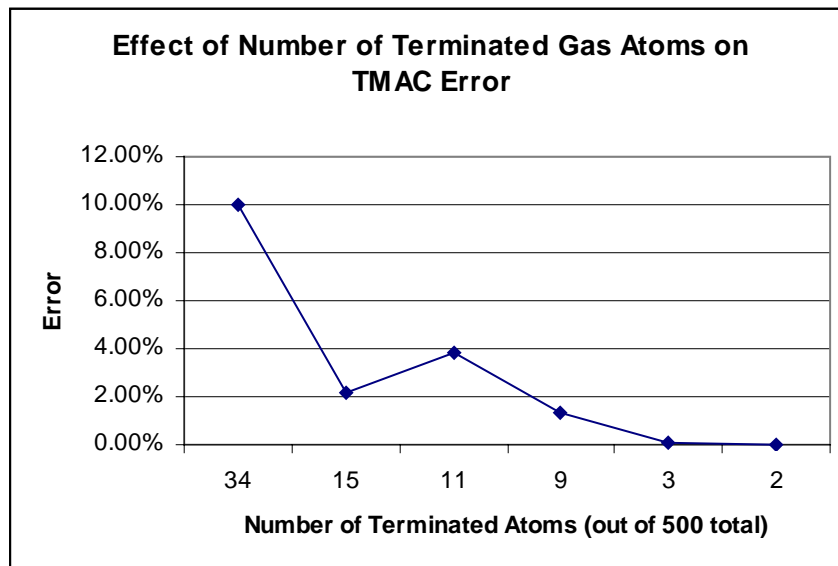


Figure 17 Effect of Terminated Gas Atoms on TMAC Error

Again, it is interesting to note that terminating less than 10% of the atoms can result in a 10% error. This means we have to be very careful with any MD terminating function with these analyses and maintain a very low amount of terminated atoms.

Therefore, the Time Step Cutoff (varies: 15,000 to 75,000 time steps) and the Bounce Cutoff (nominally 6 bounces) were selected and varied to result in less than 1% of the involved gas atoms being affected, thereby limiting this error.

Gas Starting Height and Mean Free Path

It is important for the gas atom to start its travel toward the solid surface from a distance greater than the Cutoff Radius. Likewise, the MD simulation proceeds until the gas atom has again moved outside the Cutoff Radius from all the solid atoms. In this manner the complete interaction is evaluated. Therefore, the starting height above the solid for the simulation was set greater than the Cutoff Radius.

For some MD runs, nanoscale surface irregularities were created. This necessitated increasing the starting height slightly to assure the Cutoff Radius distance minimum would be maintained.

A logical question relates to what is the appropriate Mean Free Path, appropriate characteristic length and resulting Knudsen Number for these simulations.

- Mean Free Path:
 - The Mean Free Path is implied to be larger than the Cutoff Radius: ($\lambda > R_c$).
 - The Mean Free Path was previously specified to be an order of magnitude greater than the starting height. ($\lambda > 10 * \text{Height}$).
- The candidate Characteristic Lengths include
 - Cut Off Radius (R_c)
 - Atomic lattice spacing (order of R_c)
 - Starting Height (order of R_c)
 - Average distance between surface irregularities (order of R_c)

- Overall length of solid model surface (order of 10 times R_c)
- Mean Free Path (order of 10 times R_c)
- The Knudsen Number (Ratio of λ / Characteristic Length) for these MD analyses is therefore:
 - $Kn > 1$.

Limitations of the Model

The following Model Limitations exist for the reasons stated:

Simulation is limited a 2-D model: The actual gas to solid interaction events are 3-D. In order to manage computer time the initial simulation is created as a 2-D model.

Simulation does not model making or breaking of atomic bonds: The model is not intended to model effects such as making or breaking of atomic bonds. It is a collision type model to aid in the understanding of TMAC.

Development of the MD Simulation Model

The following Technical Approach was used to develop the MD model.

Technical Approach to MD Simulation Model

Main Issues in Computer Simulations

Landman et al [105] outlines the main issues in developing computer simulations, which are:

1. “The faithfulness of the simulation model, focusing mainly on our knowledge of the interaction potentials
2. The spatial dimension, i.e. finite size of the computational cell and imposed periodic boundary conditions in the case of simulations of extended systems
3. The finite time span of the simulation”

Each of these were considered early in the process to avoid creating fundamental problems with the simulation. The following risk management measures were used to abate problems with the model:

- The interaction potentials were modeled using Lennard-Jones, the most widely used and understood of the potential models.
- The subject to be modeled was verified to be of small enough size so that the spatial dimensions were manageable. Additionally, their repetitive nature of the crystal solid allowed reintroduction of the moving atoms at the opposite side to extend the useful solid length dimension.
- The time period involved in these impacts was verified to be sufficiently small that the entire collision can be modeled from the time the moving atom enters the cut off radius, until the time it leaves the cut off radius.

Select Software

Specify Mathcad: Mathcad was selected as the software to use because it is already on my computers at work, at home and on my laptop for travel. To date, Mathcad has not presented limitations which affect the outcome of the work.

Other numerical simulations of free molecular flows have been performed using similar commercial off the shelf programming software such as MATLAB [106] .

Gather the Key Input Data

Specify the type of MD analysis: Currently the only option is a “Directed Beam” analysis, where the angle of incidence of the gas atoms and their velocity are specified. (Follow on work could include an analysis option for a “Flow with Temperature Distribution.” This will require input of a gas temperature and a gas flow velocity.)

Specify the static material & geometric characteristics: Specify the gas and solid materials involved; specify the type of solid crystal involved; specify the crystal cutting plane; specify the special surface characteristics of the solid.

Specify the dynamic characteristics: Specify the average gas atom’s initial position and velocity vector (if “Directed Beam”). Specify the average atom’s temperature and the average gas flow velocity (if “Flow with Temperature Distribution”)

Set the limits of the MD analysis: Set the number of gas atoms to be involved; cut off radius desired; time step factor desired; the height above the solid each gas atom starts its evaluation and the maximum number of time steps allowed for each gas atom desired.

Setup Variables for MD Simulation

Generate the Gas and Solid properties: Based on the gas and solid materials involved, lookup the Lennard-Jones coefficients (ϵ and σ); lookup the atomic mass, lookup the atomic radius. Such data is available from the following key references: [103], [104], [51] .

Calculate variables required for simulation: Calculate the composite Lennard-Jones values; the time scale; the cut off radius; define the Lennard-Jones potential expression, the Lennard-Jones gradient (force) expression; check plot.

Calculate the initial conditions for the gas atoms: For each gas atom calculate its initial position. Vertically, this is set to be one mean free path above the highest point of the solid surface. Horizontally, in order to distribute the gas atoms along the solid's lattice distance each gas atom is equally spaced such that typically two lattice distances are covered.

Calculate the initial conditions for the solid atoms

For each solid atom, calculate its x, y and z position in space according to the crystal structure (FCC or BCC) and cutting plane (111 or 100) specified. Relaxation effects are neglected [107].

Locate extra solid molecules above the crystal plane as required to simulate irregular surfaces.

Check plot the solid in plan, elevation and section.

Run the MD Simulation for each gas atom

Sum of Forces: For each time step, evaluate the gas atom's position with respect to each of the atoms in the solid surface. If its separation distance is less than the cut off radius, calculate the Lennard-Jones potential and force. Sum over all involved solid atoms for the gas atom.

F=ma: Using to forces summed above and the mass of the gas atom, calculate the acceleration on the gas atom.

Calculate new position and velocity. Based on the acceleration and using step wise integration (second order accurate in space), calculate the new position and velocity at the completion of the time step.

Save the data. Save the time step, force, position, velocity and acceleration data within Mathcad for later plotting.

Analyze and Post Process the MD Model Data

Check plots: For selected gas atoms, check plot the positions, velocities, accelerations, Lennard-Jones potentials, Lennard-Jones forces. total energy and number of atoms within the cut off radius at each time step. Visually review for reasonableness.

Perform Energy Checks

Energy (kinetic): For all gas atoms, calculate and plot the ratio of kinetic energy (final time step / initial time step) on an individual and moving average basis. Set the moving average amount equal to the number of gas atoms spread across one lattice distance. Kinetic energy should be conserved. The ratio should be close to one. If not, it is an indicator of too large a time step or other errors in the simulation.

Perform Momentum Analyses and Checks

Momentum (normal): For all gas atoms, calculate and plot the ratio of normal momentum (final time step / initial time step) on an individual and moving average basis. Set the moving average amount equal to the number of gas atoms spread across one lattice distance. Check to see if the moving average and total averages have stabilized or need more atoms in the sample to do so.

Momentum (tangential): For all gas atoms, calculate and plot the ratio of tangential momentum (final time step / initial time step) on an individual and moving average basis. Set the moving average amount equal to the number of gas atoms spread across one lattice distance. Check to

see if the moving average and total averages have stabilized or need more atoms in the sample to do so.

Estimate TMAC: The moving average or total average of the Tangential Momentum ratio calculated above represents the portion of the tangential momentum which was maintained in the gas and not transferred to the wall. This represents the incomplete momentum transfer portion.

$$\text{TMAC} := \frac{\sum_N m \cdot V_i - \sum_N m \cdot V_f}{\sum_N m \cdot V_i}$$

Therefore, the TMAC is estimated as 1 minus this average ratio.

$$\text{TMAC} = 1 - \frac{\sum_N m \cdot V_f}{\sum_N m \cdot V_i}$$

Visualization Plots: For numerous gas atoms, plot their path for visual confirmation and understanding of the process taking place.

Technical Approach to Design of the Experiments

General Topics in TMAC Experiment Design

According to Barber and Emerson [19], experiments indicate the TMAC is a substantially a function of the following:

- Molecular weight of the gas
- Energy of the incoming molecules
- Wall material
- Temperature of the surface
- Condition (roughness) of the surface

To investigate TMAC in a rational manner, while managing the total combinations of influencing factors, the following approach was used:

Utilize Energy Ratio as a way to evaluate three factors simultaneously: The first three items (molecular weight of the gas, gas energy and wall material) are all considered simultaneously in the term “Energy Ratio”. The Energy Ratio (ER) is defined as the ratio of the gas atom’s kinetic energy to the Lennard Jones energy constant (ε):

$$ER := \frac{\frac{1}{2} \cdot m \cdot V^2}{\varepsilon}$$

Where m is the molecular weight of the gas, the numerator is the kinetic energy of the gas and the denominator is determined by the wall material and the gas material.

Set the wall and the gas to the same temperature: In this manner effects of surface temperature are not considered and do not influence the results (adiabatic approximation).

Expand “wall material” to consider the actual surface material: Evaluate layers of adsorbed contaminants with different material characteristics than the base material.

Utilize various surface roughness atomic geometry: Create varying surface roughness geometric models to evaluate effects on TMAC.

Therefore, the overall approach to the experiments is to evaluate on three variables: Energy Ratio, Adsorbed Layers and Surface atomic / nano Roughness.

Specific Experiments Planned

Based on the above factors the following experiments were planned. Each are described further in the subsequent sections:

- Validation Experiments:
 - Baseline Validation with Data
 - Reasonableness Inspection of Typical Results

- Investigative Experiments:
 - Energy Ratio Analysis
 - Adsorbed Layers Analysis
 - Atomic / nanoscale Geometry Analysis

Baseline Validation with Data Methodology

As described in Chapter 3, “Experimental Work of Primary Interest – Seidel” [33], of the data surveyed, the Seidel data is most appropriate for validating this model because it provides not just a single TMAC value, but separate TMAC values for each of 7 impact angles on a prepared, cleaned and characterized surface with a known impact velocity. The data set chosen for validation is shown and highlighted below:

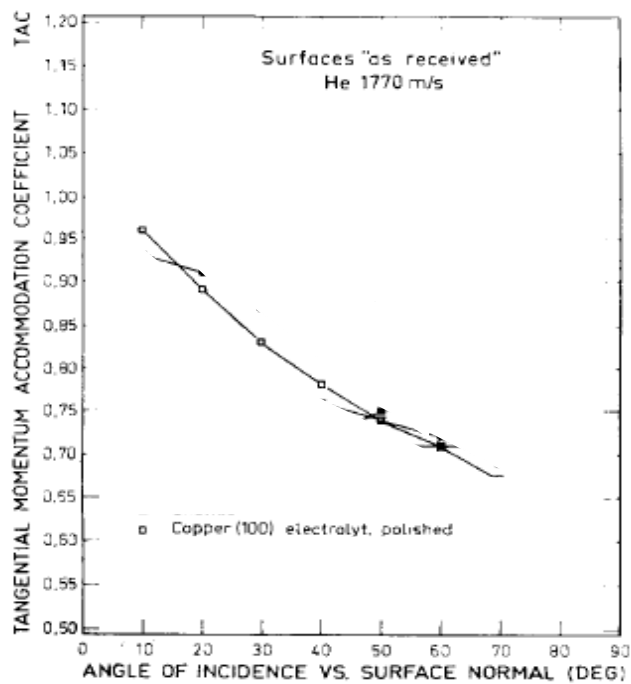


Figure 18 Seidl Data

This represents a copper crystal surface, face 100 being impacted by Helium atoms at 1770 m/s.

Seidl also evaluated the accuracy and repeatability of his experimental process. The accuracy was greater at the larger angles of approach than at the smaller angles. Using the plus and minus limits he suggests, the actual TMAC values are bounded as follows:

Table 11 Seidl Experimental Error

Angle	Seidl Variability	Seidl Lower TMAC Exp Value	Seidl Upper TMAC Exp Value
10	0.100	0.86	1.06
20	0.080	0.81	0.97
30	0.065	0.77	0.90
40	0.050	0.73	0.83
50	0.040	0.71	0.79
60	0.030	0.69	0.75
70	0.020	0.66	0.70

Seidl states that the material was electrolytically polished. Material which has been electrolytically polished does not present an “Ideal Crystal Surface”. The actual condition of the surface was not reported further, but can be deduced from the typical performance of electropolishing, which typically reduces surface roughness readings by about 50% and smoothes or eliminates discernable features. [108] . In this case, the copper with 5 micrometer grinding grooves was stated to be electropolished. The resulting copper surface would be expected to be in the 2.5 micrometer roughness category with a smooth, featureless surface.

Seidl goes on to describe a contaminant layer was described as follows, “the surfaces are completely covered by adsorbent layers, which are ... made up mainly of hydrocarbons and

water.” The stated contaminants (hydrocarbons and water) therefore exist in more than one layer mixed in with the irregular surface of a copper 100 crystal.

Based on this material and surface description, a series of “Directed Beam” analyses were performed for the following conditions:

Table 12 Baseline Data MD Experimental Conditions

Baseline Data MD Experimental Conditions		
Condition	Constant Value	Variable Values
Type of Analysis	Directed Beam	Varied from 10° to 70° in increments of 10°
Energy Ratio	Not Specified, determined by materials involved	Held Constant
Number of Gas Atoms	500 atoms over 2 lattice spacings	Held Constant
Cut Off Radius	3.5 σ	Held Constant
Time Step	.0005 τ	Held Constant
Time Step Cut Off	45,000 steps	Varied to maintain less than 1% of atoms being terminated
Number of Impacts (Bounces) Cut Off	6 impacts	Varied to maintain less than 1% of atoms being terminated
Solid Face	FCC, 100 Plane, Cu geometry	Held Constant
Solid Base Material	Copper	Held Constant
Adsorbed Layers on Top of Solid Base		2 & 3 adsorbed layers of composite material
Solid Atom Positions	Fixed	Held Constant
Velocity of Gas Atom	1770 m/s	Held Constant
Mass of Gas Atom	6.65 x 10 ⁻²⁷ kg	Held Constant

Diameter of Gas Atom (σ)	2.28×10^{-10} m	Held Constant
Energy of Gas Atom (ϵ)	1.41×10^{-22} J	Held Constant

Regarding the approach the modeling of the adsorbed composite layers: Based on the material description, a weighted mix of Hydrogen, Oxygen, Carbon and Copper atoms was developed. The exact geometry or pattern at nanoscale was not provided. This presented a substantial number of possible combinations and it was decided to try to model all the involved atoms in the composite layer with a single set of Lennard – Jones coefficients. The single coefficients were determined using weighted averages, based on the anticipated material ratios of the composite or their involved energies. mix for all atoms in these adsorbed composite layers. The assumed mix was in the following ratio: 1 Carbon atom, 1 Oxygen atom, 2 Hydrogen atoms and 2 Copper atoms. This resulted in an $\epsilon_{\text{composite}}$ of 3.13×10^{-20} J, weighted on number of atoms and a $\sigma_{\text{composite}}$ of 2.308×10^{-10} m weighted on the number of atoms and their individual ϵ .

The findings from this experiment are described in Chapter 5.

Reasonableness Inspection of Typical Results Methodology

As a validation technique in addition to comparison to actual data (as described above) output from a typical MD run were plotted visually analyzed for reasonableness with regards to the following quantifiable factors:

- Lennard Jones potential vs. separation distance
- Lennard Jones force vs. separation distance
- Gas atom position vs. time step
- Gas atom velocity vs. time step
- Gas atom acceleration vs. time step
- Lennard Jones potential vs. time step
- Number of solid atoms involved in the collision vs. time step
- Kinetic Energy ratio (final/initial) vs. each gas atom
- Tangential Momentum ratio (final/initial) vs. each gas atom
- Normal Momentum ratio (final/initial) vs. each gas atom

The findings from this experiment are described in Chapter 5.

Energy Ratio Analysis Methodology

The energy ratio (ER) is defined as the ratio of the gas atom's kinetic energy to the Lennard Jones energy constant (ϵ):

$$ER := \frac{\frac{1}{2} \cdot m \cdot V^2}{\epsilon}$$

At typical Energy Ratio for still gas (He) at room temperature (300° K) impacting metal (Cu) would in the 1.5 to 3.0 range. For the case of atoms in outer space impacting at very high velocities of several kilometers /second, the ER could be 20 or more.

This experiment seeks to determine how the TMAC changes with Energy Ratio. The TMAC was evaluated over a wide range of energy ratios, angles of approach and points of contact with respect to the atomic spacing of the solid.

The Lennard-Jones value of ϵ represents magnitude of the attractive “well depth” energy of the interaction. Prior to running the simulation, one can reason that the expected are results as follows:

- If the Lennard-Jones ϵ is much greater than an atom's Kinetic Energy, the gas atom path would be dominated by these attractive surface forces. It would likely experience multiple "bounces" before leaving the Rc, or could conceivably be captured by the surface, thereby "wetting" it or being adsorbed by it.
- If the Lennard-Jones ϵ is much less than an atom's Kinetic Energy, the gas atom path would be expected to be dominated by the inertial momentum of the atom, moving quickly past the attractive potential zone into the strongly repulsive zone, then being ejected in a similar manner, with few "bounces".
- If the Lennard-Jones ϵ is about equal than an atom's Kinetic Energy, the gas atom path would be expected to be less obvious, and depend upon the specific geometry of the approach.

The effect of Energy Ratio on TMAC analysis was performed in the following manner. A series of "Directed Beam" analyses were performed for the following conditions:

Table 13 Energy Ratio MD Experimental Conditions

Energy Ratio MD Experimental Conditions		
Condition	Constant Value	Variable Values
Type of Analysis	Directed Beam	Varied from 10° to 70° in increments of 10°
Energy Ratio		Evaluated at 1, 2.9, 5, 10 and 70 by varying the ϵ of the solid atom
Number of Gas Atoms	500 atoms over 2 lattice spacings	Held Constant
Cut Off Radius	3.5 σ	Held Constant

Time Step	.0005 τ	Held Constant
Time Step Cut Off	15,000 steps	Varied to maintain less than 1% of atoms being terminated
Number of Impacts (Bounces) Cut Off	6 impacts	Varied to maintain less than 1% of atoms being terminated
Solid Face	FCC, 100 Plane	Held Constant
Irregularities on Top of Solid Face	None	Held Constant
Adsorbed Layers on Top of Solid Face	None	Held Constant
Ratio Gas Atom Diameter to Solid Atom Diameter	1	Held Constant
Ratio Gas Atom Mass to Solid Atom Mass	1	Held Constant
Ratio Gas Atom Diameter to Crystal Lattice Constant	0.77	Held Constant
Solid Atom Positions	Fixed	Held Constant
Velocity of Gas Atom	1770 m/s	Held Constant
Mass of Gas Atom	6.65×10^{-27} kg	Held Constant
Diameter of Gas Atom (σ)	2.28×10^{-10} m	Held Constant
Energy of Gas Atom (ϵ)	1.41×10^{-22} J	Held Constant

The findings from this experiment are described in Chapter 5.

Adsorbed Layer Analysis Methodology

The surface of a crystal solid may be covered with multiple adsorbed layers of other materials.

This experiment seeks to provide insight into how the TMAC changes with depth and makeup of potential adsorbed layers. The TMAC was evaluated with different quantities of adsorbed layers, angles of approach and points of contact with respect to the atomic spacing of the solid.

The effect of Adsorbed Layers on TMAC analysis was performed in the following manner. A series of “Directed Beam” analyses were performed for the following conditions:

Table 14 Adsorbed Layer MD Experimental Conditions

Adsorbed Layer MD Experimental Conditions		
Condition	Constant Value	Variable Values
Type of Analysis	Directed Beam	Varied from 10° to 70° in increments of 10°
Energy Ratio		Allowed to vary as determined by the number and type of adsorbent layers
Number of Gas Atoms	500 atoms over 2 lattice spacings	Held Constant
Cut Off Radius	3.5 σ	Held Constant
Time Step	.0005 τ	Held Constant
Time Step Cut Off	15,000 steps nominal	Varied to maintain less than 1% of atoms being terminated

Number of Impacts (Bounces) Cut Off	6 impacts nominal	Varied to maintain less than 1% of atoms being terminated
Solid Face	FCC, 100 Plane	Held Constant
Irregularities on Top of Solid Face	None	Held Constant
Adsorbed Layers on Top of Solid Face		Varied from 0, 1, 2
Adsorbed Layer Material ϵ	3.13×10^{-20} J	Held Constant
Adsorbed Layer Material σ		Varied from 2.308×10^{-10} m to 2.42×10^{-10} m
Ratio Gas Atom Diameter to Solid Atom Diameter	1	Held Constant
Ratio Gas Atom Diameter to Crystal Lattice Constant	0.77	Held Constant
Solid Atom Positions	Fixed	Held Constant
Velocity of Gas Atom	1770 m/s	Held Constant
Mass of Gas Atom	6.65×10^{-27} kg	Held Constant
Diameter of Gas Atom (σ)	2.28×10^{-10} m	Held Constant
Energy of Gas Atom (ϵ)	1.41×10^{-22} J	Held Constant

The findings from this experiment are described in Chapter 5.

Atomic / Nano Scale Geometry Analysis Methodology

The surface of a crystal solid may be covered with multiple types of nanoscale surface irregularities.

This experiment seeks to provide insight into how the TMAC changes with geometry and frequency of certain irregularities. The TMAC was evaluated with different types and spacings, angles of approach and points of contact with respect to the spacing of the irregularity.

A series of “Directed Beam” analyses were performed for the following conditions:

Table 15 Nanoscale Geometry MD Experimental Conditions

Nanoscale Geometry MD Experimental Conditions		
Condition	Constant Value	Variable Values
Type of Analysis	Directed Beam	Varied from 10° to 70° in increments of 10°
Energy Ratio	ER(Cu Base) = 2.9 ER(Adsorbed Layer) = 48	Held Constant
Number of Gas Atoms	500 atoms over 2 lattice spacings	Held Constant
Cut Off Radius	3.5σ	Held Constant
Time Step	$.0005 \tau$	Held Constant
Time Step Cut Off	15,000 steps nominal	Varied to maintain less than 1% of atoms being terminated
Number of Impacts (Bounces) Cut	6 impacts nominal	Varied to maintain less than

Off		1% of atoms being terminated
Solid Face	FCC, 100 Plane	Held Constant
Irregularities on Top of Solid Face		Varied in type and spacing. See below.
Adsorbed Layers on Top of Solid Face		Varied from 0, 1, 2
Adsorbed Layer Material ϵ	3.13×10^{-20} J	Held Constant
Adsorbed Layer Material σ	2.3×10^{-10} m	Held Constant
Ratio Gas Atom Diameter to Solid Atom Diameter	1	Held Constant
Ratio Gas Atom Diameter to Crystal Lattice Constant	0.77	Held Constant
Solid Atom Positions	Fixed	Held Constant
Velocity of Gas Atom	1770 m/s	Held Constant
Mass of Gas Atom	6.65×10^{-27} kg	Held Constant
Diameter of Gas Atom (σ)	2.28×10^{-10} m	Held Constant
Energy of Gas Atom (ϵ)	1.41×10^{-22} J	Held Constant

The following types of irregularities were modeled and evaluated in the Nano Scale Geometry Investigation:

Crystal Plane 100 Surface (Surface Type 1): The perfect 100 crystal surface.

Single Atom Irregularity (Surface Type 2): The perfect 100 crystal surface with a single atom placed atop the surface at periodic intervals.

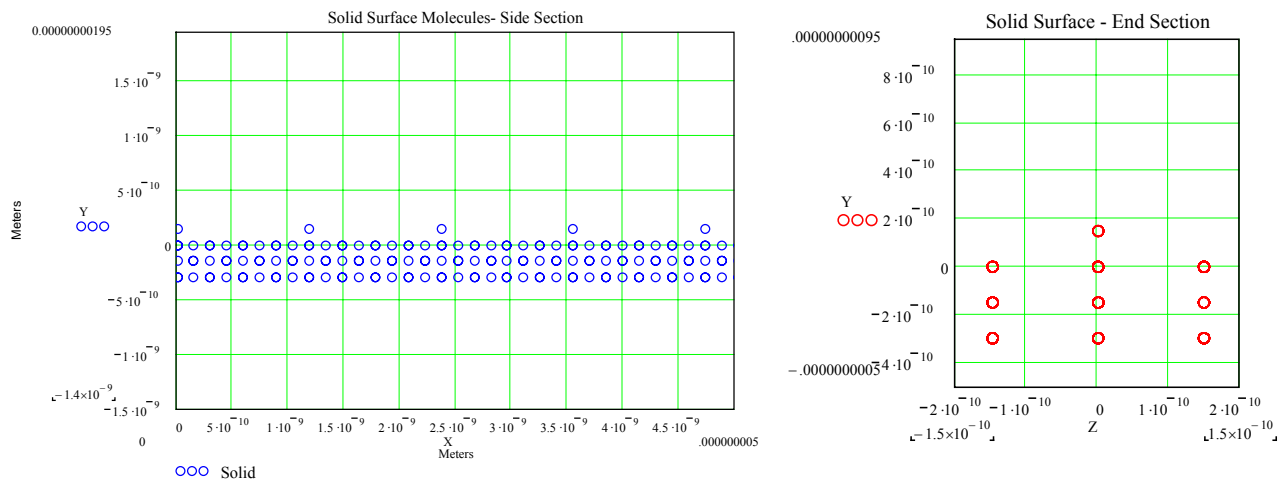


Figure 19 Atomic / Nano Scale Irregularities

The findings from this experiment are described in Chapter 5.

CHAPTER FIVE: FINDINGS

Baseline Validation Findings

The results of the Baseline Validation Experiment confirm the basic usefulness of the model.

The experimental data reported “layers” of contaminant, but did not quantify if this were 2, 3 or more layers.

If more than 3 layers, no effect would be determined by the model, since the cut off ratio is set at 3.5. Therefore MD experiments were performed with 2 and 3 adsorbed contaminant layers.

Validation Experiment with Two Layers of Adsorbent

The following MD simulation included two layers of characteristic adsorbent at a nominal ER of 5 (4.94). Note that 6 of the 7 MD data points fall within the experimental error limits of Seidl.

Note also that the average TMAC difference from Seidl’s data set is less than 3%.

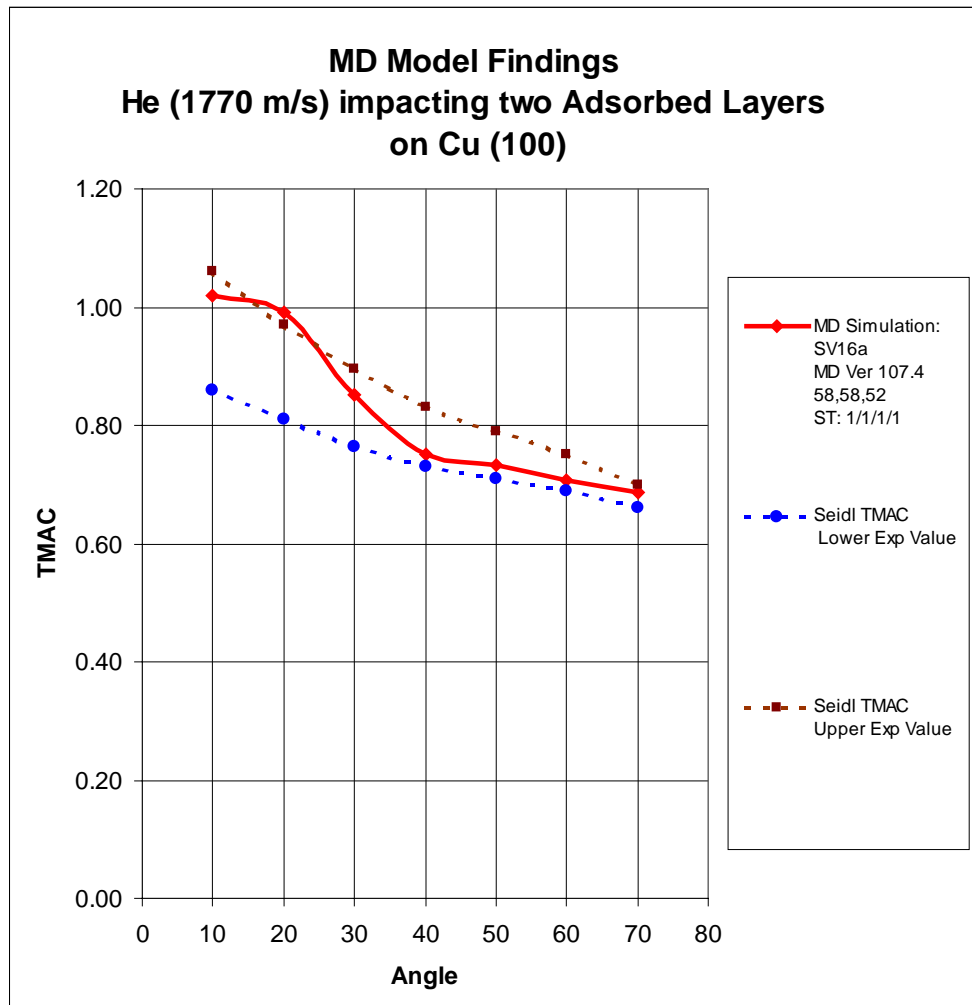


Figure 20 Baseline Validation Data Summary – 2 Layer Model

Table 16 Comparison MD Model Results (2 Layers) to Seidl Data

Angle (Degrees)	TMAC Seidl Atomically Rough; Electrolytically Polished	TMAC MD Simulation: SV16a MD Ver 107.4 58,58,52 ST: 1/1/1/1	Difference in %
10	0.86	1.02	18%
20	0.81	1.00	23%
30	0.76	0.85	12%
40	0.73	0.75	3%
50	0.71	0.73	3%
60	0.69	0.70	1%
70	0.66	0.68	3%

10	0.96	1.020	6.3%
20	0.89	0.992	11.5%
30	0.83	0.851	2.5%
40	0.78	0.750	-3.8%
50	0.75	0.732	-2.4%
60	0.72	0.706	-1.9%
70	0.68	0.687	1.0%
Average	0.80	0.82	2.3%

Validation Experiment with Three Layers of Adsorbent:

The following MD simulation included three layers of characteristic adsorbent at a nominal ER of 5.

Note that all 7 of the 7 MD data points fall within the experimental error limits of Seidl.

Note also that the average TMAC difference from Seidl's data set is less than 3%.

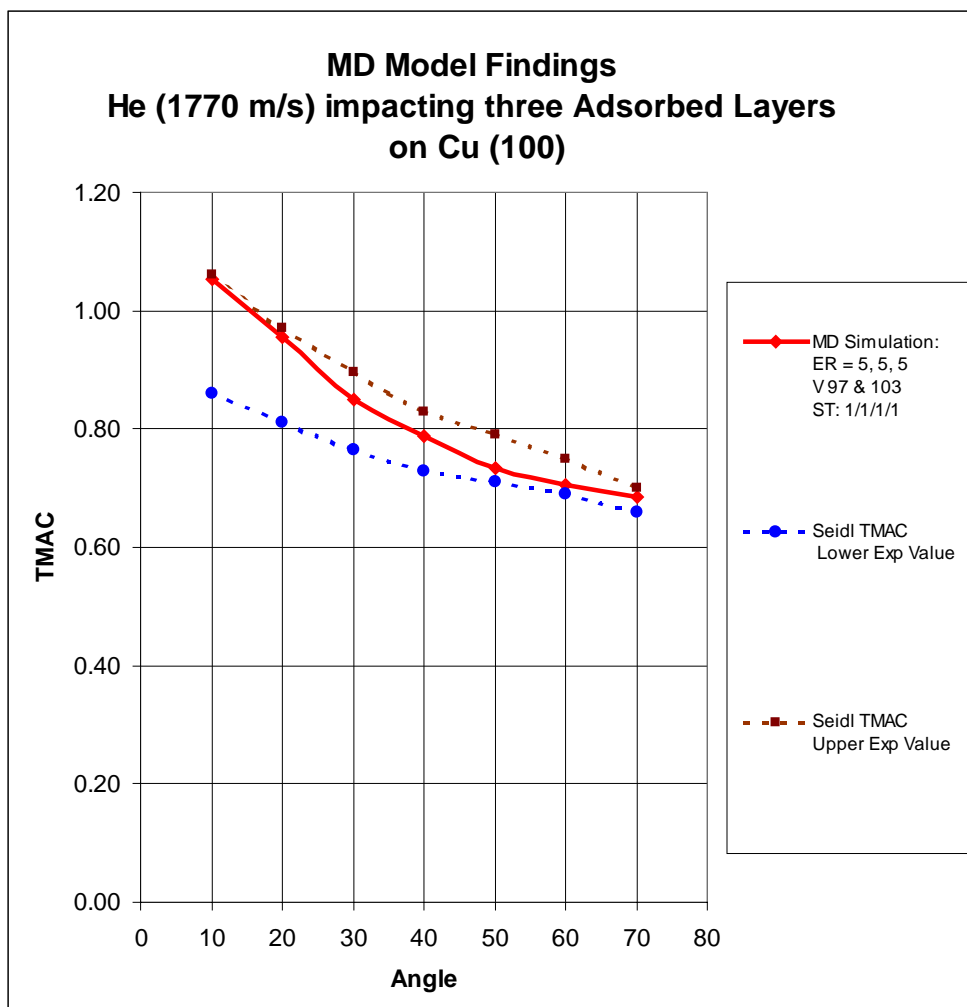


Figure 21 Baseline Validation Data Summary – 2 Layer Model

Table 17 Comparison MD Model Results (3 Layers) to Seidl Data

Angle (Degrees)	TMAC Seidl Atomically Rough; Electrolytically Polished	TMAC MD Simulation: ER = 5, 5, 5 V 97 & 103 ST: 1/1/1/1	Difference in %
10	0.85	1.05	22.4
20	0.81	0.95	16.0
30	0.77	0.85	10.4
40	0.73	0.78	6.7
50	0.71	0.72	1.4
60	0.69	0.70	1.4
70	0.66	0.68	3.0

10	0.96	1.052	9.6%
20	0.89	0.955	7.3%
30	0.83	0.85	2.4%
40	0.78	0.788	1.0%
50	0.75	0.735	-2.0%
60	0.72	0.705	-2.1%
70	0.68	0.684	0.6%
Average	0.80	0.82	2.8%

MD Model Validation Summary

The MD model can provide useful estimates of many factors:

- The MD simulation correctly predicted that the TMAC changes with the angle of impact.
- The MD simulation correctly estimated the direction of the slope regarding changes of the TMAC with the angle of impact.
- The magnitude of difference between the MD simulation data average and the Seidl data average is just a few per cent. It is generally more accurate as the angle of approach is increased.
- Overall, for these two runs, the MD model produced 13 of 14 data points within the experimental data range.

This MD model can therefore be used to provide greater insight into the characteristics which affect TMAC.

Reasonableness Inspection of Typical MD Results

A sample MD simulation run was selected to be analyzed for reasonableness. This was the 60 degree approach angle from the initial validation analysis. This was a run of 500 Helium atoms at 1770 m/s impacting a copper material with 2 adsorbed layers on top.

Gas atom position vs. time step

For this MD simulation the gas atom paths fall into three typical types of collisions. These are described and illustrated in the figures below:

(Note all the following gas atom numbers are rounded based on 500 total gas atoms positioned equally over two lattice cycles.)

- Single “bounce” with negative final tangential momentum (backscattered)
 - Gas atoms 1 to 40; 210 to 250
 - Gas atoms 251 to 290; 460 to 500

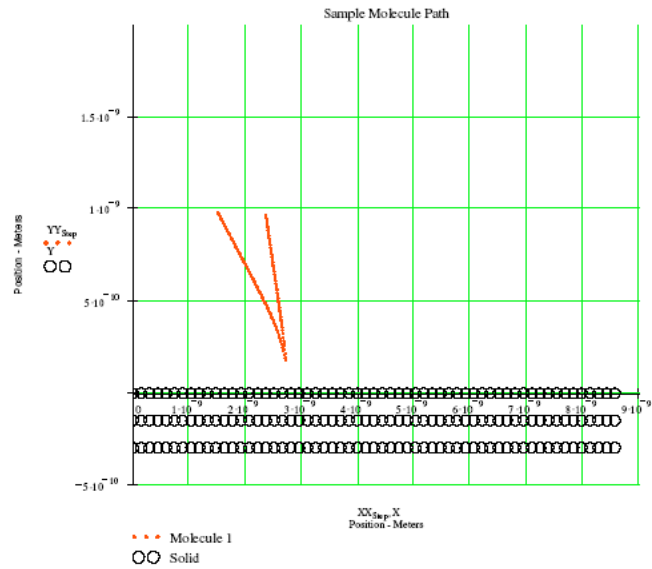


Figure 22 Typical Gas Atom Path – Single “Bounce”; Negative Final Tangential Momentum

- Single “bounce” with positive final tangential momentum
- Gas atoms 41 to 99; 161 to 209
- Gas atoms 291 to 349; 411 to 459

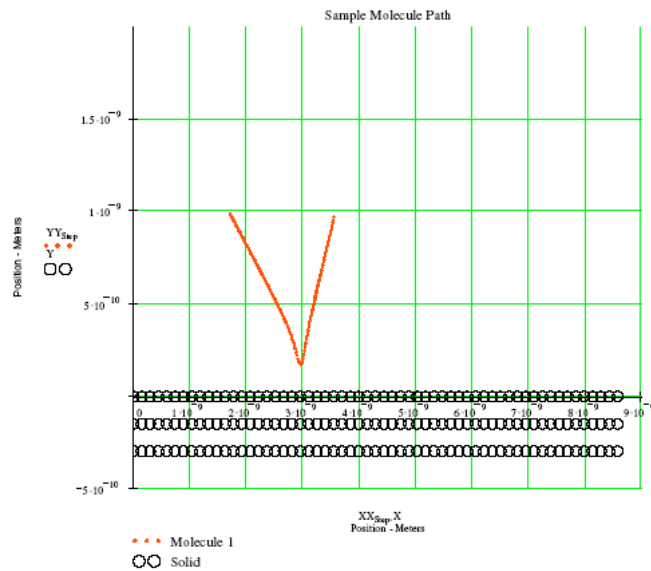


Figure 23 Typical Gas Atom Path – Single “Bounce”; Positive Final Tangential Momentum

- Multiple “bounces” with variable final tangential momentum
 - Gas atoms 100 to 160
 - Gas atoms 350 to 410

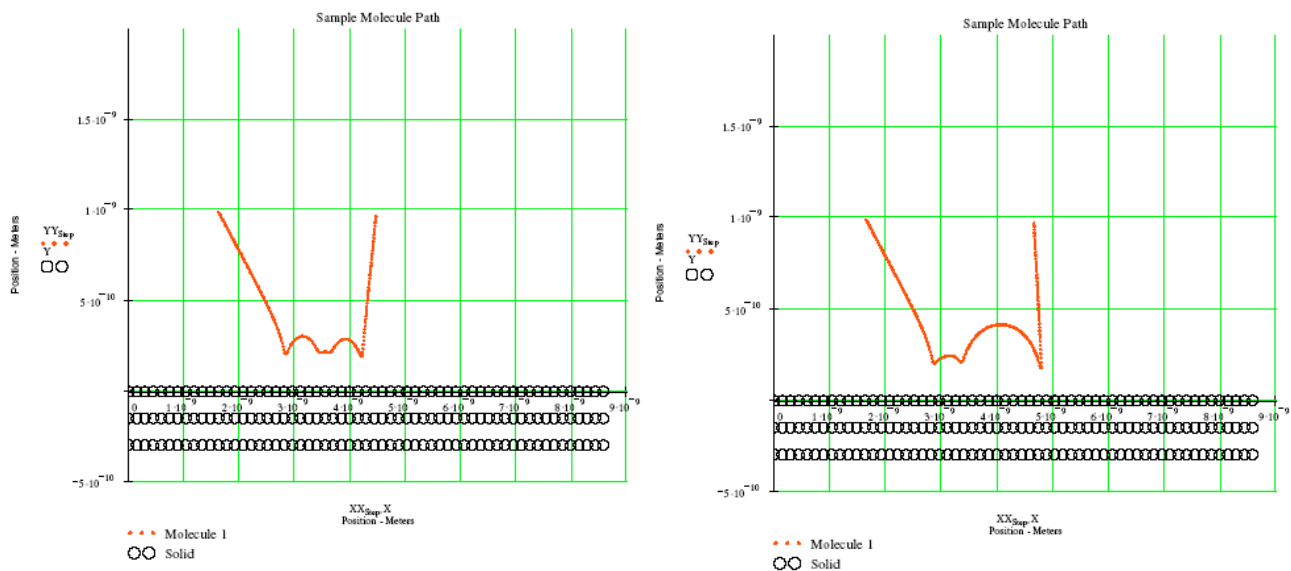


Figure 24 Typical Gas Atom Paths – Multiple “Bounces”; Variable Result

These paths show reasonable movement of the gas atoms.

Gas atom velocity vs. time step

This plot shows the velocity of a gas atom (“Single “bounce” with positive final tangential momentum “) over the period of time steps required to impact and leave the surface. As

expected, the Normal (Y) velocity is substantially reversed and the Tangential (X) velocity is somewhat maintained.

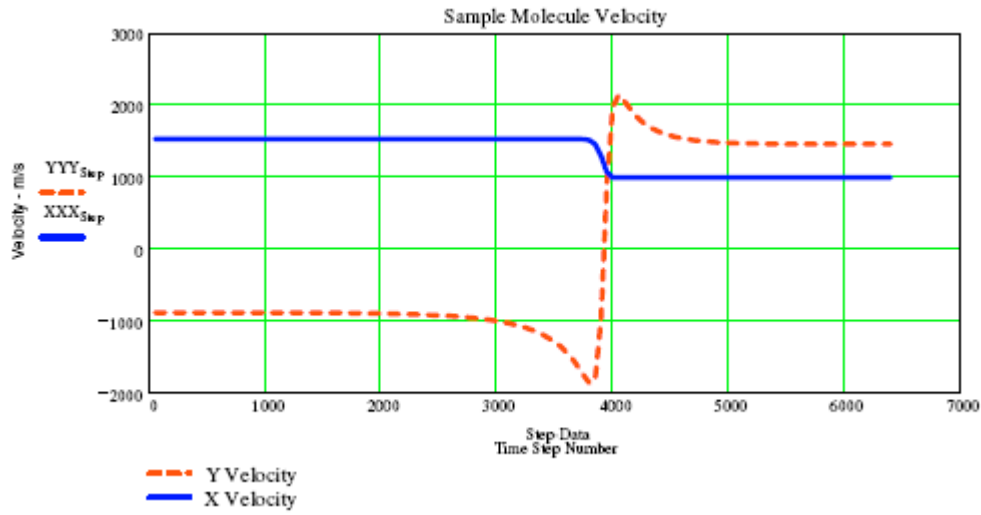


Figure 25 Typical Gas Atom Velocity vs. Time Step

Gas atom acceleration vs. time step

This plot shows the acceleration of a gas atom over the period of time steps required to impact and leave the surface. As expected, the acceleration is zero for most of the period. Then, as the gas atom gets within the cut off radius of the solid atoms, a weak Normal (Y) negative (attractive) acceleration exists, followed by a strong positive (repulsive) Normal (Y) acceleration. For this geometry a moderate negative Tangential (X) acceleration exists during the event.

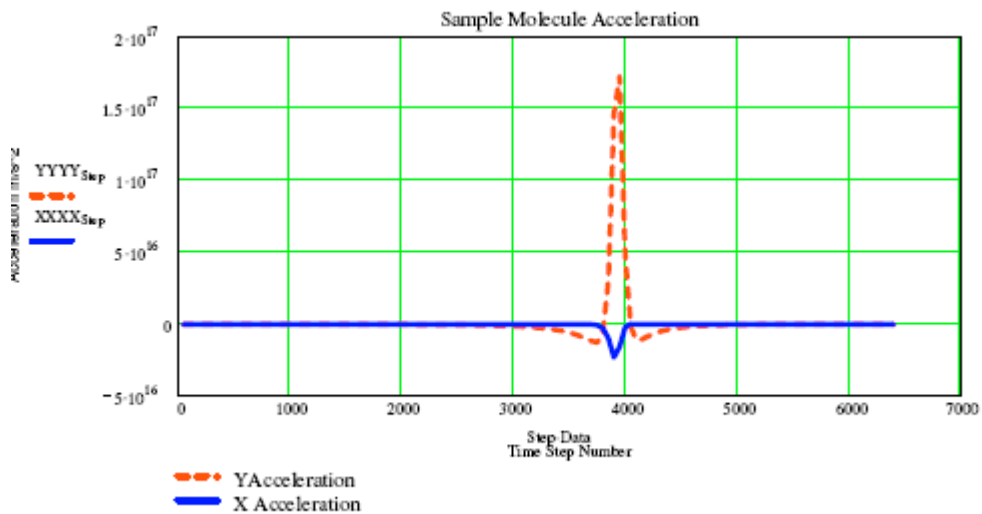


Figure 26 Typical Gas Atom Acceleration vs. Time Step

Lennard Jones potential vs. time step

This plot shows the Lennard-Jones potential over the period of time steps required to impact and leave the surface. As expected, it is zero for most of the period. Then, as the gas atom gets within the cut off radius of the solid atoms, a weak attractive potential exists, followed by a strong repulsive potential.

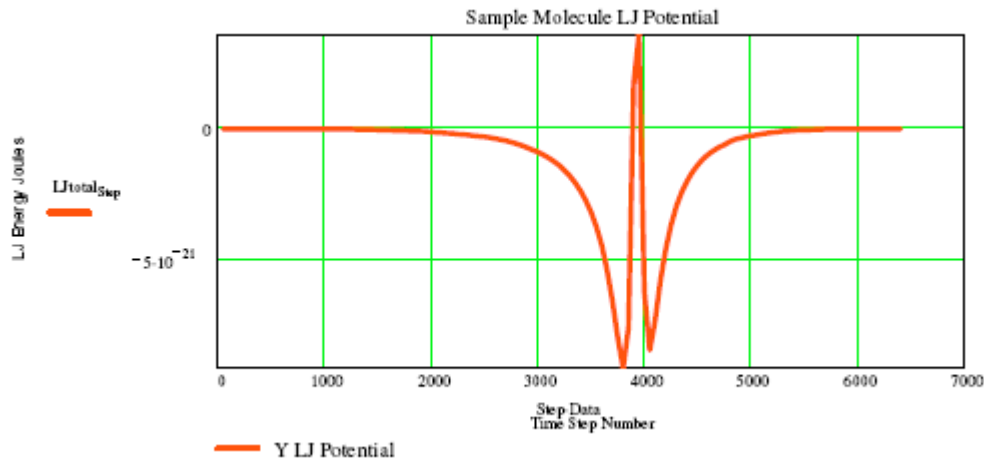


Figure 27 Typical Lennard Jones Potential vs. Time Step

Number of solid atoms involved in the collision vs. time step

As long as the gas atom is outside the cut off radius, no other atoms affect its path and it proceeds in a straight line. Then as it approaches the solid more and more solid atoms are within the cutoff radius and each affects its travel. As it departs the solid, the reverse happens. Finally, it is again outside the cut off radius and is unaffected by the solid.

The following plot illustrates that for this gas atom up to 43 solid atoms affected its travel. Note that this particular collision took place in nearly 5000 time steps.

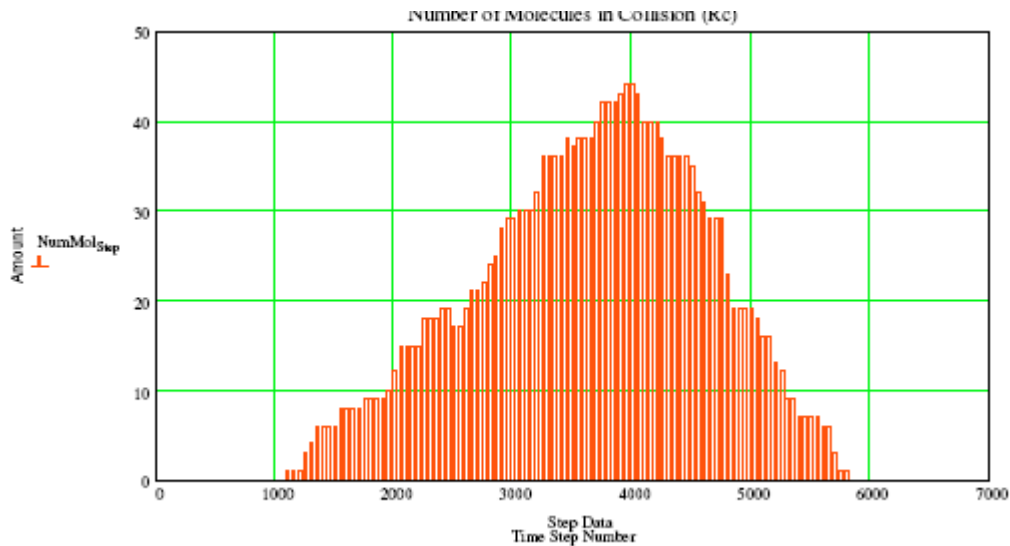


Figure 28 Typical Number of Solid Atoms Involved in Collision vs. Time Step

Total energy vs. time step

The following illustrates that as the Lennard – Jones energy well is entered, the kinetic energy of the gas atom is increased, keeping the total energy constant. As the gas atom leaves the influence of the solid, the reverse happens.

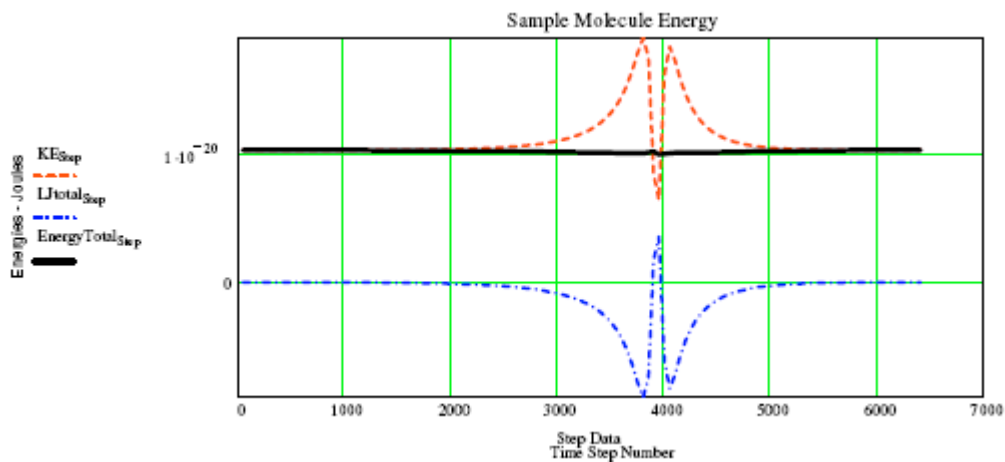


Figure 29 Typical Total Energy vs. Time Step

Kinetic Energy ratio (final/initial) vs. each gas atom

The following shows that for each gas atom the ratio of the final kinetic energy value to the initial kinetic energy was between 0.99998 and 1.00002. This indicates that over the course of the MD simulation of the gas impact with the solid surface energy was conserved within 0.002%.

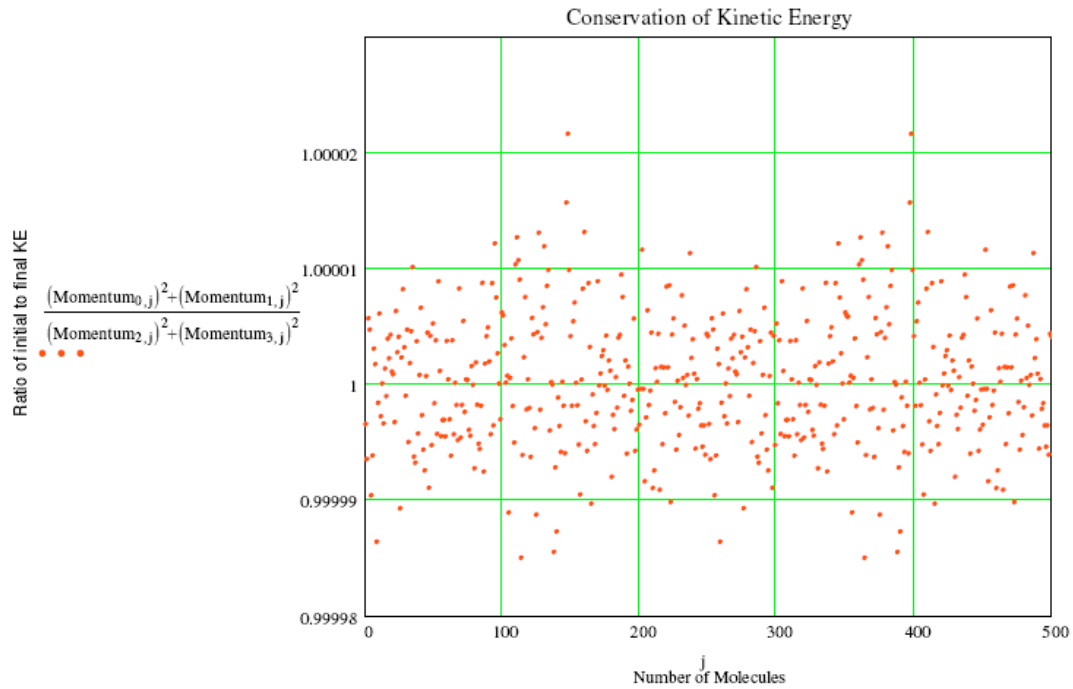


Figure 30 Typical Kinetic Energy Ratio for Each Gas Atom

Tangential Momentum ratio (final/initial) vs. each gas atom

The following shows for each gas atom the ratio of the final momentum to the initial momentum.

There are 500 gas atoms impacting the surface over two lattice spacings. Therefore, based on geometry one would expect a repeated pattern of gas atom momentum ratios. The figure clearly demonstrates these two cycles.

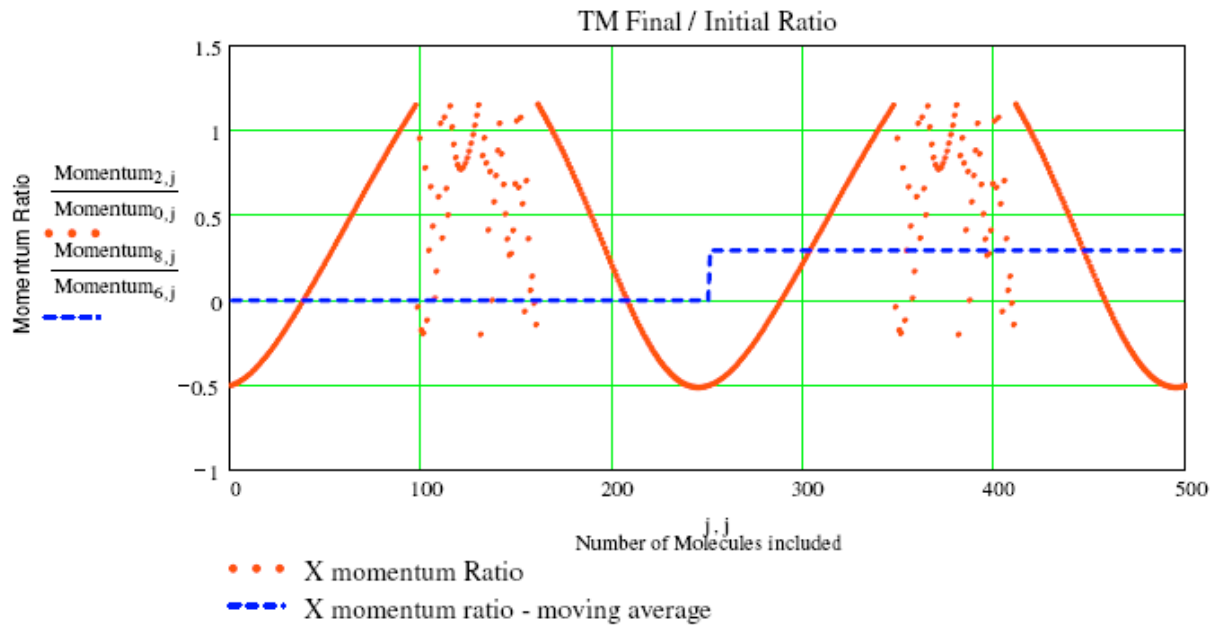


Figure 31 Typical Tangential Momentum Ratio Plot for Each Gas Atom

- Note that the tangential momentum is a continuous function over large portions of the sample. It becomes discontinuous as the type of collision changes from a single “bounce” to multiple “bounces”.
- Note that for portions of the cycle the ratio is less than 1. This indicates backscattering for that portion of the sample.
- Note that the horizontal blue line is a moving average value. For the first 250 gas atoms it is zero, because data for a complete cycle of 250 gas atoms has not been gathered. From atoms 251 through 500, it represents the moving average. The fact that this is a horizontal line over the second half of the plot indicates the repeatability of the data. It is the final value of this moving average (or the total average over all 500 gas atoms) which is used for calculating the TMAC value.

Normal Momentum Ratio (final/initial) vs. each gas atom

Although, not specifically of interest in this work, the MD simulation also outputs the Normal Momentum Accommodation Coefficient (NMAC), and calculates its moving average.

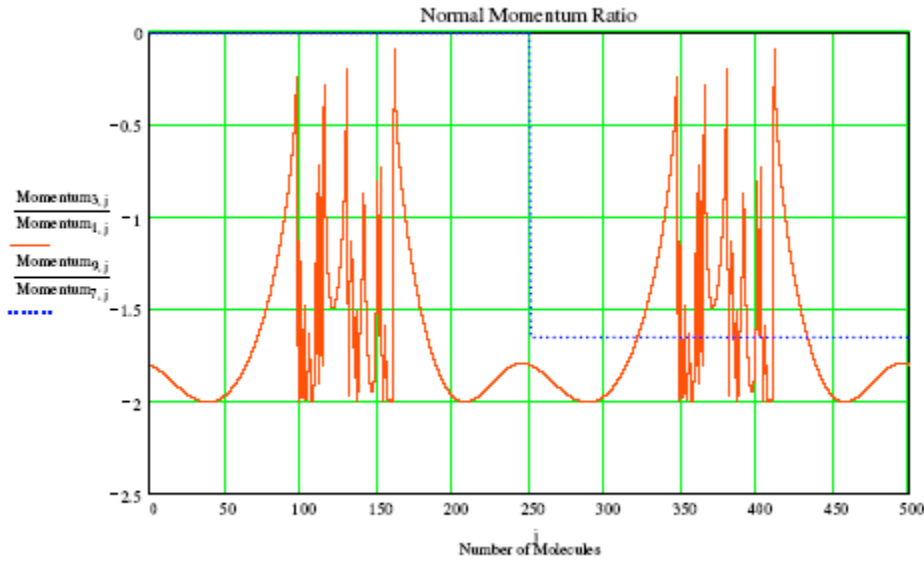


Figure 32 Typical Normal Momentum Ratio Plot for Each Gas Atom

Summary – Reasonableness Check

In summary, a detailed review of the MD simulation output indicates that the results have been examined and dispositioned as credible.

Energy Ratio Analysis Findings

The evaluation TMAC as a function of Energy Ratio presents many interesting findings. The summary data for five different Energy ratios is shown below:

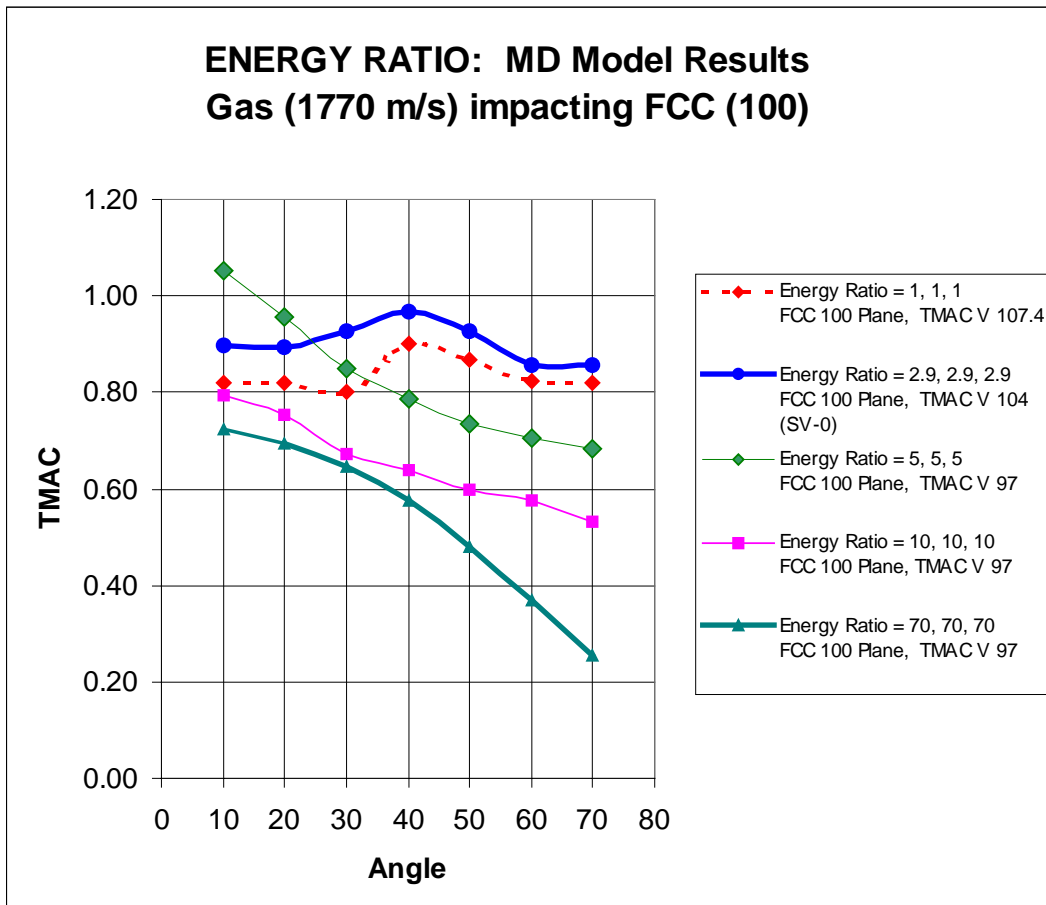


Figure 33 Energy Ratio - Data Summary

For large angles of approach, decreases in Energy Ratio generally increase the TMAC value.

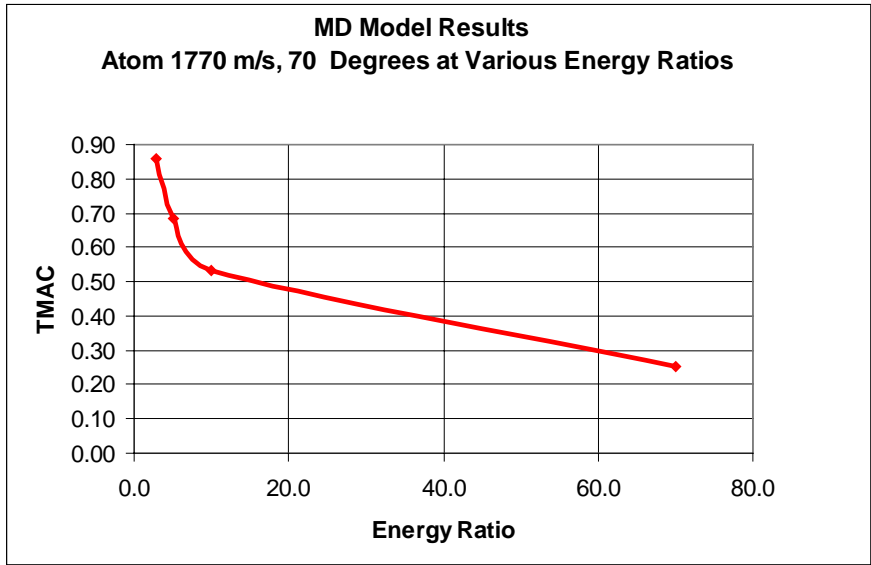


Figure 34 Energy Ratio – Effect at Large Angles

However, at small angles it increases to maximum and then decreases again:

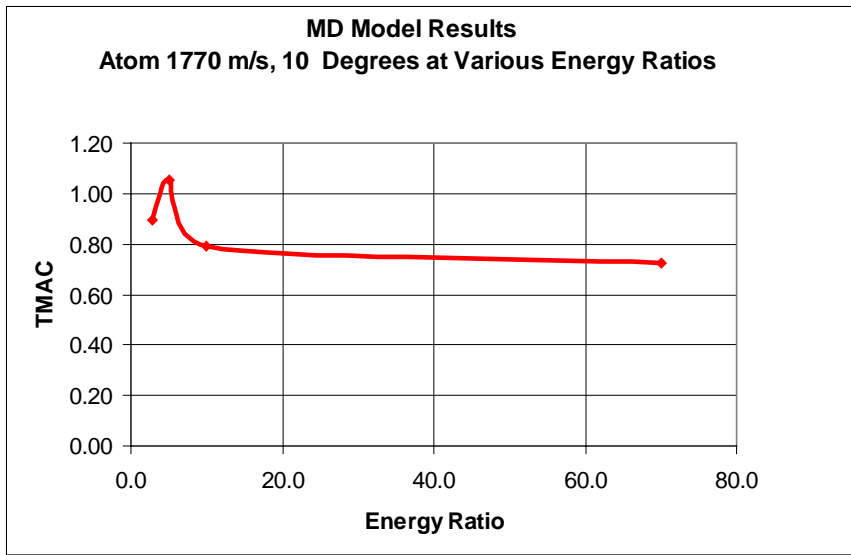


Figure 35 Energy Ratio – Effect at Small Angles

These findings are in general agreement with previous models of the effects of ER on TMAC by Jackson [93] .

This prompts further examination of the collisions themselves and what is different about those at:

- Large and small energy ratios
- Large and small angles of approach

Comparing plots of the ratio of final to initial tangential momentum in four such different cases, we find the following:

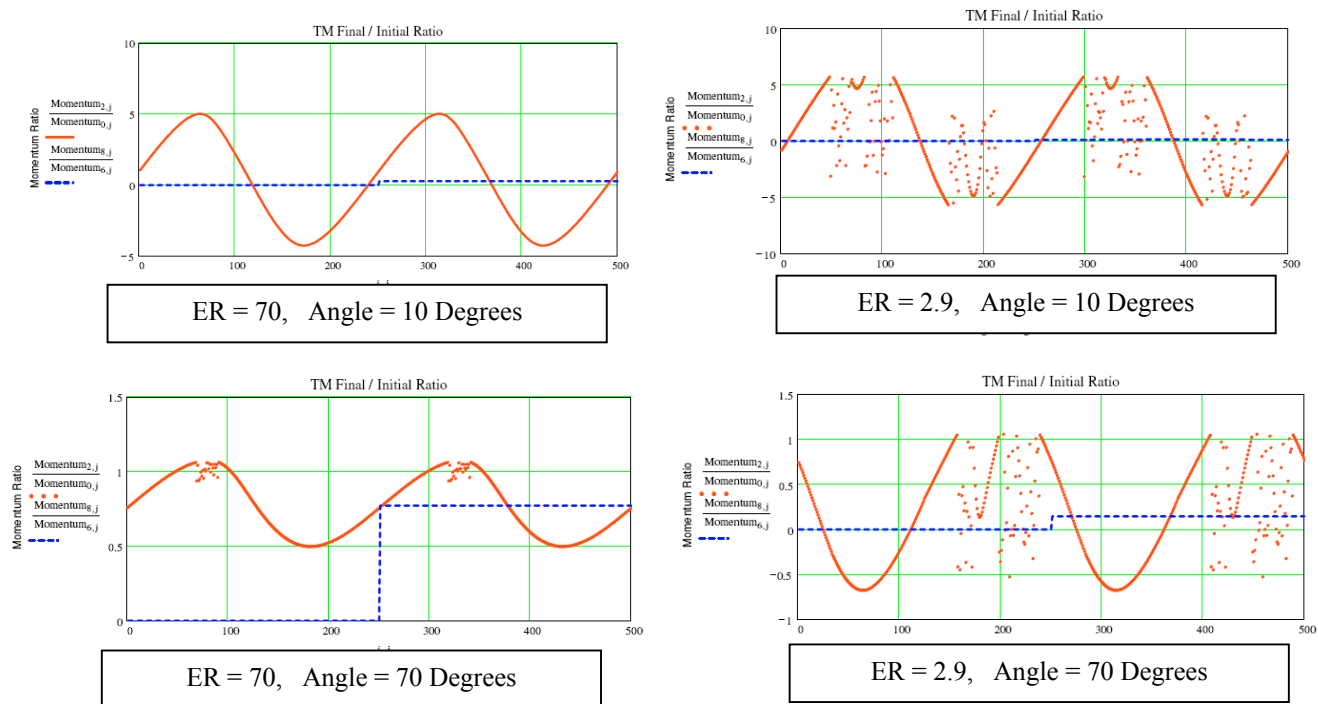
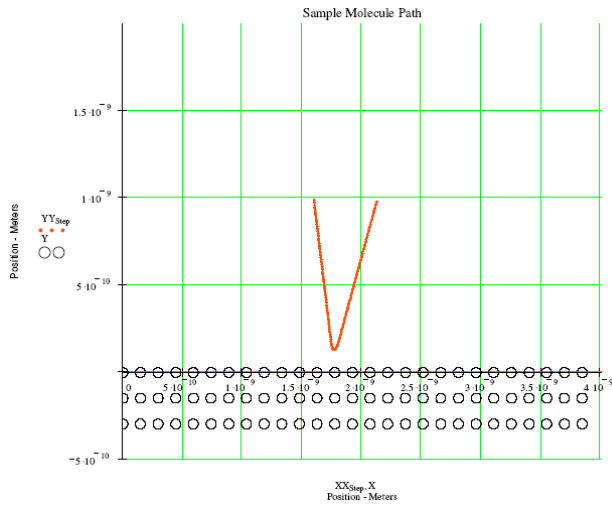


Figure 36 Energy Ratio - Tangential Momentum Ratio - 4 Cases

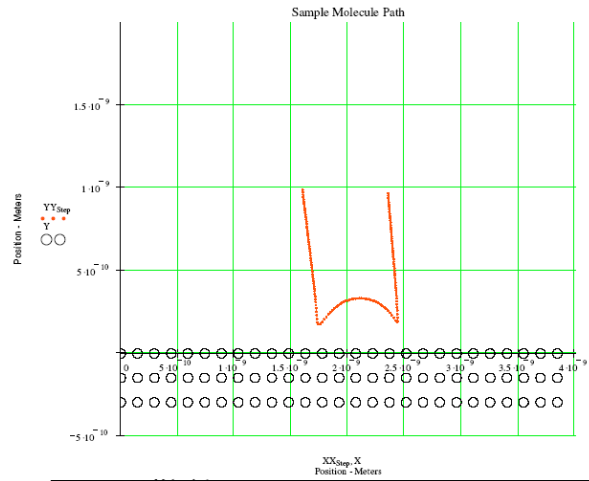
- At large energy ratios and at small angles (top left of figure), all impacts are single “bounce” impacts creating a continuous curve throughout the range of gas atoms. This includes both the forward scattering and the backscattering impacts..
- At large energy ratios and at large angles (bottom left of figure), most impacts are single “bounce” impacts. All impacts are forward scattering. However, some of the forward scattering impacts become multiple “bounces” with more variability and a lower overall average for tangential momentum. This creates a discontinuous area at the top of each curve.

- At small energy ratios and at large angles (bottom right of figure), most impacts are single “bounce” impacts. However, more of the forward scattering impacts become multiple “bounces” with more variability and a lower overall average for tangential momentum. This creates a discontinuous area at the top of each curve. All of the backscattering impacts are single “bounce” and present a continuous curve throughout this portion of the gas atoms.
- At small energy ratios and at small angles (top right of figure), single “bounce” impacts and multiple “bounce” impacts are about equal in number. Some of both the forward scattering and backscattering impacts become multiple “bounces” with more variability, and a lower overall average for tangential momentum. This creates a discontinuous area at the top and bottom of each curve. This is more neutral with regards to the overall impact to TMAC because the formerly backscattered gas atoms exhibit more variability.

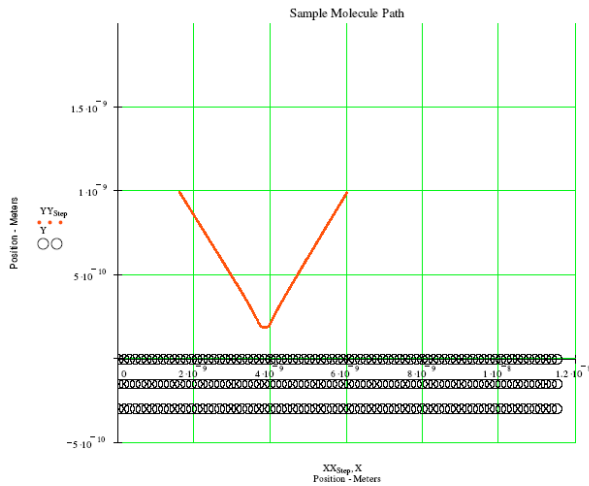
This finding is verified by examination of individual gas atom impacts. Consider gas atom number 100 under the four cases described:



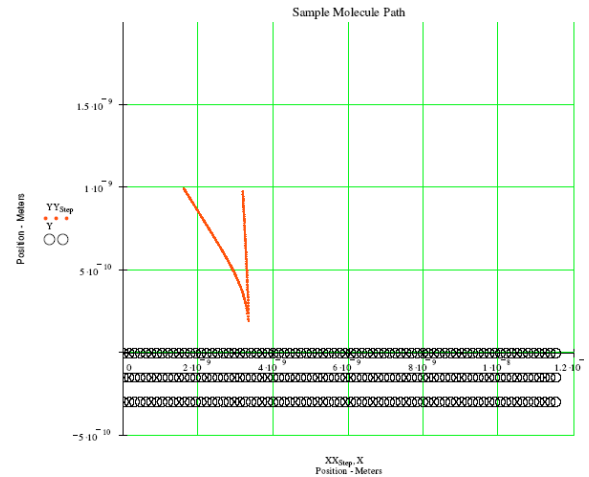
Atom # 100, ER = 70, Angle = 10 Degrees



Atom # 100, ER = 2.9, Angle = 10 Degrees



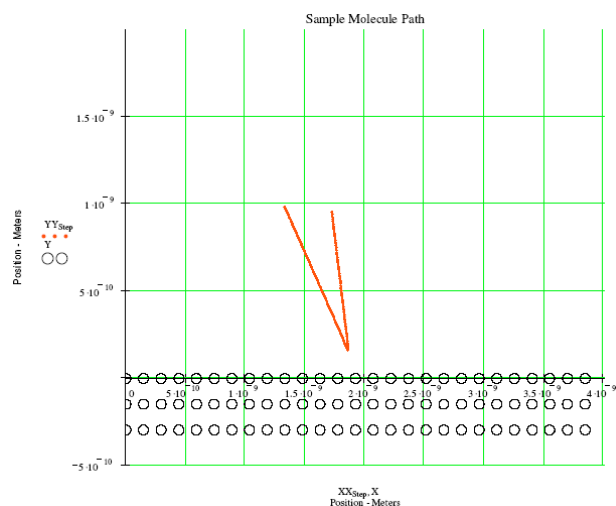
Atom # 100, ER = 70, Angle = 70 Degrees



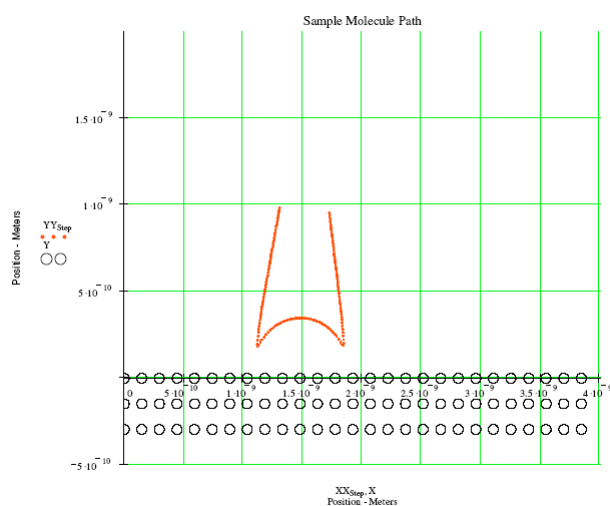
Atom # 100, ER = 2.9, Angle = 70 Degrees

Figure 37 Energy Ratio - Gas Atom 100 in 4 Cases

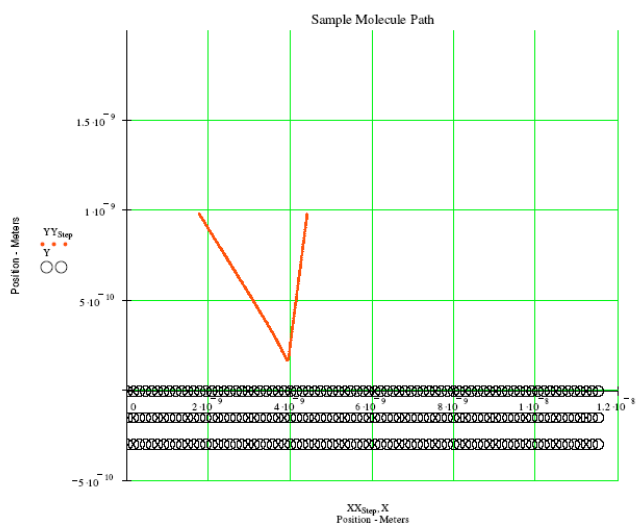
This finding is also verified by considering gas atom number 200 under the four cases described:



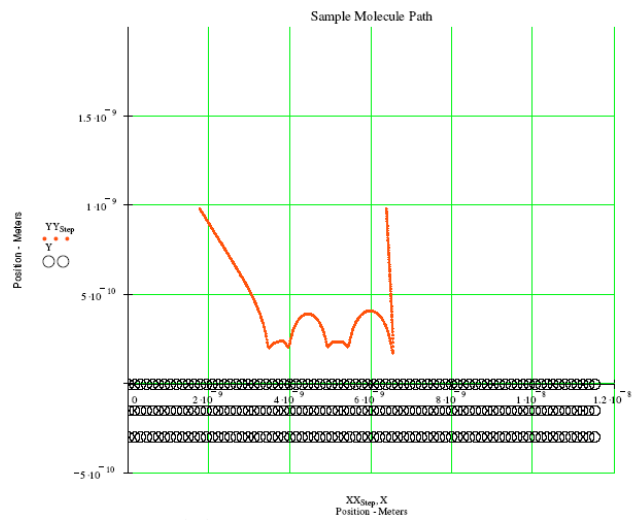
Atom # 200, ER = 70, Angle = 10 Degrees



Atom # 200, ER = 2.9, Angle = 10 Degrees



Atom # 200, ER = 70, Angle = 70 Degrees



Atom # 200, ER = 2.9, Angle = 70 Degrees

Figure 38 Energy Ratio - Gas Atom 200 in 4 Cases

Therefore, decreasing the Energy Ratio results in more of a breakdown of the continuous tangential momentum ratio curve, in the both the forward scattering and backscattering portions,

depending on the angle of approach. It is not known if at even lower Energy Ratios if this effect is also duplicated at the lower angles.

-

Adsorbed Layer Analysis Findings

The effects of layers of adsorbents on TMAC presents many interesting findings.

Effect of Single and Multiple Adsorbed Layers with large ER difference

For this analysis, the ER of the adsorbed layer was 48 vs. an ER for the base material of 2.9.

The summary data for single and double adsorbent layers is shown below:

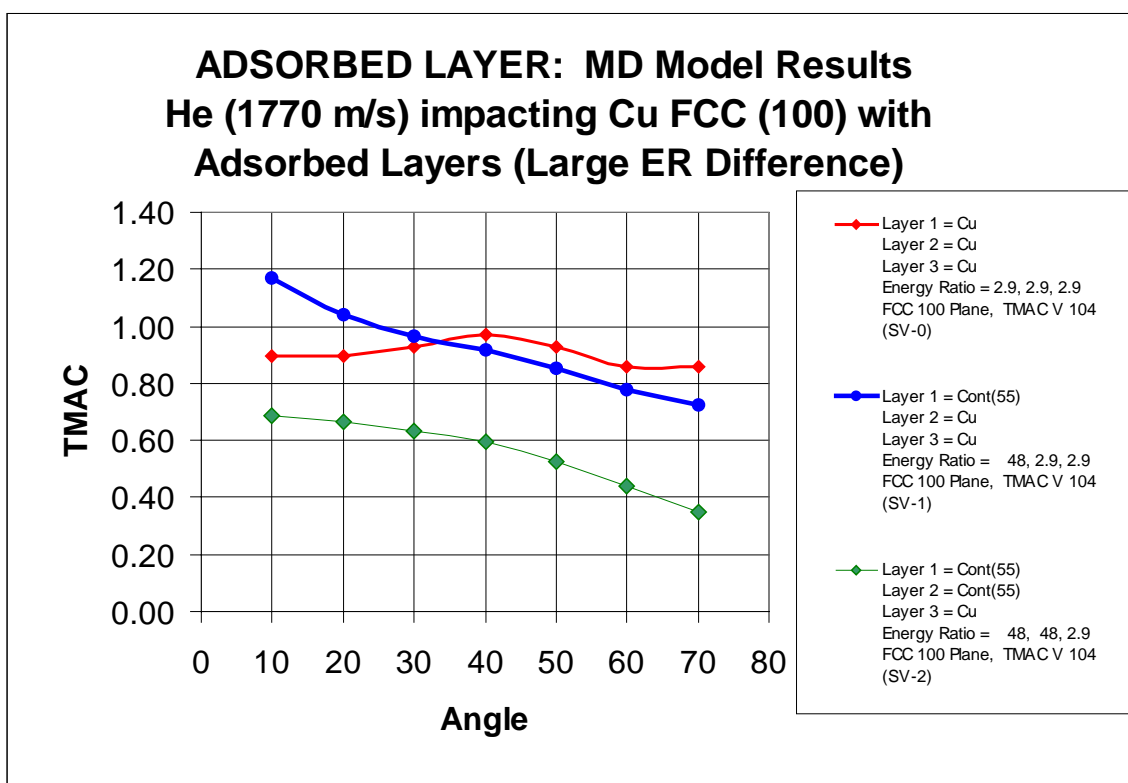


Figure 39 Adsorbed Layers - Data Summary for Large ER Difference

The above figure illustrates the effect of adding one or two layers of an adsorbent atop a Copper type FCC 100 crystal plane. The adsorbent atoms are located in the same FCC arrangement as

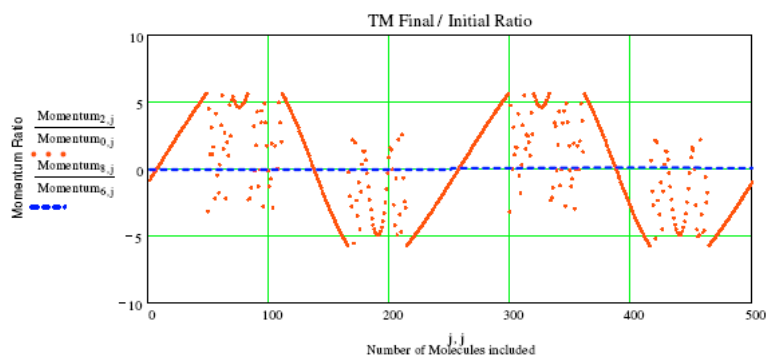
the base material. However, the Energy Ratio resulting from the adsorbent material is much different than for the base material. ($ER_{\text{adsorbant}} = 48$; $ER_{\text{base}} = 2.9$).

The result is that the gas atom impacting the surface now sees a combination of solid atoms which have a varying ER within the solid. As it approaches it is exposed to atoms with high ER. At the bottom of the impact it is exposed to atoms with both large and small ER. The result is a markedly different TMAC result.

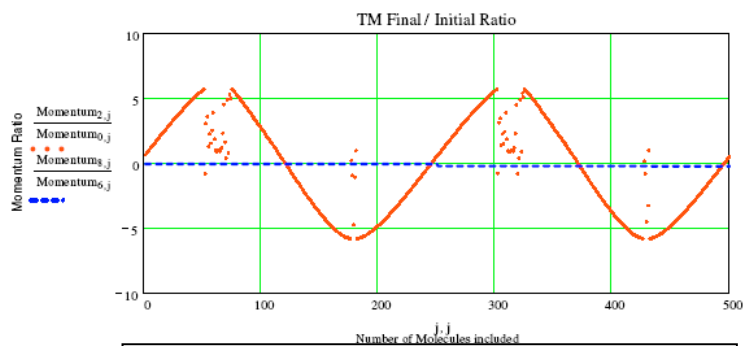
For the single adsorbent layer, the high ER top layer has restored many of the forward scattering gas atoms and most of the potentially backscattering gas atoms to a single “bounce” situation, substantially raising the TMAC at 10degrees.

For the two adsorbent layers, the third layer of atoms (base solid) has only a small effect. The result is nearly the same as if all the material were of the ER of the adsorbent. The plot is nearly the same as the high ER plot from the prior experiment.

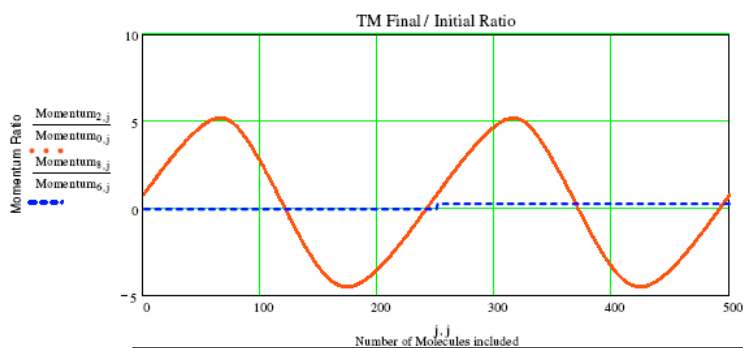
This is evident in the following plot of final to initial tangential momentum for the three cases:



No Adsorbed Layers, Angle = 10 Degrees



1 Adsorbed Layer, Angle = 10 Degrees



2 Adsorbed Layers, Angle = 10 Degrees

Figure 40 Adsorbed Layers – Examples at 10 Degrees

This is further illustrated by the following figure showing the plots of the gas atoms. Each plot shows the same 10 different gas atoms as they impact the surface. The effect of the additional adsorbed layers is to change the type of impact from a multiple “bounce” to a single “bounce”.

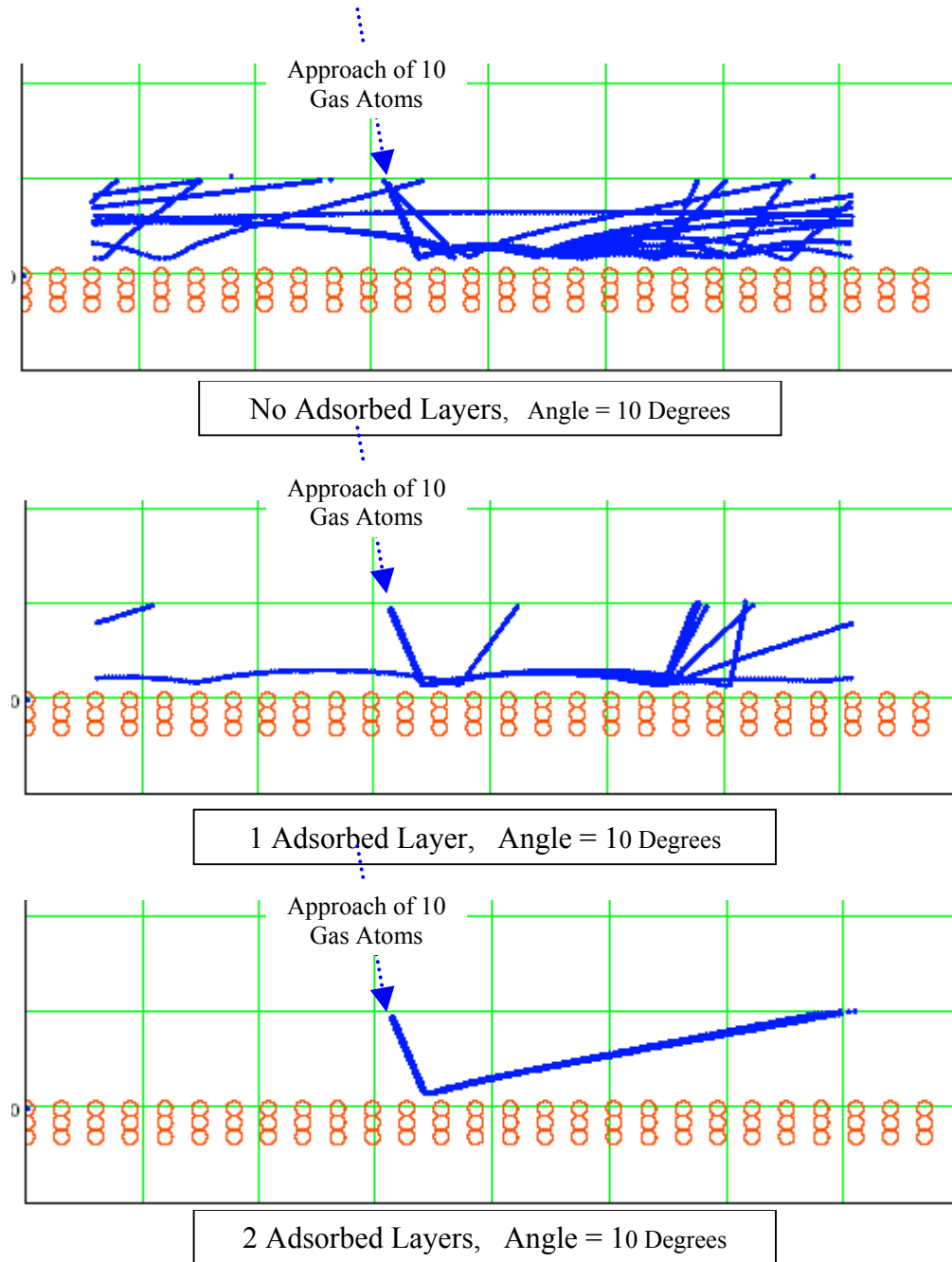


Figure 41 Adsorbed Layers – Gas Atom Path Plots (10 sample atoms each)

Effect of Single and Multiple Adsorbed Layers with small ER difference

For this analysis, the ER of the adsorbed layer was 4.9 or 5.0 vs. an ER for the base material of 2.9.

The summary data for single, double and triple adsorbent layers is shown below:

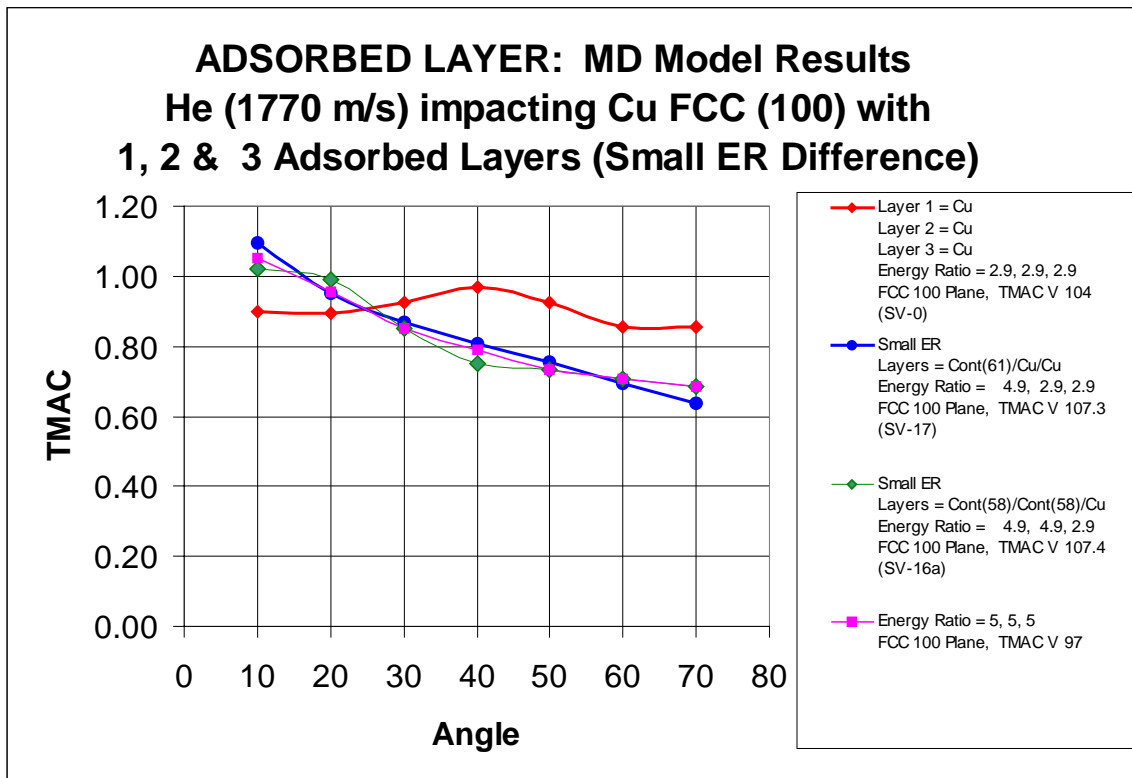


Figure 42 Adsorbed Layers - Data Summary for Small ER Difference

Effect of Change of ER of Adsorbed Layer

The summary data for a single and double adsorbent layers at varying ER are shown below:

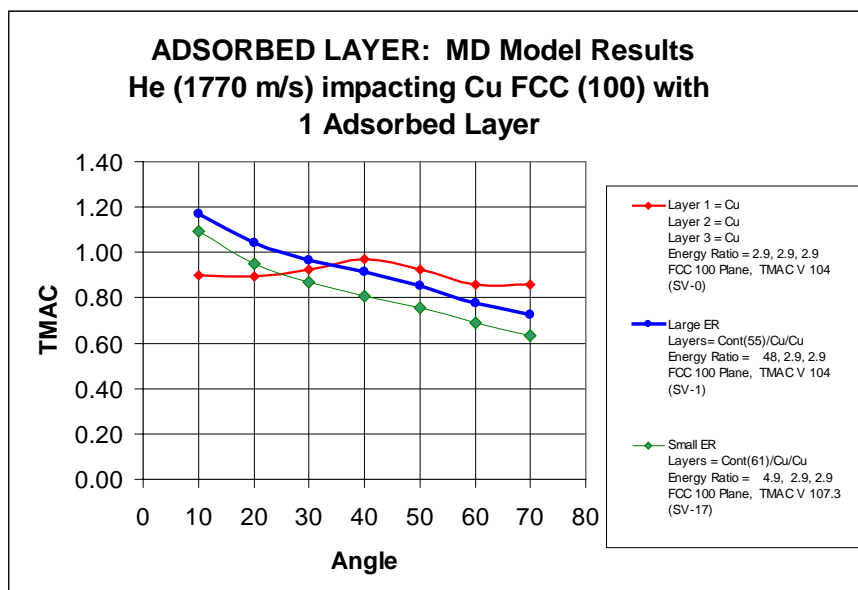


Figure 43 Adsorbed Layers – ER 1 Layer

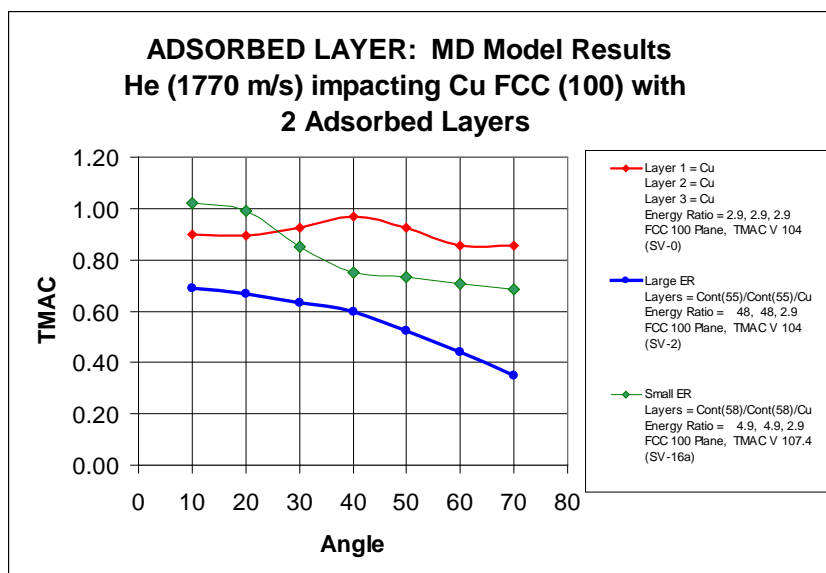


Figure 44 Adsorbed Layers – ER 2 Layers

Nano & Sub Nano Geometry Analysis Findings

The experiments regarding the nano and sub nanogeometry present many interesting findings, as described below.

Sub Nano Geometry Findings (Ratio of σ / Lattice Spacing)

The Lennard Jones σ is a measure of the characteristic distance around the atom. The Solid Lattice Spacing is a measure of the distance between solid atoms. The ratio of these two values provides a measure of the effective sub nanoscale surface roughness of the FCC crystal, as shown below.

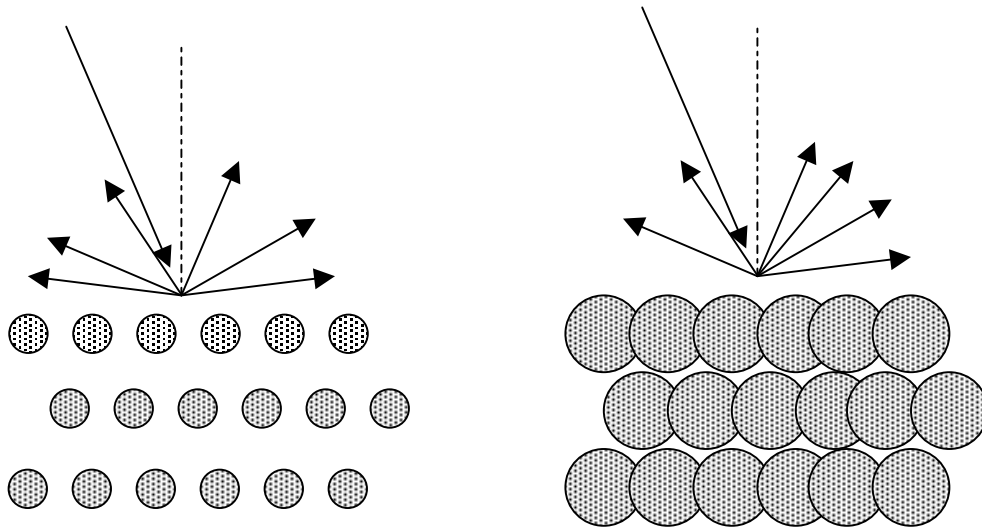


Figure 45 Nano Geometry - Ratio of Sigma to Solid Lattice Spacing Concept

Following is a summary of the experiment regarding the effect of the ratio of Lennard Jones “sigma” to the solid Lattice Spacing on the TMAC.

The two solid structures illustrated above have the same lattice spacing, but differing Lennard Jones σ values. As the ratio of σ to the lattice spacing is increased, the solid presents a different surface, with less nano geometric irregularities, thereby altering TMAC.

Ratios of 0.77 and 0.81 were evaluated over the complete range of angles. A ratio of 0.97 was evaluated at the extreme angles to provide additional insight.

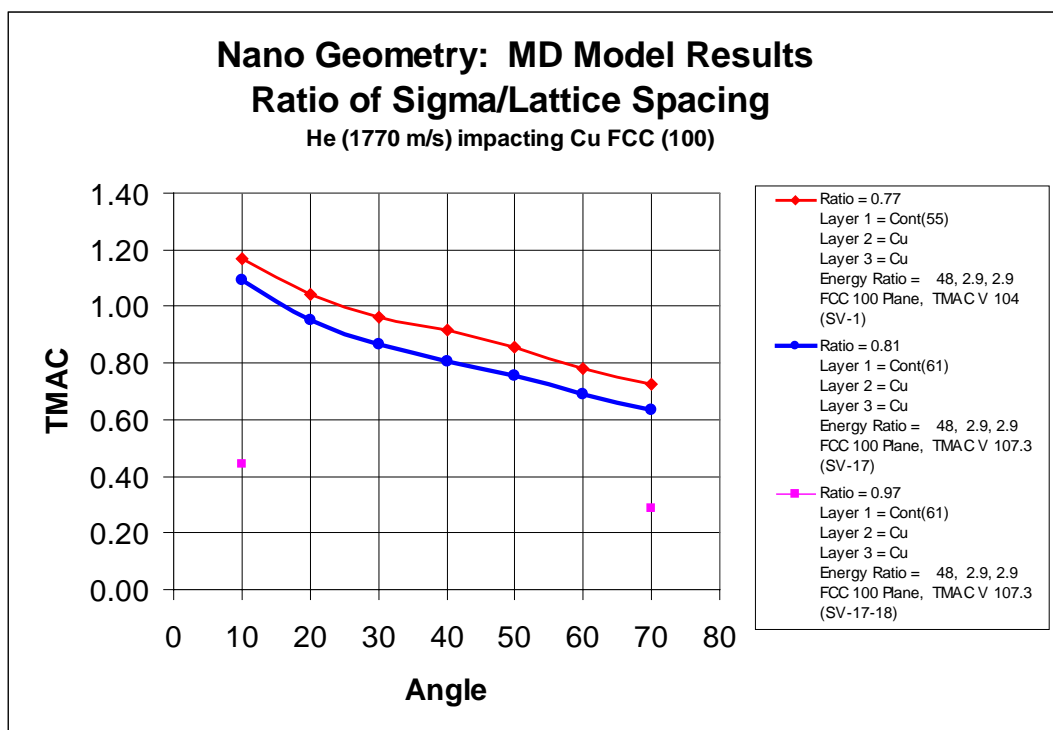


Figure 46 Nano Geometry – Ratio of Sigma to Solid Lattice Spacing Data

Note that increasing the σ to lattice spacing ratio in general lowers TMAC over all angles.

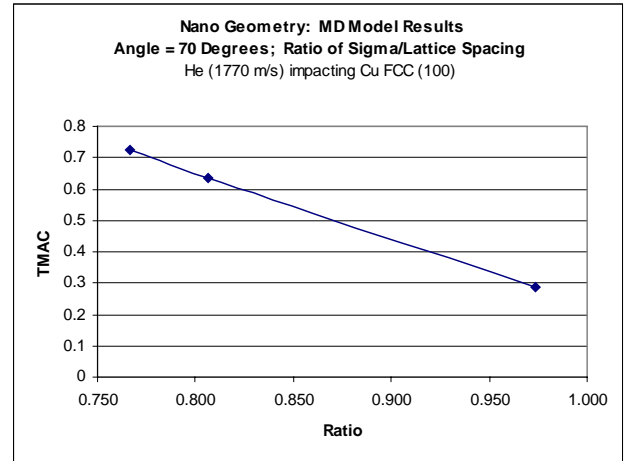
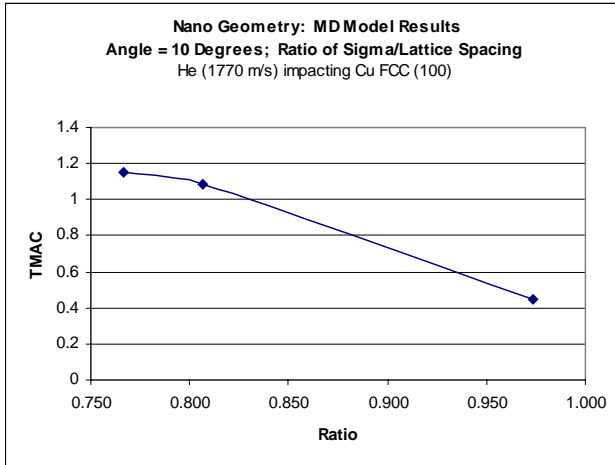


Figure 47 Nano Geometry – Ratio of Sigma to Solid Lattice Spacing, 10 & 70 Degrees

Nano Geometry Findings – Single Atom Bumps Atop FCC 100 Crystal

Single atom “bumps” were added atop an FCC 100 surface to evaluate the potential effect on TMAC. Two different spacings of “bumps” were evaluated. The first spacing was 1 “bump” every Unit Cell. The second spacing evaluated was 1 “bump” every 8 Unit Cells.. This resulted in significantly different effects. The data summary is plotted below.

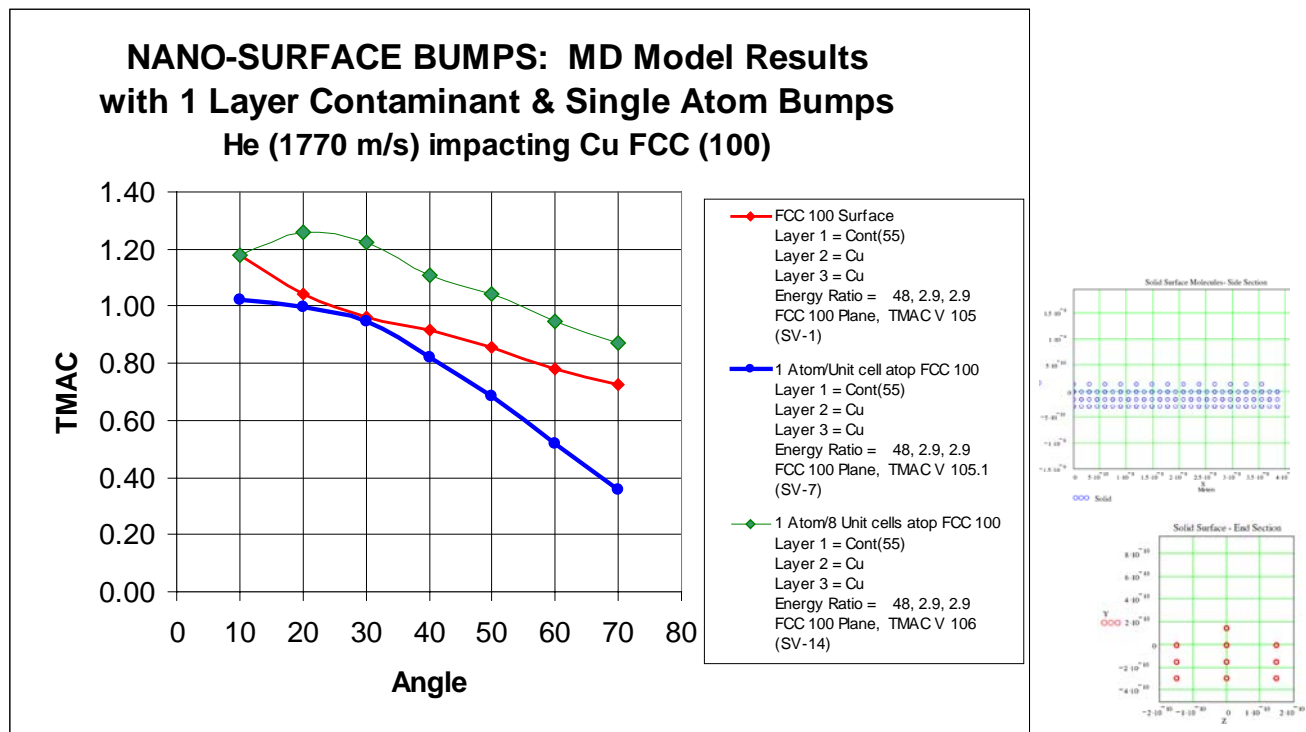


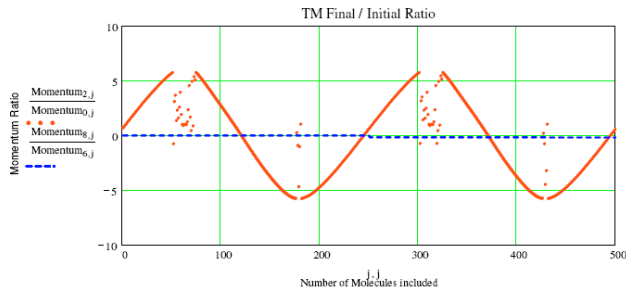
Figure 48 Nano Geometry – Surface “Bumps” Summary Data

“Bumps” spaced every unit cell:

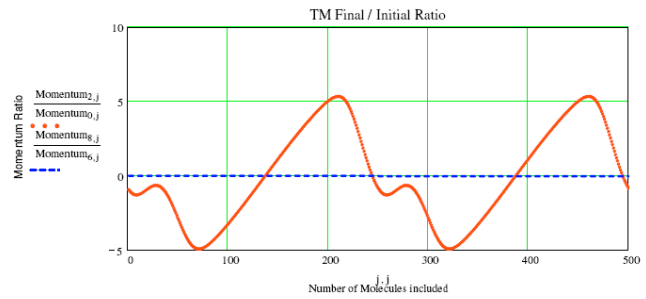
The experiment with the “bumps” spaced every unit cell (every other surface atom) provides some interesting findings:

- The TMAC is reduced (instead of increased) by such an irregularity at a shallow angle of approach.
- The TMAC is reduced (instead of increased) by such an irregularity at a steep angle of approach.

For the 10 degree case, we examine the ratio of final to initial tangential momentum for each gas atom involved. Notice that the backscattering period for the surface with “bumps” is disturbed from a simple wave function.



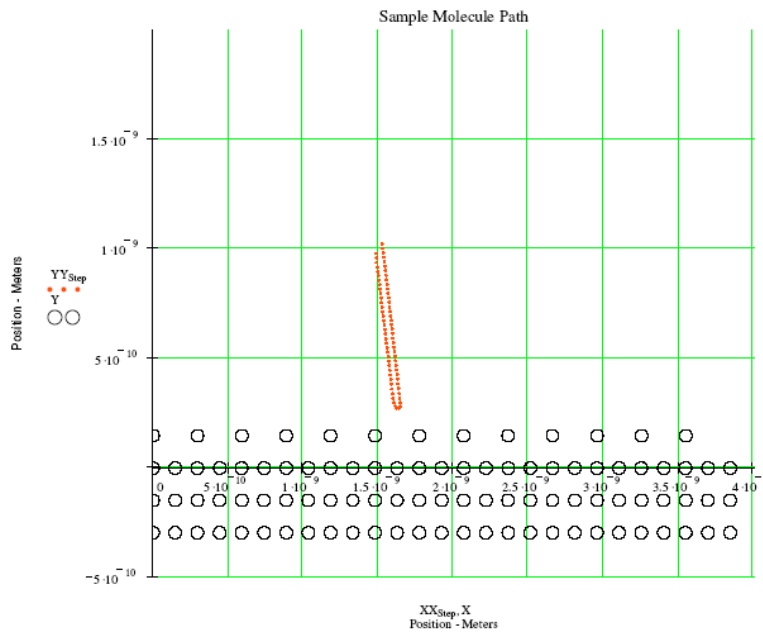
No "Bumps", Angle = 10 Degrees



1 "Bump" per Unit Cell, Angle = 10

Figure 49 Nano Geometry – Surface "Bumps"

Examining the path of such a gas molecule, we find that the nano geometry is such that its backscattering amount is reduced by the presence of another "bump" in close proximity.



1 "Bump" per Unit Cell, Angle = 10

Figure 50 Nano Geometry – Surface "Bumps" Reducing Backscattering

"Bumps" spaced every 8 unit cells:

The experiment with the "bumps" spaced every 8 unit cells provides some interesting findings:

- For most of the involved angles, the TMAC is increased, as would be expected by a nano roughening of the surface.
- However, the TMAC is substantially unchanged (instead of increased) by such an irregularity at a 10 degree angle of approach.

A possible explanation is that at the larger angles of approach, there is more opportunity for the “bumps” to interact with the gas atoms due to their shallower approach and departure paths. At the 10 degree angle of approach, most gas atoms approach and leave the surface without interacting with the “bumps”.

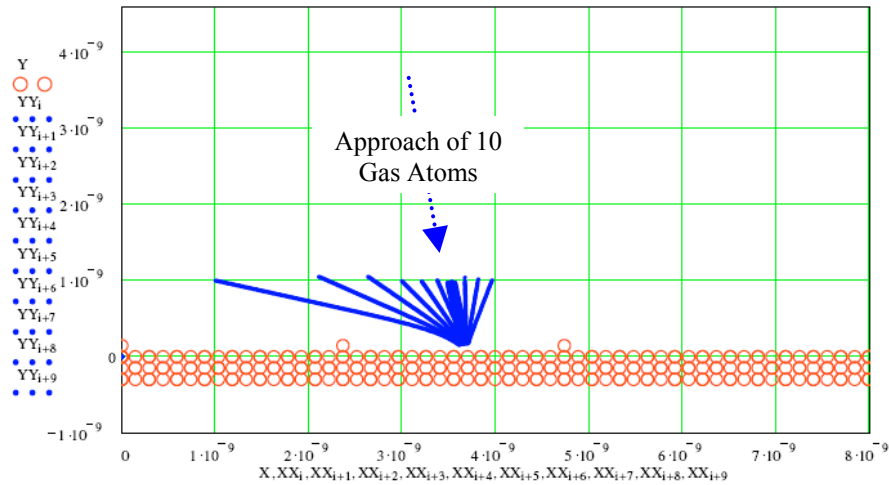


Figure 51 Nano Geometry - 1 /8: Most Gas Atoms miss "Bump" (10 sample atoms)

Energy Ratio Surface Plot Analysis

As a separate follow-up analysis, the surface of the FCC crystal was analyzed to evaluate L-J potential at various heights above the atoms of the crystal. A solid 7 atoms by 7 atoms by 3 atoms deep, comprised of 9 unit cells was analyzed over the center unit cell only. The outlying unit cells were included in the solid to assure all atoms within the cut off radius were part of the analysis. From this data, contour plots of constant L-J potential were made. Such plots can be considered imaginary “surfaces” which indicate how close a gas atom would come to the solid, given the Energy Ratio between the gas atom and the solid surface.

Fig 51 shows a contour plot of a single unit cell for an ER of 1. One can clearly see the 5 top atoms of the FCC unit cell. Fig. 52 shows the same data over a large surface.

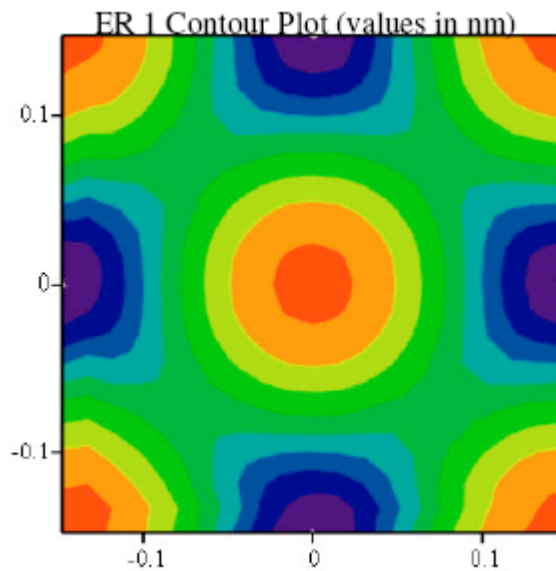


Figure 52 Height Contour Plot of L-J Potential Corresponding to ER of 1 (Unit Cell)

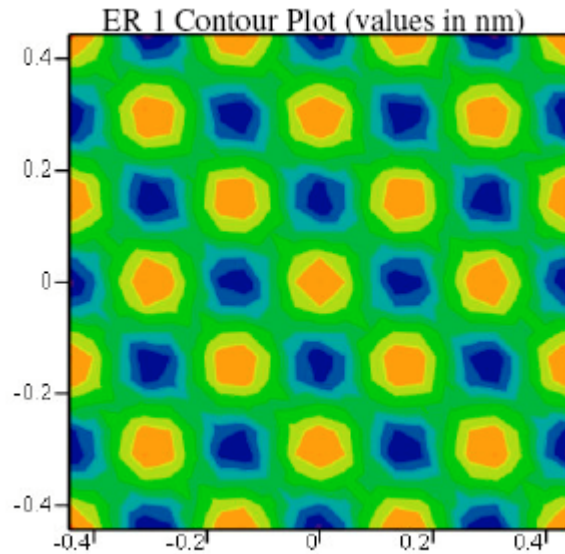


Figure 53 Height Contour Plot of L-J Potential Corresponding to ER of 1 (Larger Surface)

The variation in height for a variety of Energy Ratios is shown in Fig 53. This plot shows the high, low and average values for the contour plot for the range of Energy Ratios evaluated. The difference in the contour plots between the highest and lowest point is on the order of 5×10^{-11} m. Note as Energy Ratio is increased, the gas atom penetrates the L-J potential field closer to the solid atoms.

The standard deviation in surface height as a function of ER is shown in Fig. 54. Note for a broad range of ER (0.5 to 10) the standard deviation is essentially constant. Over the range from 10 to 100, it increases about 20%. This standard deviation could be considered a measure of the surface subatomic roughness which would increase TMAC with increasing ER. However, for the range of ER and materials simulated, this effect has not been detected. In general, TMAC was

reduced with increasing ER rather than vice versa. One can infer that this subatomic scale roughness does not have an significant affect on TMAC for these conditions..

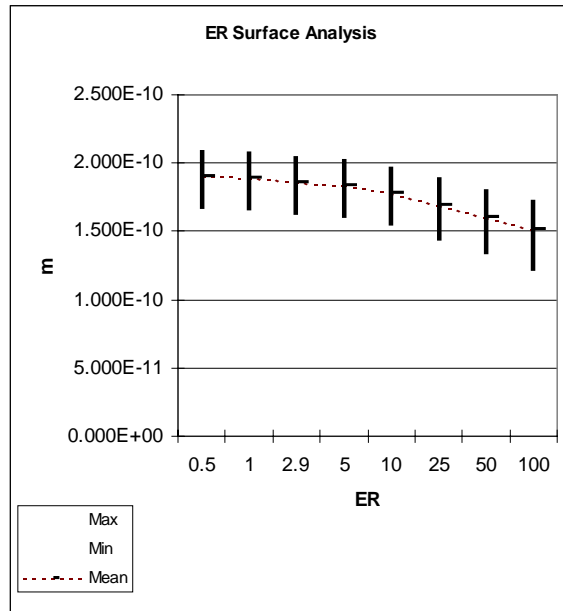


Figure 54 Height High-Low-Average Corresponding to Various ER

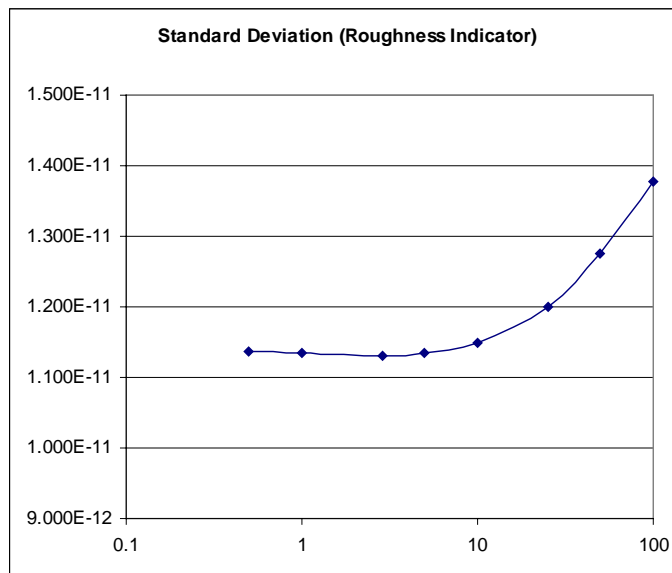


Figure 55 Standard Deviation of Height Corresponding to Various ER

CHAPTER SIX: CONCLUSION

An MD model has been developed and shown to be a useful tool in understanding many of the various factors which affect tangential momentum transfer and in quantitatively evaluating the TMAC at various angles.

Basic Conclusions about TMAC

The variance of TMAC with angle of approach, as detected in experiments has been demonstrated to be reproducible with deterministic calculations.

The ratio of final momentum to initial momentum for a given sequence of gas molecules follows a piecewise continuous curve for most situations evaluated. This curve frequently demonstrates regular cycles of both forward scattering and backscattering. It is the sum for all the involved gas atoms which determines whether backscattering occurs overall.

During the discontinuous portions of these curves, impacts between the gas atom and the solid involve multiple “bounces” before the gas atom finally leaves the surface. It is this area of multiple “bounce” impacts which initially raises TMAC as the forward scattering continuity is disturbed. Subsequently it reduces TMAC as the backscattering continuity is disturbed.

Conclusions Based on Broad Parameters

Energy Ratio has been shown to be a major determinant in the overall value of TMAC.

Decreasing the Energy Ratio tends to increase the number of multiple “bounce” impacts of the gas atom to the surface. Increasing Energy Ratio above a value of 5 tends to decrease TMAC at all angles of approach. Decreasing Energy Ratio below a value of 5 tends to increase TMAC at large angles of approach, but not necessarily at the small angles.

Adsorbed layers or layers of contaminant atop a surface have been shown to significantly change the TMAC values in a manner consistent with the Energy Ratio of the added layer.

Nanoscale geometry in the form of Lennard Jones σ to Lattice Spacing ratio affects TMAC. In general, increasing this ratio decreases TMAC.

Nanoscale irregularities in the form of single atoms may increase or decrease TMAC depending on their frequency of spacing.

Thoughts on MD Modeling of TMAC

An MD model has been developed and shown to be a useful tool in understanding many of the various factors which affect tangential momentum transfer. It was useful to consider cut off ratios larger than 2.5 as a method to improve accuracy of the results.

Use of commercial off the shelf software, such as Mathcad presented a viable option for small, deterministic MD simulations.

Modeling of specific real world macro or micro scale systems with contaminants or certain geometry is problematic because of the uncertainty regarding the makeup and geometry of those systems. However, simplified even models of such systems have been shown to provide useful results.

APPENDIX: RECOMMENDATIONS FOR FOLLOW ON RESEARCH

The work described in this Dissertation has been rewarding and provides a new basis for follow on work in the area of TMAC analysis.

The following is an outline for follow on research for future, post doctoral work:

- Phase 1: Convert this basic MD code to become more compatible with ongoing MD and DSMC work at UCF:
 - Using the techniques developed in this MATHCAD code, develop an improved basic functionality in C :
 - Program the existing code into C to take advantage of the UCF higher speed computers and parallel computer systems, so that analysis runs may be accomplished faster.
 - Incorporate a Predictor – Corrector algorithm. Evaluate if it allows use of larger time steps to speed up the analyses. If so, continue its use. If not, return to use of Verlet algorithm.
 - Validate convergence on TMAC as time step is reduced.
 - Validate improved conservation of energy as time step is reduced.
 - Validate with Seidl experimental data using values described in this dissertation.
 - Survey the other MD, CFD and DSMC software being used for similar research at UCF. Develop C input and output formats compatible with supporting these other software.
 - Survey the 3D movie software in use at UCF. Develop C output formats compatible with this software so that movies of the gas atoms trajectories may be made.

- Phase 2: Use / expand the MD code to perform new research:
 - The existing code is a 2 dimensional simulation. It models gas atoms impacting the crystal surface at varying angles normal to the crystal plane (zenith), but at a single angle with respect to a orientation of the surface atoms (azimuth). Expand the code to evaluate TMAC combinations of zenith and azimuth angles – full 3 dimensional analysis. This will involve enlarging the solid crystal base and keeping track of gas positions, velocities, accelerations, energies, forces, etc. in all 3 dimensions. (This might become a journal article on the topic of, “Comparison of 2D and 3D MD Models for Estimating TMAC”.)
 - The existing code estimates TMAC by angle. This approach aides in analysis, but it is not what is typically used in engineering calculations. The code is expandable to allow addition of a thermal velocity distribution to superimpose onto the flow velocity. This would allow estimation of a statistical set of gas atoms to estimate a single TMAC value similar to what is usually recorded as data and used in calculations. For a given set of gas atoms, a Maxwellian velocity distribution would be applied for the given gas temperature. This would be added to the flow velocity and the TMAC estimated. TMAC convergence based on the number of gas atoms involved should be demonstrated, as well as agreement with experimental data. (This might become a journal article on the topic of, “Estimation of TMAC using Maxwellian Temperature Distribution in Combination with Flow Velocities”.)
 - The existing code provides both TMAC and NMAC data. The focus of this doctoral research was on TMAC. The Normal Momentum Accommodation Coefficient data

- could be extracted and evaluated in a manner to that used for TMAC. This would then be related to heat transfer mechanisms in the gas. (This might become a journal article on the topic of, “Estimation of Normal Momentum Accommodation Coefficient using MD Simulation”.)
- The data currently in the code is complete only for Helium and Copper. Look up tables have been outlined to record complete data for other materials of interest. Other materials need to be included. Add Lennard – Jones material data for more gasses and solids. Some additional experimental TMAC data exists for Helium on Aluminum and Argon on Aluminum [35] which could also be used to validate further analyses and for validation at gas velocities similar to those of Spacecraft on orbit.
 - The code is currently configured to model a FCC crystal 100 plane. Incorporate coordinate transforms to convert the basic crystal structure to 110 or 111 planes. Incorporate BCC and other crystal structures. Evaluate how basic crystal structure and orientation effects TMAC. (This might become a journal article on the topic of, “Effects of Crystal Plane Nano Geometry on TMAC using MD Simulation”.)
 - The existing code provides for limited nanoscale geometric irregularities. Add more nanoscale geometry features, such as missing surface atoms and larger irregularities. Evaluate their effect on TMAC. Incorporate surface relaxation effects, then evaluate those effects on TMAC. (This might become a journal article on the topic of, “Estimation of Relaxation and Surface Nano Defects on TMAC using MD Simulation”.)
 - Expand the Energy Ratio envelope evaluated. The existing work evaluated over a limited ER range. At the lower ER values, the time step has to be very small in order

to assure convergence. This resulted in some individual data runs lasting several days each. It is hoped that in a C form on a higher speed computer lower ER can be practicably evaluated in a reasonable time period and the results analyzed. Higher ER results would also be of interest for spacecraft on orbit. (This might become a journal article on the topic of, “Estimation of TMAC at High Energy Ratios”.)

- Examine trajectory convergence. Rapaport makes the statement, “ Obtaining a high degree of accuracy in the trajectories is neither realistic nor a practical goal.” [46] This work has, through the use of very small time steps and simplifying assumptions, demonstrated that useful gas atom trajectory information is in fact obtainable from MD simulations. For follow on work, trajectories at a high degree of accuracy must also be the goal and must be generally achievable. Individual trajectories, especially multiple bounce trajectories should demonstrate convergence on time step and or other factors. Perhaps the gas atom’s position in space after certain time periods could be compared and demonstrated to formally converge. This initial work examined trajectories in the single and multiple bounce arena and demonstrated that the tangential momentum ratio plot is piecewise continuous. If you notice, in the “discontinuous” regions of many of these plots there exists subsets of continuity, which are likely 2 or 3 bounce situations. After demonstrating trajectory convergence, the discontinuous portions of the ratio plots can be analyzed and useful conclusions drawn. (This might become a journal article on the topic of, “Abilities of MD Simulations to Predict Trajectories With Adequate Convergence”.)
- What is the TMAC inside a carbon nanotube? What is the TMAC for flow past the outside of carbon nanotubes? The solid geometry for a single or multiple walled

carbon nanotube could be inserted into the code and the TMAC evaluated for the desired materials and conditions. (This might become a journal article on the topic of, “Estimation of TMAC Within and Around Carbon Nanotubes”.)

- The existing code models nano geometry. Most actual surface irregularities are in the micro geometry regime. Topics such as grinding or polishing grooves and electropolishing are more likely to be micro geometry irregularities than nano. This would require expanding the MD simulation solid geometry to allow analysis of micro geometry, including the 5 micro meter grinding grooves of Seidel or micro channel roughness of Turner et al [109] . It would be valuable to incorporate calculation acceleration techniques so that whenever the gas atom is outside the cut off radius of any solid surface, it proceeds in a straight line until it again reaches a cut off radius. (This might become a journal article on the topic of, “Estimation of Micro Geometry Effects on TMAC using MD Simulation”.)
- To assist in ongoing MD and DSMC flow analyses, perform a series of MD analyses using the TMAC MD model developed to generate a series of curves for the involved materials, geometry and energy ratios. Analyze to develop curve fitting equations or create look up tables so that the data may be directly used in the DSMC or MD simulation on a real time basis.
- Phase 3: Eliminate many of the simplifying assumptions from the model to perform new research:
 - The existing code models single atom gasses, such as Helium. There is much interest in H₂ and other diatomic gasses. The existing code models the solid atoms as fixed in space. In reality, the solid atoms are not fixed in space, but constantly moving and

interacting. Incorporating these new motions will necessitate keeping track of much more data about the gas and solid molecules, an order of magnitude more calculations and substantial expansion of the code. However, it will then allow investigation of such topics as: How much TMAC and NMAC variability is introduced by these vibrations; and How temperature differences between the gas and solid affect TMAC and NMAC.

LIST OF REFERENCES

1. Moore, P. and A. Sowter, *Application of a Satellite Aerodynamics Model Based on Normal and Tangential Momentum Accommodation Coefficients*. Planetary and Space Science, 1991. 39(10): p. 1405-1419.
2. Griffin, M.D. and J.R. French, *Space Vehicle Design*. Education Series, ed. AIAA. 1991: AIAA.
3. Herrero, F.A., *The Lateral Surface Drag Coefficient of Cylindrical Spacecraft in a Rarefied Finite Temperature Atmosphere*. AIAA Journal, 1985. 23(6): p. 862-867.
4. Knuth, E., *Free Molecule Normal Momentum Transfer at Satellite Surfaces*. AIAA Journal, 1980. 18(5): p. 602-605.
5. Collins, F. and E.C. Knox, *Parameters of Nocsilla Gas/Surface Interaction Model from Measured Accommodation Coefficients*. AIAA Journal, 1994. 32(4): p. 765-773.
6. AIAA, ed. *AIAA Aerospace Design Engineers Guide*. Fifth ed. 2003: Reston, VA.
7. Thonon, B. and p. Marty. *Micro Thermal Systems in France: From Knowledge to Technological Development*. in *First International Conference on Microchannels and Minichannels*. 2003: ASME.
8. Bari, A., et al. *Frictional Characteristics of Microchannel Gas Flow*. in *First International Conference on Microchannels and Minichannels*. 2003. Rochester, NY, USA.
9. Arkilic, E.B., K.S. Breuer, and M.A. Schmidt, *Gaseous Flow in Micro channels*. Application of Micro fabrication to Fluid Mechanics, 1994. ASME FED- Vol 197: p. 57-66.
10. Pfahler, J., et al. *Gas and Liquid Flow in Small Channels*. in *Winter Annual Meeting*, ASME. 1991. Atlanta, GA: ASME.
11. Barber, R.W., D.R. Emerson, and X. Gu, *Rarefied Gas Dynamics in Micro-devices*. 2004, Council for the Central Laboratory of the Research Councils (CCLRC). p. <http://www.cse.clrc.ac.uk/ceg/rgd.shtml>.
12. Hsieh, S., et al. *Gaseous Slip Flow in a Microchannel*. in *First International Conference on Microchannels and Minichannels*. 2003. Rochester, NY, USA: ASME.
13. Yang, R. *A Micro Channel Flow and Heat Transfer Study by Lattice Boltzmann Method*. in *First International Conference on Micro channels and Mini channels*. 2003. Rochester, NY, USA: ASME.
14. Finger, G., J. Kapat, and L. Chow. *Design and Analysis of a Rotary Wankel Compressor*. in *ASME International Mechanical Engineering Congress and Exhibition*. 2001. New York, NY: ASME.
15. Finger, G., *Design and Analysis of a Miniature Rotary Wankel Compressor*, in *Department of Mechanical, Materials and Aerospace Engineering*. 2002, University of Central Florida: Orlando, Florida. p. 72.

16. Garcia, A.L. and F. Baras, *Direct Simulation Monte Carlo: Novel Applications and New Extensions*, in *Department of Physics*. 1997, San Jose State University: San Jose, CA. p. 17.
17. Beskok, A., *A Model for Flows in Channels, Pipes and Ducts at Micro and Nano Scales*. *Microscale Thermophysical Engineering*, 1999. 3: p. 43-77.
18. Veijola, T., H. Kuisma, and J. Lahdenpera, *The Influence of gas-surface interaction on gas-film damping in a silicon accelerometer*. *Sensors and Actuators A-Physical*, 1998. 66: p. 83-92.
19. Barber, R.W. and D.R. Emerson. *Numerical Simulation of Low Reynolds Number Slip Flow past a Confined Sphere*. in *23 rd International Symposium on Rarefied Gas Dynamics*. 2002. Whistler, Canada.
20. Eckert, E.R. and R.M. Drake, *Analysis of Heat and Mass Transfer*. 1987: Hemisphere Publishing Co. 806.
21. Choondal, B. and S. Garimella, *A Comparative Analysis of Studies on Heat Transfer and Fluid Flow in Microchannels*. *Microscale Thermophysical Engineering*, 2001. 5: p. 293-311.
22. Barwinkel, K. *Physical Parameters Governing Slip-Conditions and Their Influence on Momentum and Energy Transfer*. in *Second Symposium: Fluid-Solid Surface Interaction*. 1974. Bethesda, Maryland.
23. Gampert, B., K. Homman, and H.B. Rieke, *The Drag Reduction in Laminar and Turbulent Boundary Layers by Prepared Surfaces with Reduced Momentum Transfer*. *Israel Journal of Technology*, 1980. 18: p. 287-292.
24. Halliday, D. and R. Resnick, *Fundamentals of Physics*. 1970: Wiley & Sons, Inc.
25. Arkilic, E.B., M.A. Schmidt, and K.S. Breuer, *Gaseous Slip Flow in Long Microchannels*. *J. of Microelectromechanical Systems*, 1997. 6(2): p. 167-178.
26. Shih, J., et al., *Monatomic and Polyatomic Gas Flow Through Uniform Microchannels*. *Micromechanical Systems*, ASME, 1996. DSC-Vol 59: p. 197-203.
27. Maxwell, J.C., *On Stresses in Rarified Gases Arising from Inequalities of Temperature*. *Philosophical Transactions of the Royal Society of London*, 1879. 170: p. 231-256.
28. Arkilic, E.B., K.S. Breuer, and M.A. Schmidt, *Mass Flow and tangential momentum accommodation in silicon micromachined channels*. *Journal of Fluid Mechanics*, 2001. 437: p. 29-43.
29. Gad-el-Hak, M., *The Fluid Mechanics of Microdevices - The Freeman Scholar Lecture*. *Journal of Fluids Engineering*, 1999. 121: p. 5 - 33.
30. Berman, A.S. and W.J. Maegley, *Internal Rarefied Gas Flows with Backscattering*. *The Physics of Fluids*, 1972. 15(5): p. 772-779.
31. Davis, D.H., L.L. Levenson, and N. Milleron, *Effect of "Rougher- than-Rough" Surfaces on Molecular Flow through Short Ducts*. *Journal of Applied Physics*, 1964. 35(3): p. 529 - 532.
32. Maegley, W.J. and A.S. Berman, *Transition from Free - Molecule to Continuum Flow in an Annulus*. *The Physics of Fluids*, 1972. 15(5): p. 780 - 785.
33. Seidl, M. and E. Steinheil, *Measurement of Momentum Accommodation Coefficients on Surfaces Characterized by Auger Spectroscopy, SIMS and LEED*. *Rarefied Gas*

Dynamics, Eighth International Symposium, Stanford University, 1974. 9(11): p. E 9.1 - E 9.12.

34. Thomas, L.B. and R.G. Lord, *Comparative Measurements of Tangential Momentum and Thermal Accommodations on Polished and Roughened Steel Spheres*. Rarefied Gas Dynamics, Eighth International Symposium, Stanford University, 1972: p. 405 - 412.
35. Doughty, R. and W. Schaetzle, *Experimental Determination of Momentum Accommodation Coefficients at Velocities up to and Including Earth Escape Velocity*. Rarefied Gas Dynamics, Eighth International Symposium, Stanford University, 1969. Supplement 5(2): p. 1035 - 1054.
36. Bentz, J.A., R.V. Tompson, and S.K. Loyalka, *The spinning rotor gauge: measurements of viscosity, velocity slip coefficients, and tangential momentum accommodation coefficients for N-2 and CH4*. VACUUM, 1997. 48(10): p. 817-824.
37. Knechtel, E. and W. Pitts, *Experimental momentum accommodation on metal surfaces of ions near and above earth satellite speeds*. Rarefied Gas Dynamics., 1969. 5(2): p. 1257 - 1266.
38. Lord, R.G., *Tangential Momentum Accommodation Coefficients of rare Gases on Polycrystalline Metal Surfaces*. Rarefied Gas Dynamics, Eighth International Symposium, Stanford University, 1976. 10: p. 531-538.
39. Porodnov, B.T., et al., *Experimental investigation of rarefied gas flows in different channels*. J. Fluid Mech, 1973. 64(3): p. 417-437.
40. Liu, S.M., P.K. Sharma, and E.L. Knuth, *Satellite Drag Coefficients Calculated from Measured Distributions of Reflected Helium Atoms*. AIAA Journal, 1979. 17(12): p. 1314-1319.
41. Dadzie, S.K. and J.G. Meolans, *Anisotropic scattering kernel: Generalized and modified Maxwell boundary conditions*. Journal of Mathematical Physics, 2004. 45(5): p. 1804-1819.
42. Cercignani, C. and M. Lampis, *New scattering kernel for gas-surface interaction*. AIAA Journal, 1997. 35(6): p. 1000-1011.
43. Bird, G., *Molecular Gas Dynamics and the Direct Simulation of Gas Flows*. 1994: Clarendon Press, Oxford.
44. Ceperley, D. *Mat SE 485, Atomic Scale Simulation Lecture Notes*. in University of Illinois. Fall 2004.
45. Skoulidas, A.I. and D.S. Sholl, *Self Diffusion and Transport Diffusion of Light Gases in Metal Organic Framework Materials using Molecular Dynamics Simulation*. J. Am. Chem. Soc., Submitted 2/9/2005.
46. Rapaport, D.C., *The Art of Molecular Dynamics Simulation*. Second ed. 2004, Cambridge, UK: Cambridge University Press.
47. Kapat, J. *Fundamental Phenomenon, Lecture Notes*. in University of Central Florida. 2003.
48. Mortimer, C.E., *Chemistry a Conceptual Approach*. 1971, Allentown, PA: Van Nostrand Reinhold Co.

49. Kruger, M., et al., *Sensitivity of Single Multi Walled Carbon Nanotubes to the Environment*. New Journal of Physics, 2003. 5: p. 138.1 - 138.11.
50. Kleiman, G. and U. Landman, *Theory of Physisorption: He on Metals*. Physical Review B, 1973. 8(12): p. 5484 - 5493.
51. Churakov, S.V., *Temperature, pressure and composition corrections for molar thermodynamic properties on non-electrolyte fluids and their mixtures*. 2003, Centro Swizzero di Calcolo Scientifico (CSCS): Manno, Switzerland.
52. Saltsburg, H. and J.N. Smith, *Molecular Beam Scattering from the (111) Plane of Silver*. The Journal of Chemical Physics, 1966. 45(6): p. 2175 - 2183.
53. Boring, J. and R. Humphris, *Drag Coefficients for Free Molecule Flow in the Velocity Range 7 - 37 km/sec*. AIAA Journal, 1970. 8(9): p. 1658 - 1662.
54. Gabis, D.H., S.K. Loyalka, and T.S. Storvick, *Measurements of the tangential momentum accommodation coefficient in the transition flow regime with a spinning rotor gauge*. J. Vac. Sci. Technol., 1996. 14(4): p. 2592-2598.
55. Suetin, P.E., et al., *Poiseuille flow at arbitrary Knudsen numbers and tangential accommodation*. J. Fluid Mech, 1973. 66(3): p. 581-592.
56. Colin, S., P. Lalonde, and R. Caen. *Gaseous Flows in Rectangular Microchannels: Experimental Validation of a Second Order Slip Flow Model*. in *First International Conference on Microchannels and Minichannels*. 2003. Rochester, NY, USA: ASME.
57. Sazhin, O.V. and S.F. Borisov, *Accommodation Coefficient of tangential momentum on anatomically clean and contaminated surfaces*. J. Vac. Sci. Technol., 2001. 19(5): p. 2499-2503.
58. Cooper, S.M., et al., *Gas Transport Characteristics through a Carbon Nanotube*. Nano Letters, 2004. 4(2): p. 377-381.
59. Jang, J., Y. Zhao, and S.T. Wereley. *Pressure distribution and TMAC measurements in near unity aspect ratio, anodically bonded microchannels*. in *MEMS 2003*. 2003. Kyoto, Japan.
60. Abuaf, N. and D. Marsden, *Momentum accommodation of argon in the 0.06 to 5 eV range*. Rarefied Gas Dynamics., 1967. Supplement 4: p. 199 - 210.
61. Logan, R.M., J.C. Keck, and R.E. Stickney. *Simple Classical Model for the Scattering of Gas Atoms from a Solid Surface: Additional Analysis and Comparisons*. in *International Symposium on Rarefied Gas Dynamics*. 1966.
62. Srivastava, D., M. Menon, and K. Cho, *Computational nanotechnology with carbon nanotubes and fullerenes*. Computing in Science & Engineering, 2001. July/August 2001: p. 42-54.
63. Bayazitoglu, Y., S. Maruyama, and P. Hos, *Phase Change Studies with Molecular Dynamics: A Computer Simulation*. Calore e Tecnologia, 2000. 18(Supplement n. 1, 2000): p. 3-16.
64. Morris, D., L. Hannon, and A. Garcia, *Slip Length in a Dilute gas*. Physical Review A, 1992. 46(8): p. 5279-5281.
65. Koplik, J., J. Banavar, and J. Willemsen, *Molecular Dynamics of Poiseuille Flow and Moving Contact Lines*. Physical Review Letters, 1988. 60(13): p. 1282-1285.

66. Yang, J., J. Koplik, and J. Banavar, *Molecular Dynamics of Drop Spreading on a Solid Surface*. Physical Review Letters, 1991. 67(25): p. 3539-3542.
67. Koplik, J. and J. Banavar, *No-Slip Condition for a Mixture of Two Liquids*. Physical Review Letters, 1998. 80(23): p. 5125 - 5128.
68. Koplik, J., J. Banavar, and J. Willemsen, *Molecular Dynamics of Fluid Flow at Solid Surfaces*. Phys. Fluids A, 1989. 1(5): p. 781-794.
69. Cieplak, M., J. Koplik, and J. Banavar, *Applications of Statistical Mechanics in Subcontinuum Fluid Dynamics*. Physica A, 1999. 274: p. 281-293.
70. Cieplak, M. and J. Banavar, *Boundary Conditions at a Fluid-Surface*. Physical Review Letters, 2001. 86(5): p. 803-806.
71. Tomassone, M., et al., *Molecular Dynamics Simulation of Gaseous-Liquid Phase Transitions of Soluble and Insoluble Surfactants at a Fluid Surface*. Journal of Chemical Physics, 2001. 115(18): p. 8634-8642.
72. Vergeles, M., et al., *Stokes Drag and Lubrication Flows: A Molecular Dynamics Study*. Physical Review A, 1996. 53(5): p. 4852-4864.
73. Oman, R., et al., *Interactions of Gas Molecules with an Ideal Crystal Surface*. AIAA Journal, 1964. 2(10): p. 1722 - 1730.
74. Oman, R., *Numerical calculations of gas-surface interactions*. AIAA Journal, 1967. 5(7): p. 1280 - 1287.
75. Knechtel, E. and W. Pitts, *Normal and Tangential Momentum Accommodation for Earth Satellite Conditions*. Astronautica Acta, 1973. 18: p. 171 - 184.
76. Finger, G., J. Kapat, and A. Bhattacharya. *Analysis of Tangential Momentum Accommodation Coefficient Using Molecular Dynamics Simulation*. in *44th AIAA Aerospace Sciences Meeting and Exhibit*. 2006. Reno, NV: AIAA.
77. Piekos, E. and K.S. Breuer, *Numerical Modeling of Micro mechanical Devices Using the Direct Simulation Monte Carlo Method*. Transactions of the ASME, 1996. 118(September 1996): p. 464-469.
78. Sun, H. and M. Faghri, *Effects of Rarefaction and Compressibility of Gaseous Flow in Micro channel Using DSMC*. Numerical Heat Transfer, Part A, 2000. 38: p. 153-168.
79. Hajiconstantinou, N.G. *The Effect of Viscous Heat Dissipation on Convective Heat Transfer in Small Scale Slipping Gaseous Flows*. in *First International Conference on Micro channels and Mini channels*. 2003. Rochester, NY, USA.
80. McNenly, M.J., M.A. Gallis, and I.D. Boyd. *Slip Model Performance for Micro-Scale Gas Flows*. in *AIAA Thermophysics Conference*. 2003. Orlando, FL: AIAA.
81. Burt, J. and I. Boyd. *Monte Carlo Simulation of a Rarefied Multiphase Plume Flow*. in *43rd AIAA Aerospace Sciences Meeting and Exhibit*. 2005. Reno, NV: AIAA.
82. Burt, J. and I. Boyd. *Development of a Two Way Coupled Model for Two Phase Rarefied Flows*. in *42nd AIAA Aerospace Sciences Meeting & Exhibit*. 2004. Reno, NV: AIAA.
83. Beskok, A. and G. Karniadakis, *Simulation of Heat and Momentum Transfer in Complex Microgeometries*. Journal of Thermophysics and Heat transfer, 1994. 8(4): p. 647-655.
84. Tang, G., W. Tao, and Y. He. *Gas Flow Study in MEMS using Lattice Boltzmann Method*. in *First International Conference on Microchannels and Minichannels*. 2003. Rochester, NY, USA.

85. Jie, D., et al., *Navier-Stokes simulations of gas flow in micro devices*. Journal of Micromechanics and Microengineering, 2000. 10: p. 372-379.
86. Raju, R. and S. Roy, *Hydrodynamic Study of High Speed Flow and Heat Transfer through a Microchannel*. J. Thermophysics and Heat Transfer, 2004. T2562.
87. Ebert, W. and E. Sparrow, *Slip Flow in Rectangular and Annular Ducts*. Transactions of the ASME, 1965: p. 1018-1024.
88. Morini, G. and M. Spiga, *Slip Flow in Rectangular Microtubes*. Microscale Thermophysical Engineering, 1998. 2: p. 273-282.
89. Shapiro, F., *Rarefied gas Flow through a long rectangular channel*. J. Vac. Sci. Technol., 1999. A 17(5): p. 3062-3066.
90. Barber, R.W. and D.R. Emerson, *Analytical solution of low Reynolds number slip flow past a sphere*. 2000, Centre for Microfluidics, Department of Computational Science and Engineering, CLRC Daresbury Laboratory: Daresbury, Warrington.
91. Martin, M.J. and I.D. Boyd. *Blasius Boundary Layer Solution with Slip Flow Conditions*. in *Presented at the 22nd Rarefied Gas Dynamics Symposium*. 2000. Sydney, Australia.
92. Goodman, F. *Preliminary Results of a Three Dimensional Hard Spheres Theory of Scattering Gas Atoms from a Solid Surface*. in *International Symposium on Rarefied Gas Dynamics*. 1967. Oxford, England: Academic Press.
93. Jackson, D., *A Theory of Gas Surface Interactions at Satellite Velocities*. 1968, University of Toronto Institute for Aerospace Studies: Toronto, Canada.
94. Epstein, M., *Effect of Incomplete Accommodation on the Slip Coefficient*. 1968, Aerodynamics and Propulsion Research Laboratory, Aerospace Corporation, SAMSO, AFSC, LAAFS: Los Angeles, CA. p. 1-22.
95. Srivastava, G., *The Physics of Phonons*. 1990: IOP Publishing Ltd.
96. Guinier, A. and R. Jullien, *The Solid State, From Superconductors to Super alloys*. 1989: Oxford University Press.
97. Kittel, C., *Introduction to Solid State Physics*. 1967: John Wiley & Sons.
98. Kittel, C., *Elementary Solid State Physics, a Short Course*. 1962: John Wiley & Sons, NY.
99. Harrison, W., *Electronic Structure and the Properties of Solids*. 1980: W.H. Freedman and Co.
100. Wan, J., et al., *Surface Relaxation and Stress of FCC metals: Cu, Ag, Au, Ni, Pd, Pt, Al and Pb*. Modeling Simul. Mater. Sci. Eng., 1999. 7: p. 189-206.
101. Zheng, J., et al., *Relaxation of Cu(100), (110) and (111) Surfaces Using Ab Initio Pseudopotentials*. Surface Review and Letters, 2001. 8(5): p. 541-547.
102. Gerson, A. and T. Breddow, *MgO(100) Surface Relaxation and Vacancy Defects: a Semi-empirical Quantum-chemical Study*. Phys. Chem. Chem. Phys., 1999. 1: p. 4889-4896.
103. Allen, M.P. and D.J. Tildesley, *Computer Simulation of Liquids*. 1989. 408.
104. Hess, S. and M. Kroger, *Elastic and Plastic Behavior of Solid Models*. Technische Mechanik, 2002. Band 22(Heft 2): p. 79-88.
105. Landman, U., R. Barnett, and W. Luedtke, *Simulations of Materials: from electrons to friction*. Philosophical Transactions of the Royal Society of London, 1992. 341(1661): p. 337-350.

106. McNenly, M.J. and I.D. Boyd, *Numerical Simulation of Particle Flow Conductance in a Duct Under Free- Molecular Conditions*. 2004: University of Michigan, Department of Aerospace Engineering, Ann Arbor, MI. p. 6.
107. Landman, U., et al., *Theoretical considerations of energetics, dynamics and structure at interfaces*. J. Vac. sci. Technol., 1985. 3(3): p. 1574-1587.
108. Delstar, *Electropolishing, Passivating and Mechanical Polishing*. 2005, Delstar Metal Finishing, Inc. p. www.delstar.com/polishing.htm.
109. Turner, S., et al., *Effect of Surface Roughness on Gaseous Flow Through Microchannels*. Proceedings of the ASME Heat Transfer Division, 2000. HTD-Vol 366-2: p. 291-298.